Available online at www.sciencedirect.com
ScienceDirect
Coordination Chemistry Reviews 250 (2006) 2511–2564
COORDINATION CHEMISTRY REVIEWS
www.elsevier.com/locate/ccr

Review

Lanthanides and actinides: Annual survey of their organometallic chemistry covering the years 2003 and 2004

Frank T. Edelmann *

Chemisches Institut der Otto-von-Guericke-Universität Magdeburg, D-39106 Magdeburg, Germany

Accepted 13 March 2006
Available online 28 March 2006

Contents

* Fax: +49 391 6712933.
E-mail address: frank.edelmann@vst.uni-magdeburg.de.

0010-8545/$ – see front matter
doi:10.1016/j.ccr.2006.03.018

Keywords: Lanthanides; Actinides; Cyclopentadienyl complexes; Cyclooctatetraenyl complexes; Organometallic chemistry

1. Introduction

This review summarizes the progress in organo-*f*-element chemistry during the years 2003 and 2004. "Researches on non-classical organolanthanide chemistry" have been highlighted by Lappert and co-workers in 2003 [1]. A review entitled: "Product class 12: organometallic complexes of scandium, yttrium and the lanthanides" was published by Hou and Wakatsuki in 2003 [2].

2. Lanthanides

2.1. Lanthanide carbonyls

A comparative density functional study on metal–ligand (M–L) interactions has been performed on $X_3Ln(CO)$ (X = F, I; Ln = La, Nd) species including scalar relativistic effects by means of the zero-order regular approximation (ZORA) Hamiltonian. The role of the halogen atoms in modeling the M–L interactions has been discussed for the π-ligand CO [3,4]. The equilibrium geometry for the low-lying high-spin electronic state of ScCO was studied with the ab initio method. Restricted Hartree-Fock, multireference configuration interactions, and perturbation calculations were done employing flexible basis sets. The equilibrium geometry of the ScCO molecule was found to be linear [5].

2.2. Lanthanide hydrocarbyls

Whereas complexes of unsubstituted and substituted cyclopentadienyl ligands represent the vast majority of all published compounds in organolanthanide chemistry, examples of isolated and fully characterized (including X-ray structural analyses) compounds containing only σ-bonded alkyl and aryl ligand are still fairly rare. The first structurally characterized homoleptic lanthanide alkyls became available through the use of bulky mono-, bis- and tris(trimethylsilyl)-substituted methyl ligands. Simple unsolvated alkyls of the rare earth elements have not been synthesized until 2004.

An ab initio study on the reaction of the ground state (3D) and the excited state (1D) of Sc^+ with methane leading to Sc^+-CH_2 and H_2 as well as with ethane and propane has been performed [6,7]. Related studies concerned the reaction of yttrium with cyclopropane [8].

2.2.1. Neutral homoleptic compounds

Reaction of 2 equiv. of $KN(SiMe_3)_2$ and a mixture of $CH_2(Ph_2P{=}NC_6H_2Me_3\text{-}2,4,6)_2$ and SmI_2 in THF resulted in formation of the stable samarium dialkyl $Sm[CH(Ph_2PNC_6H_2Me_3\text{-}2,4,6)_2]_2$ without additional solvent coordination. The deep purple-black crystals were isolated in 72% yield and structurally characterized by X-ray methods (Fig. 1). The two bis(phosphinimino)methanide ligands act as tridentate donors and, as a consequence, the samarium center is six-coordinate [9].

Intermediates containing Sc–C bonds have also been discussed for the reaction mechanism of CO_2 hydrogenation to formic acid in the presence of scandium oxide [10]. The structural and electronic properties of $LnMe_3$ species have been studied by DFT calculations [11] as well as electron localization function studies [12]. DFT calculations have also been carried out on the compounds $Ln[CH(SiR_2R')(SiR_3)]_3$ for Ln = La, Sm and (i) R = R′ = Me, (ii) R = H, R′ = Me, and (iii) R = R′ = H. The results were compared with the X-ray structures that are available from the literature for both metals and R = R′ = Me. The calculations correctly reproduced the experimental structural features in these complexes exhibiting the peculiar pyramidal coordination geometry. The results show significant increases in the Si–C bond lengths associated with β-Si–C agostic interactions, whereas little structural changes were found for γ-C–H agostic interactions. The latter are in fact repulsive [13]. Recent

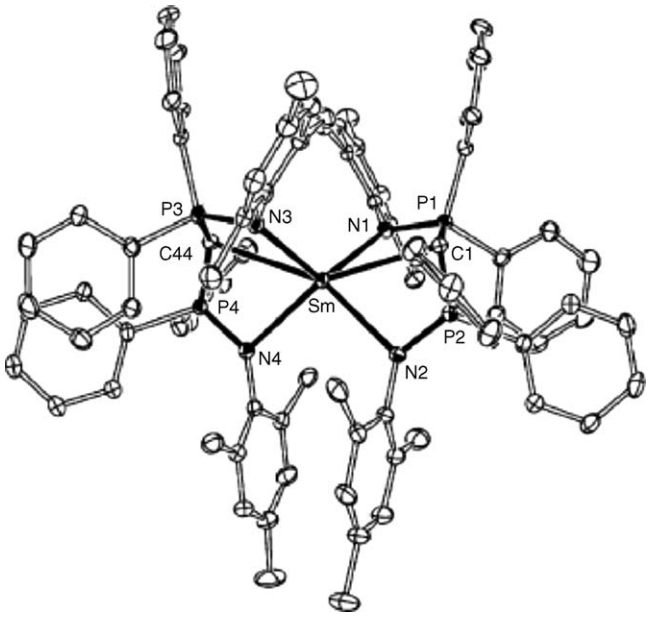

Fig. 1. Molecular structure of Sm[CH($Ph_2PNC_6H_2Me_3$-2,4,6)$_2$]$_2$ [9].

DFT calculations showed that La[CH($SiMe_3$)$_2$]$_3$, whose X-ray structure had previously been determined, should be considered as having a β-agostic Si–C bond and not a γ-agostic C–H bond [14]. Large transparent single-crystals of Ln[CH($SiMe_3$)$_2$]$_3$ (Ln = Pr, Nd, Sm) were obtained by slowly lowering the temperature of nearly saturated solutions in *n*-pentane, isopentane or methylcyclohexane from −5 to −40 °C within 3 days [15].

Still very little is known about the higher homologues of the homoleptic lanthanide alkyls, i.e. germyls, stannyls, etc. Reactions of bis(triphenylmethyl)ytterbium and bis(triphenylgermyl)ytterbium with $HgCl_2$, $BiPh_3$, I_2, Bu^tOH, HC≡CPh, and CpH have been studied [16].

2.2.2. Heteroleptic compounds

Theoretical investigations on lanthanide alkyls have been published by Eisenstein and co-workers under the title "Lanthanide complexes: electronic structure and H–H, C–H, and Si–H bond activation from a DFT perspective" [17].

The dimerization, unimolecular methane ejection, and bimolecular methane metathesis reactions of L_2LnMe species (L = H, Cl, Cp, Cp^*; Ln = Sc, Y, Lu) have been modeled at the density functional level (B3LYP) using a relativistic effective core potential basis set [18]. The use of very bulky terphenyl-type ligands allowed the isolation and structural characterization of several monoaryllanthanide dihalides (Scheme 1) [19].

Reaction of LiDpp (Dpp = 2,6-diphenylphenyl) with $SmCl_3$ in THF afforded the *ate*-complex (Dpp)$_2$SmCl(μ-Cl)Li(THF)$_3$ (Fig. 2) [20] while with the 2,6-di(*o*-anisyl)phenyl ligand (=Danip) several organolanthanide amides such as DanipYb[N($SiMe_3$)$_2$]$_2$ and DanipLn[N($SiMe_2H$)$_2$]$_2$ (Ln = Sm, Yb) have been isolated and structurally characterized. Fig. 3 depicts the molecular structure of DanipYb[N($SiMe_3$)$_2$]$_2$ as a typical example [21].

The homoleptic alkyls Ln[CH($SiMe_3$)$_2$]$_3$ (Ln = Y, Ce) react with nitriles under formation of adducts rather

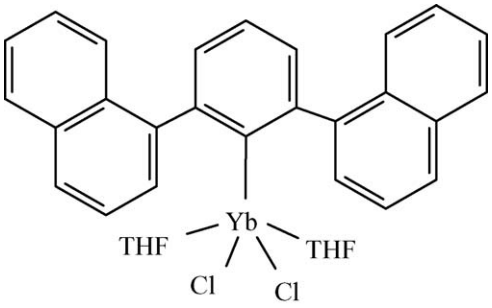

Scheme 1.

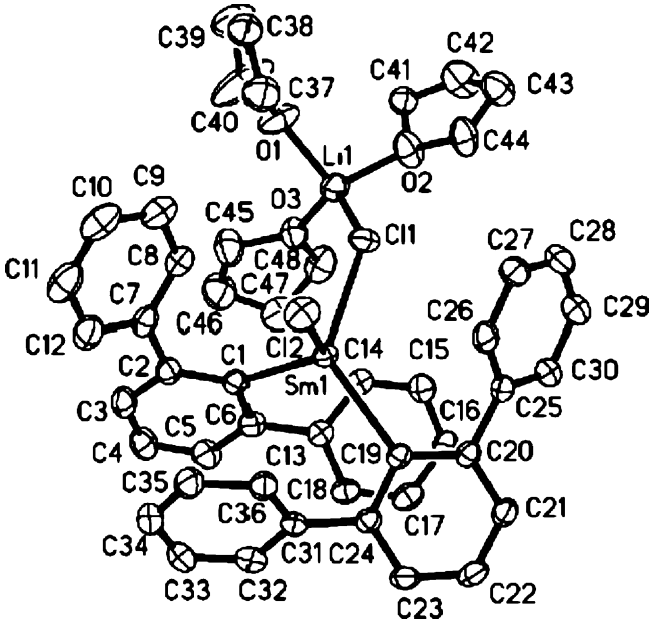

Fig. 2. Molecular structure of (Dpp)$_2$SmCl(μ-Cl)Li(THF)$_3$ [20].

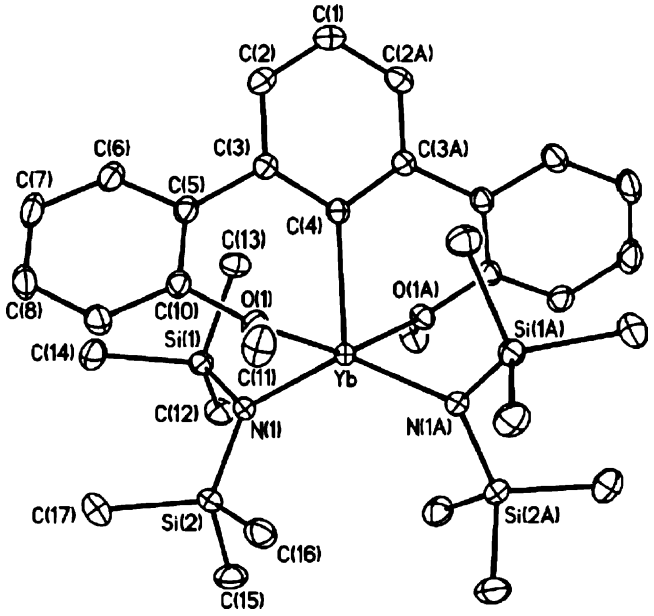

Fig. 3. Molecular structure of DanipYb[N($SiMe_3$)$_2$]$_2$ [21].

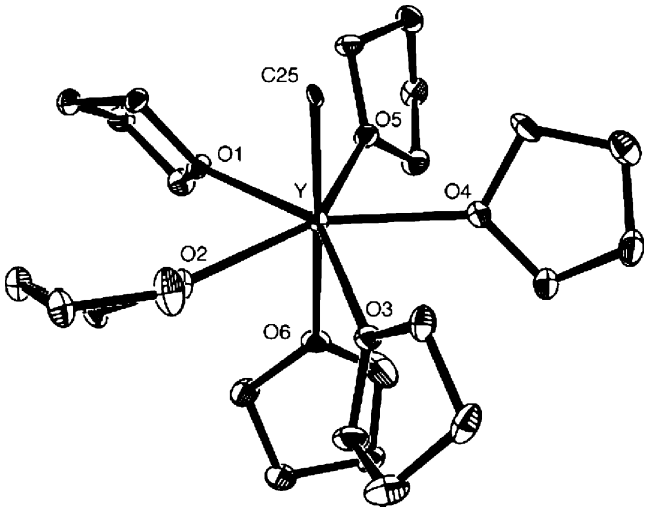

Fig. 4. Molecular structure of the cation in $[YMe(THF)_6][BPh_4]_2$ [24].

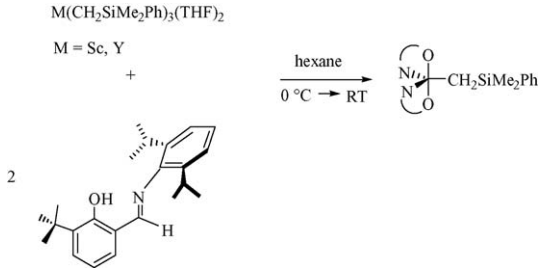

Scheme 2.

than β-diketiminato-metal insertion products [22]. In the absence of $B(C_6X_5)_3$ the thermally stable trialkyls (12-crown-4)$Ln(CH_2SiMe_3)_3$ (Ln = Sc, Y, Sm, Gd, Tb, Dy, Ho, Er, Tm, Yb, Lu) can be isolated, of which the yttrium complex was structurally characterized [23]. The unusual cationic yttrium alkyl complexes $[YMe(THF)_6][BPh_4]_2$ and $[Y(CH_2SiMe_3)_2(THF)_4][Al(CH_2SiMe_3)_4]$ have been synthesized and structurally characterized. The cationic portion of $[YMe(THF)_6][BPh_4]_2$ is shown in Fig. 4. The structure determination revealed a pentagonal bipyramidal coordination geometry around the yttrium center with the methyl group in the apical position. The Y–C bond length is 2.418(3) Å [24].

A series of bis(salicylaldiminato) mono-alkyls of scandium and yttrium has been prepared (Scheme 2) [25].

Chelating diamides of the type $[ArN(CH_2)_xNAr]^{2-}$ have been shown to be highly useful ligands for the stabilization of yttrium alkyl and hydride complexes [26].

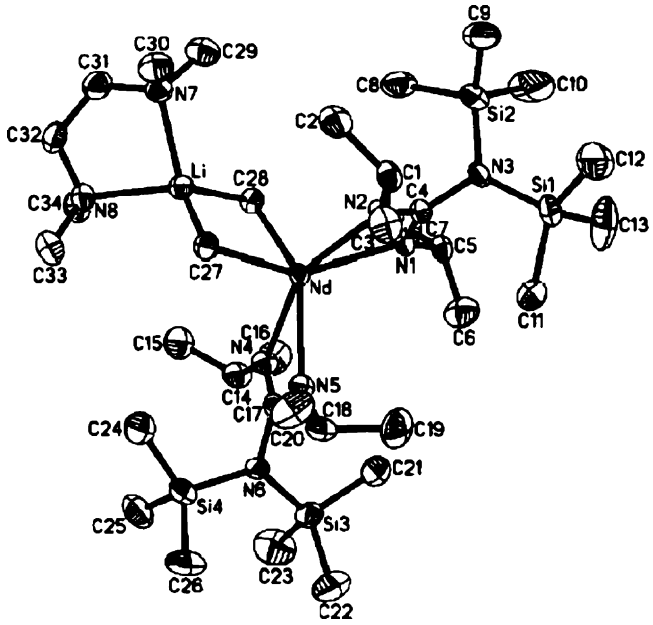

Fig. 5. Molecular structure of $[(Me_3Si)_2NC(NPr^i)_2]_2Nd(\mu\text{-}Me)_2Li(TMEDA)$ [27].

Guanidinate lanthanide methyl complexes of the type $[(Me_3Si)_2NC(NPr^i)_2]_2Ln(\mu\text{-}Me)_2Li(TMEDA)$ and $[(Me_3Si)_2NC(NPr^i)_2]_2Ln(\mu\text{-}Me)_2Li(THF)_2$ (Ln = Nd, Yb) are accessible in good yields by reacting the chloro-bridged precursors with methyllithium (Scheme 3). Fig. 5 illustrates the molecular structure of the neodymium/TMEDA derivative [27].

β-Diketiminato ("nacnac") ligands are becoming increasingly popular as ancillary ligands in organolanthanide chemistry [22,28–30]. Scheme 4 summarizes typical synthetic routes leading to diorganoscandium complexes stabilized by bulky β-diketiminato ligands [31,32].

A most remarkable achievement was the stabilization of a diamagnetic Sc^IBr molecule in a sandwich-like structure. The reaction of the β-diketiminato scandium derivative $LScBr_2$ ($L = Et_2NCH_2CH_2NC(Me)CHC(Me)NCH_2CH_2NEt_2$) with $(C_3H_5)MgBr$ gave the unexpected blue-green scandium complex $(LMgBr)_2ScBr$, whose structure was established by X-ray analysis, liquid and solid-state NMR, EPR, UV–vis, and magnetic measurements as well as DFT calculations. Correlation of all results led to the conclusion that the formal oxidation state of scandium in this complex is *one* (Sc(I)) having no unpaired electrons [33]. The same tetradentate β-diketiminato ligand has been utilized for the synthesis of $LLnBr_2$ (Ln = Y, Sm,

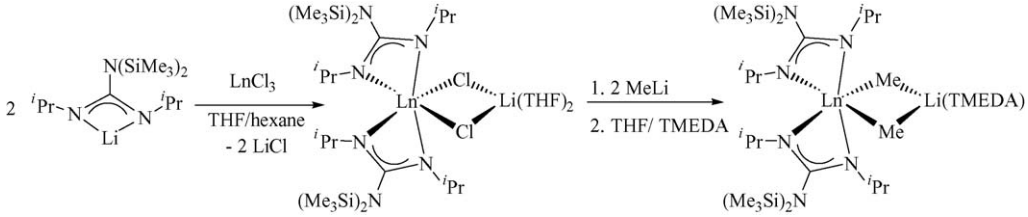

Scheme 3.

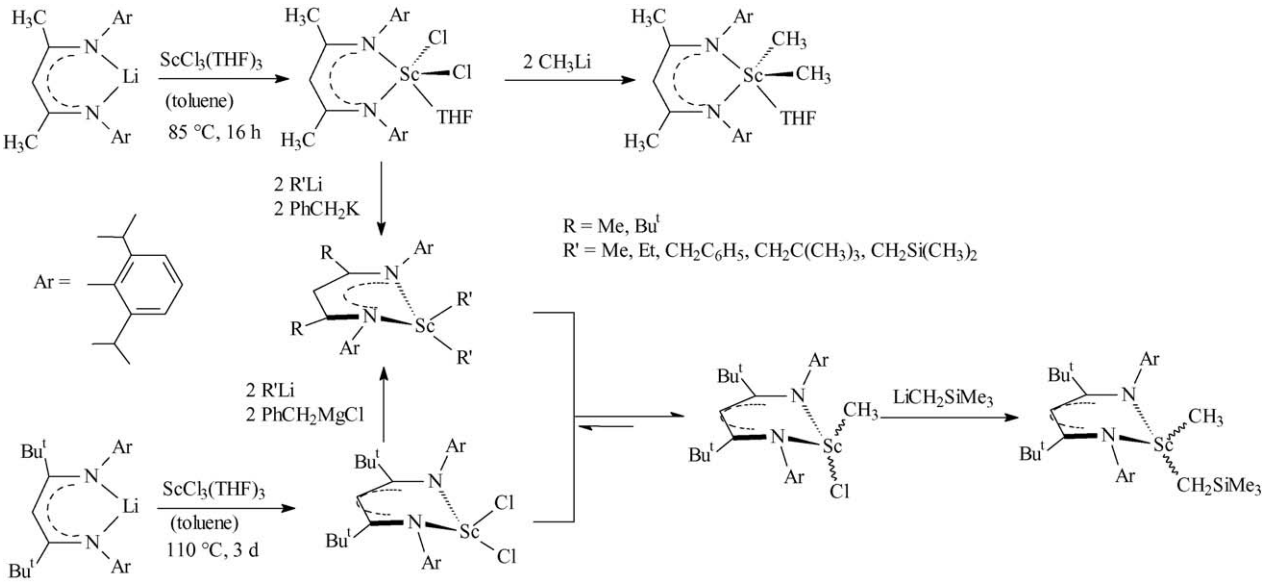

Scheme 4.

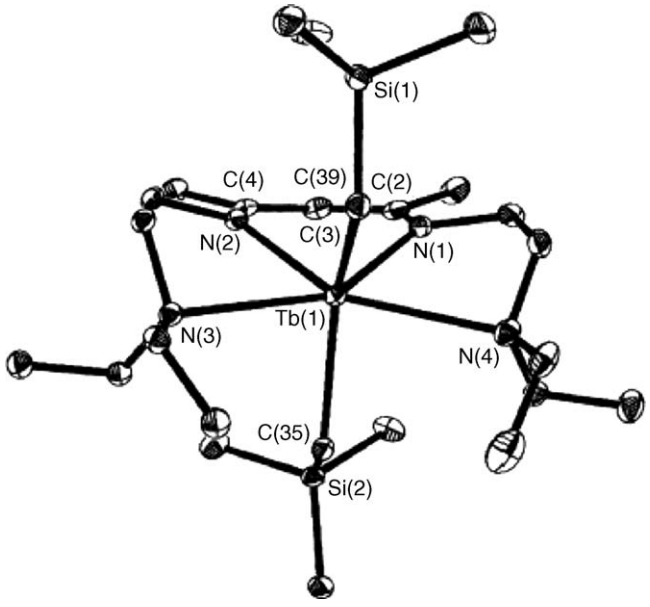

Fig. 6. Molecular structure of $LTb(CH_2SiMe_3)_2$ ($L = Et_2NCH_2CH_2NC(Me)CHC(Me)NCH_2CH_2NEt_2$) [34].

Er, Yb) and the bis(alkyl)terbium complex $LTb(CH_2SiMe_3)_2$ (Fig. 6) [34,35]. Silyl-substituted β-diketiminato ligands have been shown to be highly useful for the preparation of divalent ytterbium complexes [36].

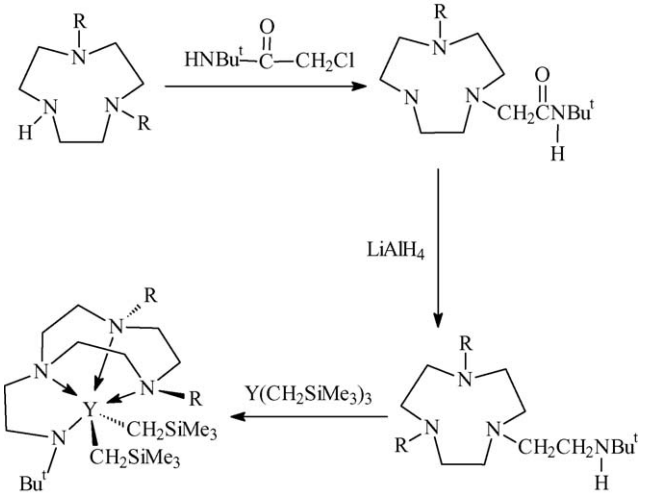

Scheme 6.

The neutral trialkyl complexes $(Me_3[9]aneN_3)Ln(CH_2SiMe_3)_3$ (Ln = Sc, Y) were made by reacting the free ligand with $Ln(CH_2SiMe_3)_3(THF)_2$ (Scheme 5) [37].

Neutral and cationic yttrium and lanthanum alkyl complexes have also been prepared with related linked 1,4,7-triazacyclononane-amide monoanionic ancillary ligands as illustrated in Scheme 6. As a typical example, the molecular

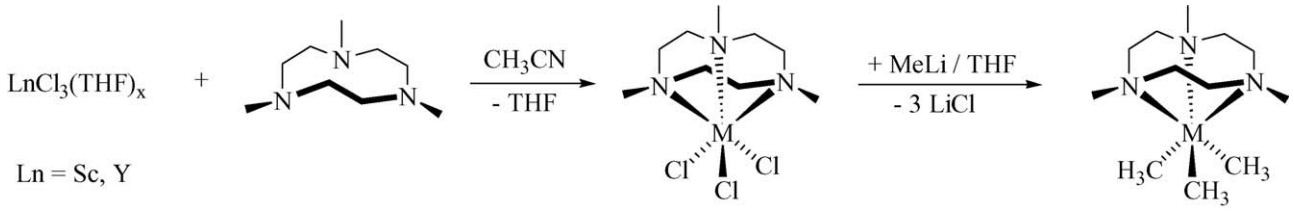

Scheme 5.

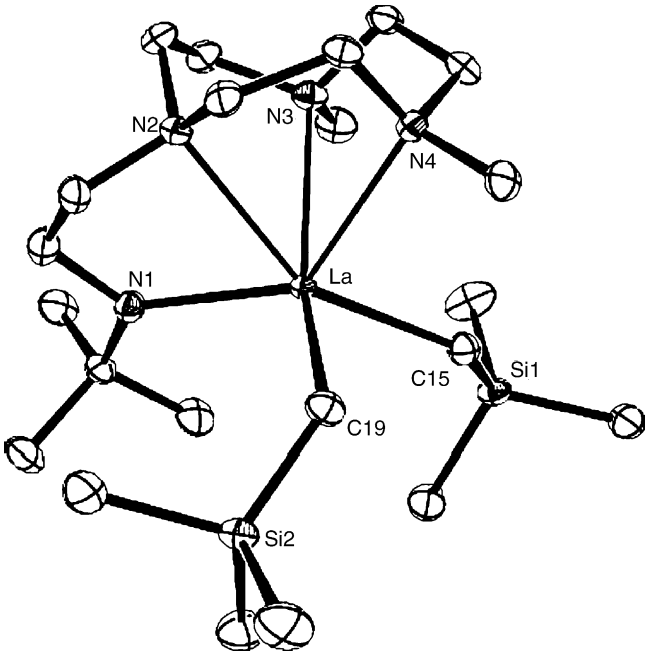

Fig. 7. Molecular structure of $[Me_2TACN(CH_2)_2NBu^t]La(CH_2SiMe_3)_2$ [38].

structure of $[Me_2TACN(CH_2)_2NBu^t]La(CH_2SiMe_3)_2$ is illustrated in Fig. 7 [38].

Related new ligand sets for the stabilization of scandium and yttrium alkyls have been introduced [39]. Also closely related is a series of triamino-amide ligands, which has been utilized to stabilize yttrium bis(alkyl) complexes [40]. A tetradentate bis(phenoxide) ligand has been used to stabilize an yttrium alkyl complex of the type $[L]Y(CH_2SiMe_3)(THF)$ [41].

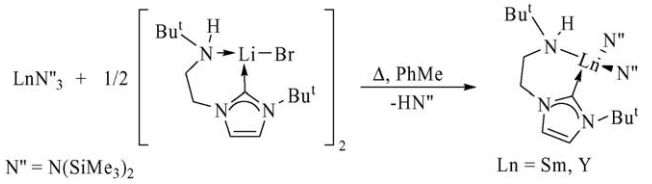

Scheme 8.

Heteroleptic lanthanide alkyls containing one or two CH_2SiMe_3 ligands have also been stabilized with the use of pyrrolylaldiminato ligands [42], chelating tridentate diamide ligands [43], bulky anilido-imine ligands [44], sterically demanding benzamidinate ligands [45], multidentate anilido-pyridine-imine ligands [46], and C_2-symmetric fluorous diamino-dialkoxide ligands [47]. The use of the neutral tris(pyrazolyl)*methane* ligand $HC(Me_2pz)_3$ allowed the synthesis of the trialkyls $[HC(Me_2pz)_3]Ln(CH_2SiMe_3)_3$ (Ln = Sc, Y) directly from $Ln(CH_2SiMe_3)_3(THF)_2$. Further reaction of the trialkyls with $[CPh_3][B(C_6F_5)_4]$ afforded the cationic species $[\{HC(Me_2pz)_3\}Ln(CH_2SiMe_3)_2(THF)][B(C_6F_5)_4]$ [37].

Protonation of a heteroleptic, cyclometalated lanthanum phosphide complex with $[NEt_3H][BPh_4]$ was shown to occur at the La–P and not at the La–C bond, which allowed the isolation of a cationic lanthanum alkyl complex as shown in Scheme 7 [48,49].

Lanthanide complexes containing anionic amido *N*-heterocyclic carbenes as ligands have been synthesized as illustrated in Scheme 8. Fig. 8 depicts the molecular structure of the samarium derivative. The geometry around Sm is *pseudo*-tetrahedral, with one possible close contact with a silicon atom suggested by a Sm–Si distance of 3.3334(5) Å. With 2.588(2) Å the $Sm–C_{carbene}$ distance is exceptionally short [50].

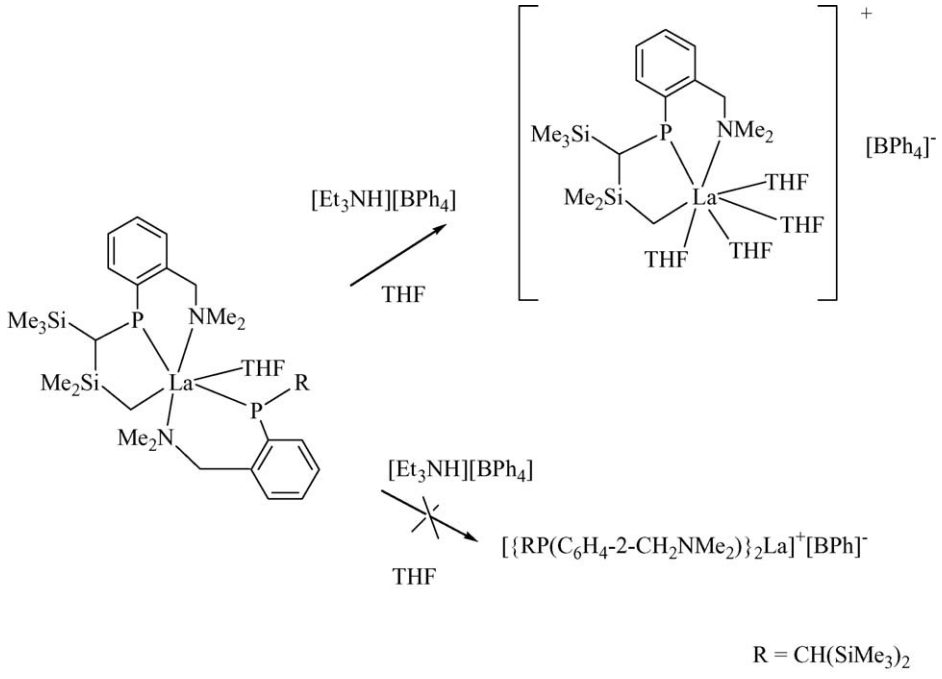

Scheme 7.

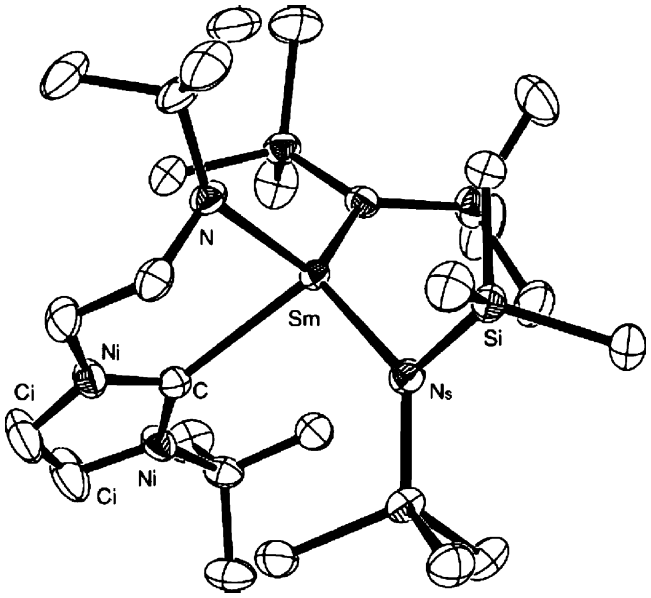

Fig. 8. Molecular structure of $[Bu^tC_3H_2N_2(CH_2)_2NBu^t]Sm[N(SiMe_3)_2]_2$ [50].

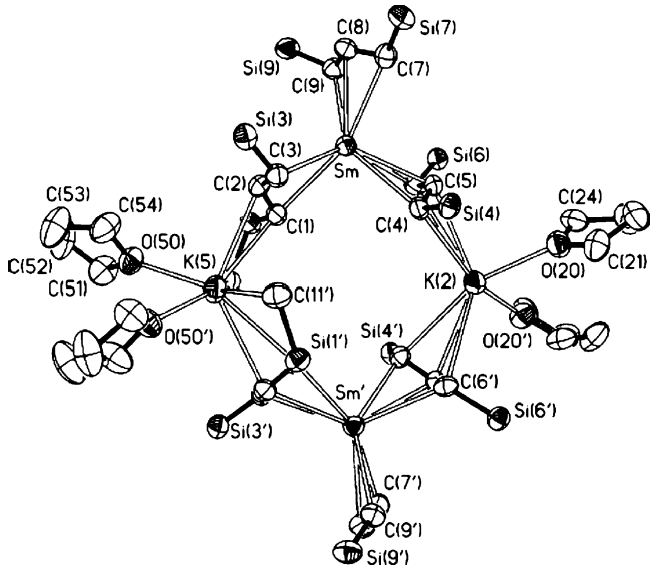

Fig. 9. Molecular structure of $[\mu\text{-}K(THF)_2]_2[Sm\{C_3H_3(SiMe_3)_2\}_3]_2$ [53].

2.3. Lanthanide alkenyl and alkynyl compounds

Reaction pathways for the Y-induced acetylene (HCCH)–vinylidene (CCH_2) rearrangement in the gas phase have been identified by density functional and coupled cluster calculations with basis set extrapolations [51]. The ytterbium(II) phenylethynyl complex $(PhC{\equiv}C)_2Yb(THF)_4$ reacts with Me_3SiCl, Ph_3GeCl, and Ph_3SnCl to give a mixture of $(PhC{\equiv}C)YbCl(THF)_2$ and $YbCl_2(THF)_2$ [52].

2.4. Lanthanide allyls

Recent contributions to the chemistry of lanthanide allyl complexes addressed the use of substituted allyl ligands [53–55]. The reaction of the bulky allyl anion $[1,3\text{-}C_3H_3(SiMe_3)_2]^-$ with $SmI_2(THF)_2$ gave the allyl-bridged dimer $[\mu\text{-}K(THF)_2]_2[Sm\{C_3H_3(SiMe_3)_2\}_3]_2$ as dark green crystals in 62% yield (Scheme 9) as the first structurally authenticated Sm(II) allyl complex. The unusual molecular structure of this compound is highlighted in Fig. 9 [53].

Similar treatment of $NdI_3(THF)_{3.5}$ with 2 equiv. of the potassium salt gave a mixture of products, from which the dark green $[1,3\text{-}C_3H_3(SiMe_3)_2]_2NdI(THF)_2$ (Fig. 10) could be isolated in 71% yield [54,55].

A new class of anionic allyl-lanthanide complexes of the type $[K(THF)_4][\{1,3\text{-}C_3H_3(SiMe_3)_2\}_3LnI]$ (Ln = Ce, Pr, Nd, Gd, Tb, Dy, Er) have been prepared and isolated by reaction of

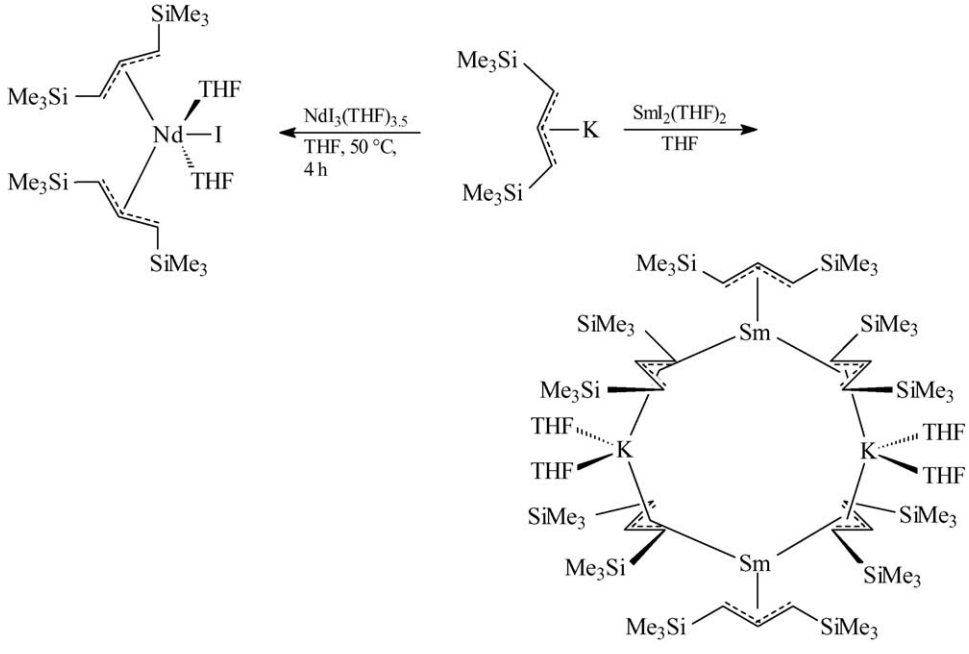

Scheme 9.

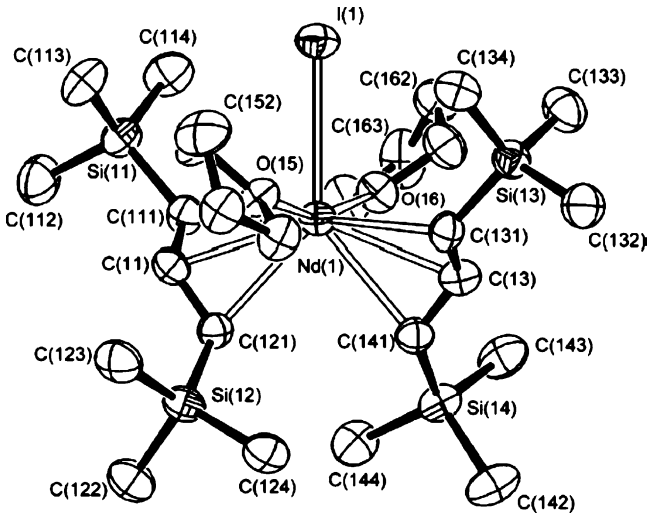

Fig. 10. Molecular structure of $[1,3\text{-}C_3H_3(SiMe_3)_2]_2NdI(THF)_2$ [55].

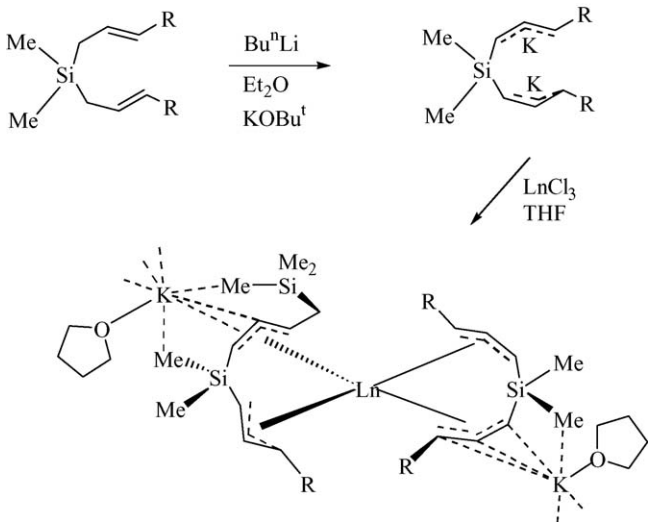

Scheme 10.

3 equiv. of the 1,3-bis(trimethylsilyl)allyl anion with LnI_3. The neutral complex $[1,3\text{-}C_3H_3(SiMe_3)_2]_3Nd(THF)$ (green crystals, Fig. 11) has been isolated from the reaction of the triflate precursor $Nd(O_3SCF_3)_3$ with 3 equiv. of $K[1,3\text{-}C_3H_3(SiMe_3)_2]$. These complexes have been structurally characterized using single crystal X-ray diffraction [56].

The synthetic route has been extended to the preparation of the first *ansa*-bis(allyl)lanthanide complexes (Scheme 10). The crystal structure determination of the La derivative (Fig. 12) revealed the presence of a coordination polymer with potassium bridging two allyl moieties of two neighboring lanthanide units and close K···CH_3Si contacts [57].

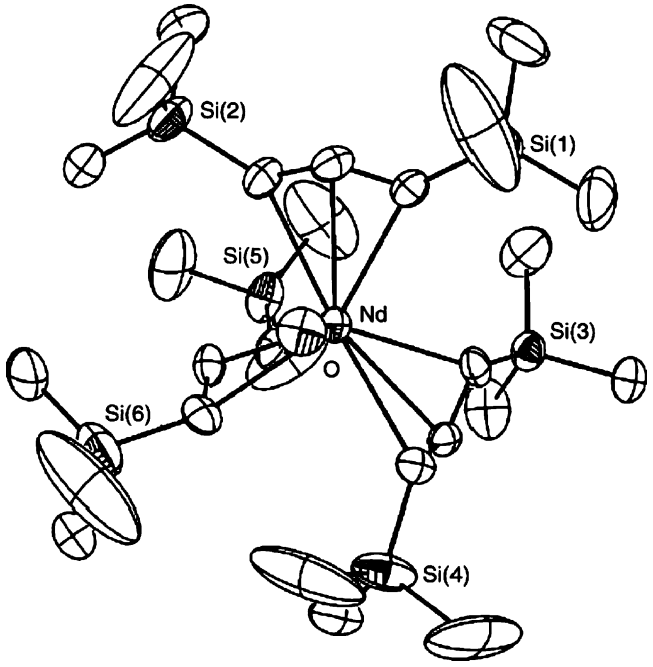

Fig. 11. Molecular structure of $[1,3\text{-}C_3H_3(SiMe_3)_2]_3Nd(THF)$ [56].

2.5. Lanthanide cyclopentadienyl compounds

2.5.1. CpLnX compounds

Reactions of the aminosilylcyclopentadienes $(C_5Me_4H)SiMe_2NHR$ (R = Et, allyl, Pr^n, Bu^t) with $YbI_2(THF)_2$ in the presence of 2 equiv. of potassium 1,2-diphenylethylenide in THF at room temperature gave the diamagnetic half-sandwich complexes $[(C_5Me_4SiMe_2NHR)YbL_n(\mu\text{-}I)]_2$ (L = THF, $n = 2$; L = DME, $n = 1$) (Scheme 11). The *t*-butylamido complex was characterized by X-ray structural analysis as a binuclear complex containing a non-chelating aminosilylcyclopentadienyl ligand. In pyridine partial dissociation into a mononuclear species occurs (Scheme 11) [58].

Exemplary synthetic routes leading to σ-alkyl complexes containing a silylene-linked cyclopentadienyl-phosphido ligand are outlined in Scheme 12. These complexes represent the first examples of rare earth alkyl and hydride complexes bearing cyclopentadienyl-phosphido ligands, which are in sharp contrast both structurally and chemically with the analogous cyclopentadienyl-amido complexes. As can be seen in Fig. 13,

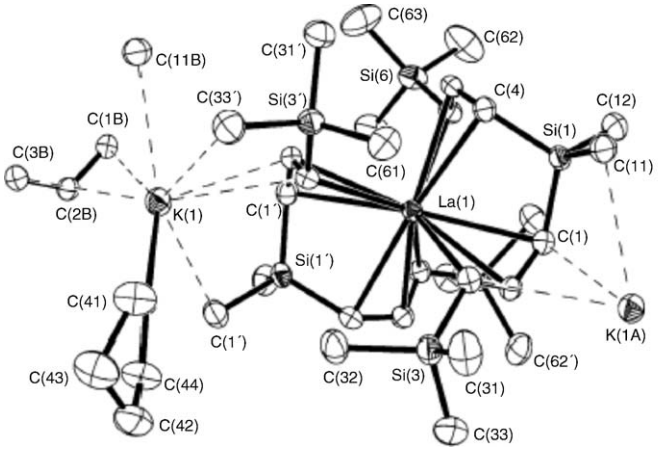

Fig. 12. Molecular structure of $[La\{(\eta^3\text{-}C_3H_3SiMe_3)_2SiMe_2\}_2\{\mu\text{-}K(THF)\}\cdot 0.5THF]_\infty$ [57].

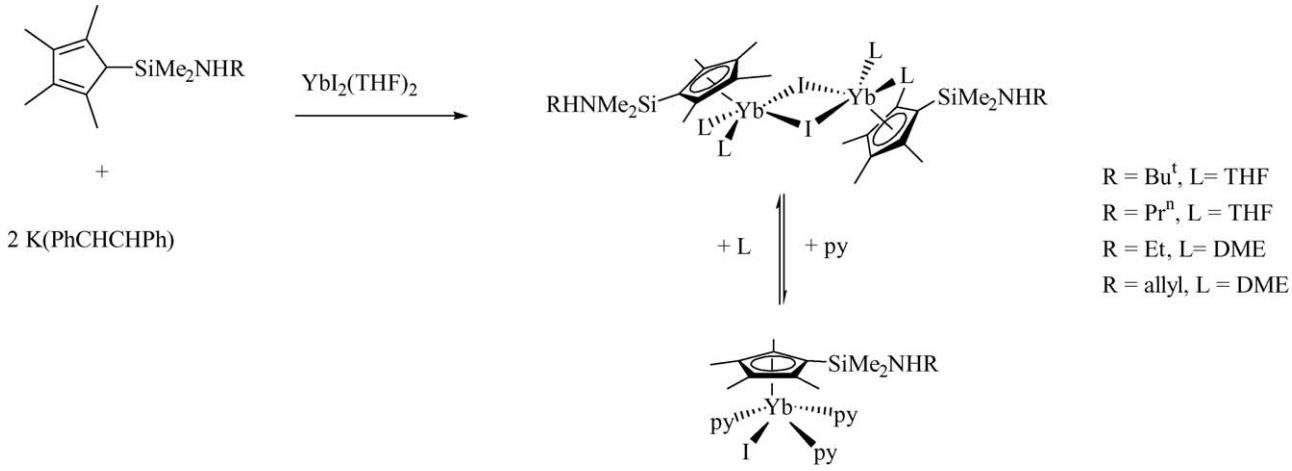

Scheme 11.

the Lu(III) center in the intermediate bis(alkyl) complex is bonded to one cyclopentadienyl unit, two CH_2SiMe_3 ligands, and one THF ligand. The main difference with respect to the cyclopentadienyl-amide analogues is that the PHAr unit is directed away from the metal center. An X-ray structure analysis of the thermolysis product confirmed the metallation at both the P atom and a methyl group of an *ortho*-Bu^t group in the PHAr unit (Fig. 14). The Y–P distance is 2.789(2) Å, and the Y–C(σ) bond length is 2.363(5) Å [59].

A theoretical study of divalent lanthanide complexes of a triazacyclononane-functionalized tetramethylcyclopentadienyl ligand has been reported [60]. Donor-functionalized amide ligands such as *N*-(methoxyphenyl)-*N*-(trimethylsilyl)amide have been employed as ancillary ligands in the preparation of dimeric mono(cyclopentadienyl)lanthanide chloride complexes. As a representative example, the molecular structure of [(*o*-$MeOC_6H_4NSiMe_3$)(MeC_5H_4)Yb(μ-Cl)]$_2$ is shown in Fig. 15 [61].

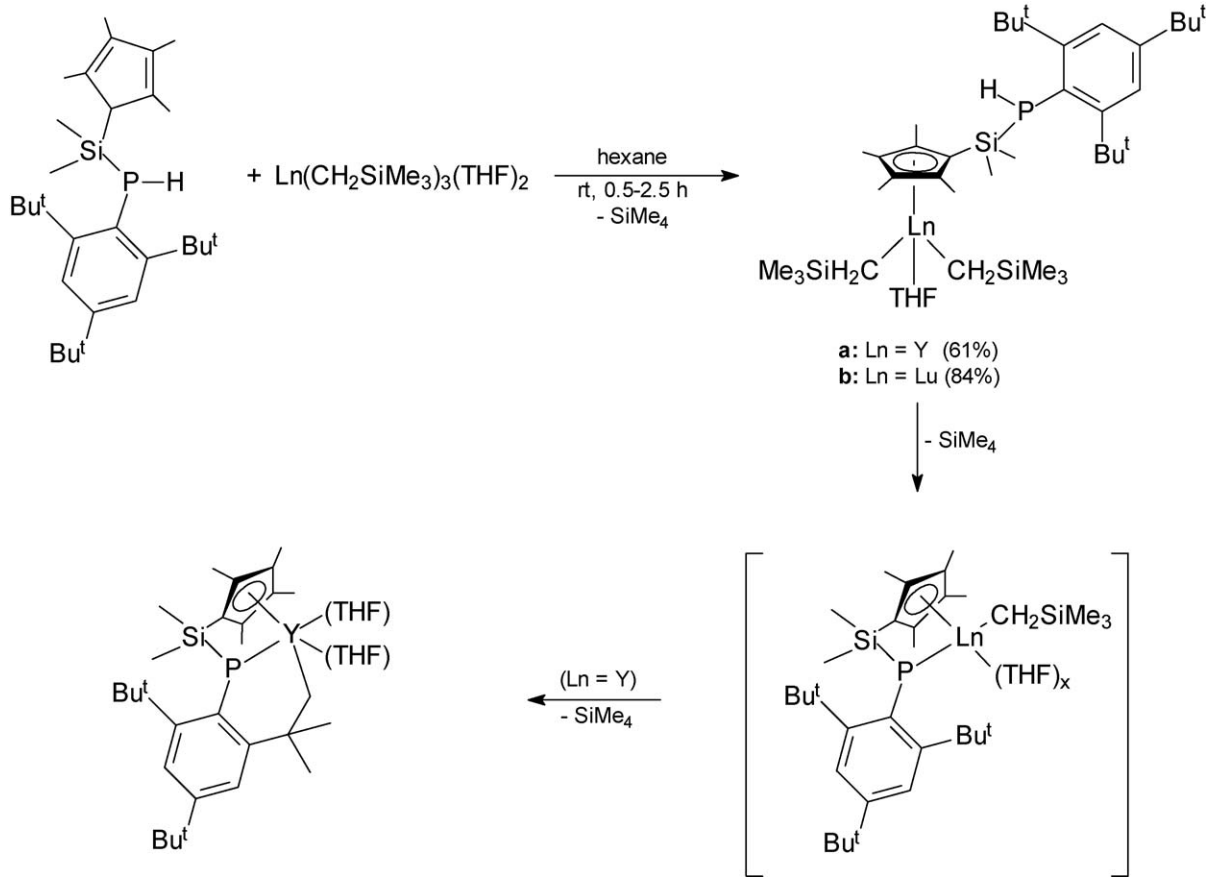

Scheme 12.

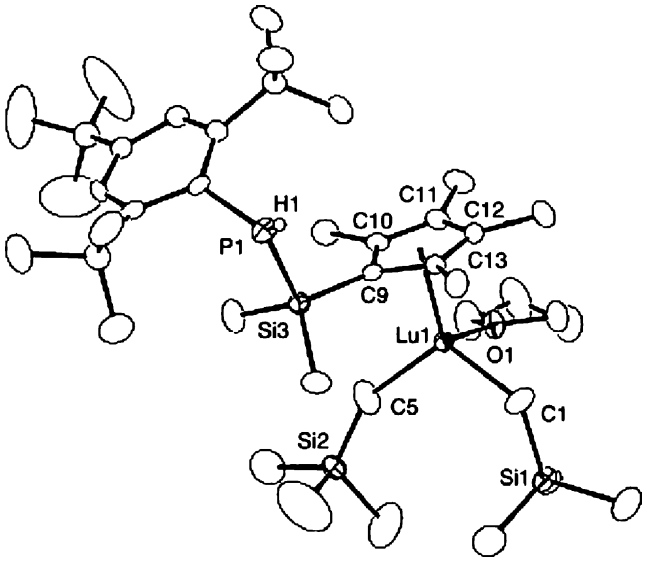

Fig. 13. Molecular structure of $[Me_2Si(C_5Me_4)P(H)Ar]Lu(CH_2SiMe_3)_2(THF)$ ($Ar = C_6H_2Bu^t_3$-2,4,6) [59].

2.5.2. Cp_2Ln compounds

The synthesis and characterization of a new class of divalent lanthanide complexes, $[Li(DME)_3]_2[\{C_5H_4(CMe_2Ph)\}_2Ln(\mu\text{-}X)]_2$ (Ln = Sm, X = I (black crystals); Ln = Yb, X = Cl (dark red crystals)) has been reported. In the solid state both complexes consist of two $[Li(DME)_3]^+$ cations and halide-bridged dimeric anions (Fig. 16) [62].

The tethered olefin cyclopentadienyl ligand $[C_5Me_4SiMe_2(CH_2CH{=}CH_2)]^-$ forms unsolvated metallocenes, $[C_5Me_4SiMe_2(CH_2CH{=}CH_2)]_2Ln$ (Ln = Sm, Eu, Yb), from $K[C_5Me_4SiMe_2(CH_2CH{=}CH_2)]$ and $LnI_2(THF)_2$ in good yield. In the solid state each complex has both tethered olefins oriented toward the Ln metal center with the Ln–C (terminal alkene carbon) distances 0.2–0.3 Å shorter than the Ln–C (internal alkene carbon) distances. Fig. 17 illustrates the molecular structure of the europium derivative as a representative example [63].

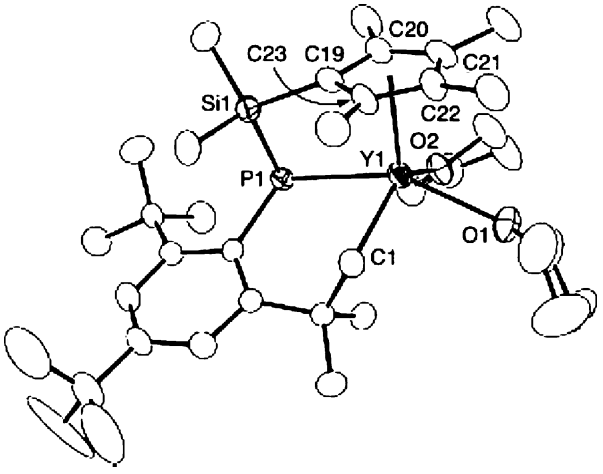

Fig. 14. Molecular structure of $[Me_2Si(C_5Me_4)PAr']Lu(CH_2SiMe_3)_2(THF)$ ($Ar' = CH_2CMe_2C_6H_2Bu^t_2$-2,4,6) [59].

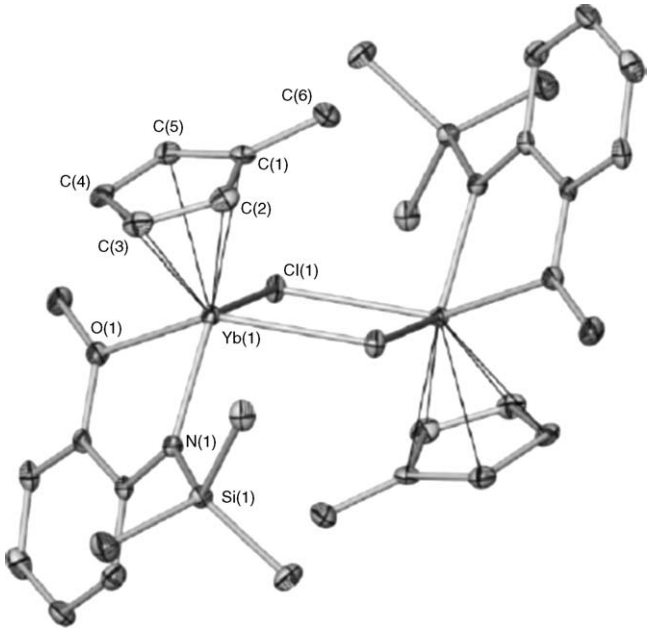

Fig. 15. Molecular structure of $[(o\text{-}MeOC_6H_4NSiMe_3)(MeC_5H_4)Yb(\mu\text{-}Cl)]_2$ [61].

2.5.3. $CpLnX_2$ compounds

The reduced lanthanide iodides of the composition LnI_x (Ln = Sc, Y, La, Ce, Pr, Nd, Gd, Dy, Ho, Er; $x < 3$), obtained by the reaction of an excess of the appropriate metal with iodine at high temperature, react with cyclopentadiene to afford the complexes $CpLnI_2(THF)_3$ with yields up to 60% [64]. $CpTbCl_2$ has been reported to form adducts with pyrazole and triphenylphosphine [65].

Mono(cyclopentadienyl)lanthanide diiodides are readily accessible utilizing the very bulky 1,2,4-tris(trimethylsilyl)-

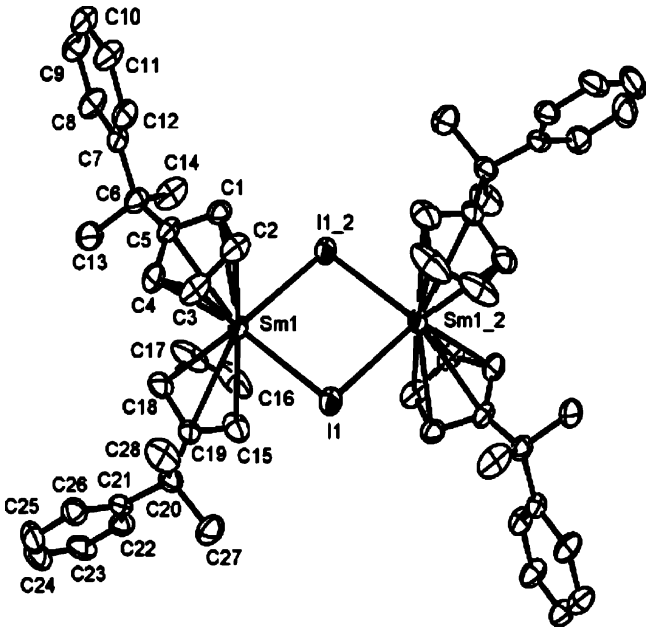

Fig. 16. Molecular structure of the $[\{C_5H_4(CMe_2Ph)\}_2Sm(\mu\text{-}X)]_2^{2-}$ dianion [62].

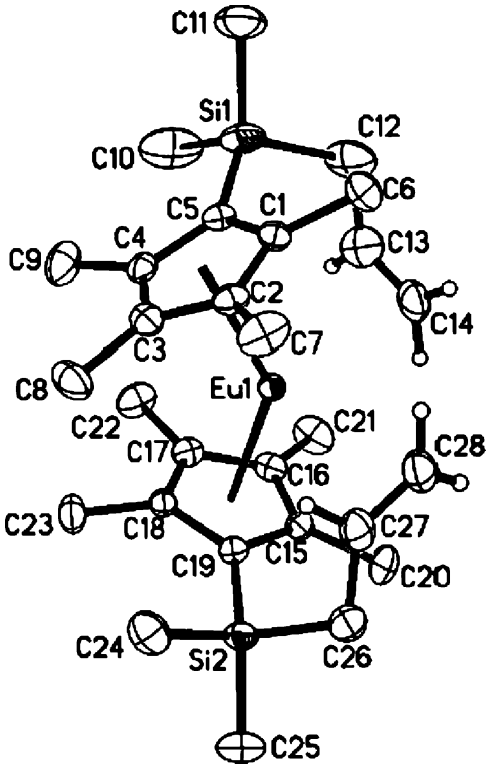

Fig. 17. Molecular structure of $[C_5Me_4SiMe_2(CH_2CH{=}CH_2)]_2Eu$ [63].

cyclopentadienyl ligand (=Cp‴). A typical example is depicted in Scheme 13 [66]. Cp‴LaI$_2$(THF)$_3$ also served as a useful starting material for the preparation of a series of mono(cyclopentadienyl)lanthanum anilido complexes. The molecular structure of Cp‴LaI(NHC$_6$H$_3$Me$_2$-2,6)(THF)$_2$ is shown in Fig. 18 [67].

Reduction of 2,5-di-*t*-butylcyclopentadienone with 2 equiv. of thulium diiodide in THF gave a binuclear thulium(III) complex containing a cyclopentadienyl oxide ligand, [η^5-C$_5$H$_2$Bu$^t_2$OTmI$_2$(THF)$_3$]TmI$_2$(THF)$_2$ as orange crystals in 76% yield [68].

The preparation and reaction chemistry of β-diketiminato ytterbium complexes containing an additional cyclopentadienyl ligand have been investigated. Reaction of Li[(DIPPh)$_2$nacnac] ((DIPPh)$_2$nacnac = *N*,*N*-diisopropylphenyl-2,4-pentanediimine anion) with 1 equiv. of anhydrous YbCl$_3$ in THF afforded the dark red monomeric complex [(DIPPh)$_2$nacnac]YbCl$_2$(THF)$_2$ in high yield. Further treatment of this complex with Na(C$_5$H$_4$Me) in a 1:1 molar ratio in THF gave the mixed-ligand ytterbium chloride (C$_5$H$_4$Me)[(DIPPh)$_2$nacnac]YbCl as red crystals in 84% yield. This compound readily undergoes

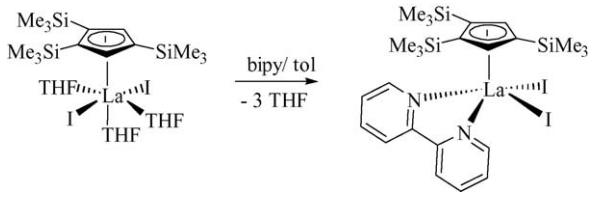

Scheme 13.

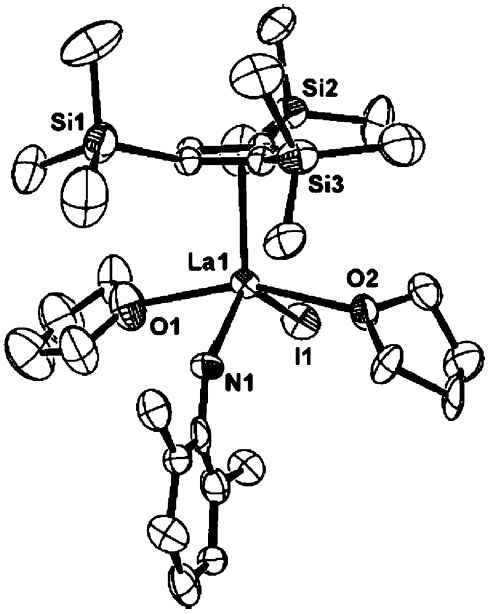

Fig. 18. Molecular structure of Cp‴LaI(NHC$_6$H$_3$Me$_2$-2,6)(THF)$_2$ [67].

metathesis reactions with LiNPh$_2$ and LiNPr$^i_2$ in THF to form the compounds (C$_5$H$_4$Me)[(DIPPh)$_2$nacnac]YbNPh$_2$ and (C$_5$H$_4$Me)[(DIPPh)$_2$nacnac]YbNPr$^i_2$, respectively [68–70]. Mono(cyclopentadienyl)lanthanide derivatives have also been isolated from reactions of Cp$_3$Ln with salicylaldehyde thiosemicarbazone [71]. The ytterbium complex Cp*Yb[N(PPh$_2$)$_2$]$_2$ contains two diphosphinoamide ligands in the coordination sphere of Sm (Fig. 19). The compound adopts a distorted square pyramidal conformation in the solid state with the diphosphinoamide ligands being both η^2-coordinated to the Yb center [72].

The synthesis of cyclopentadienyl lanthanide pyrazolate complexes and their reactivity towards dimethylsilicone has

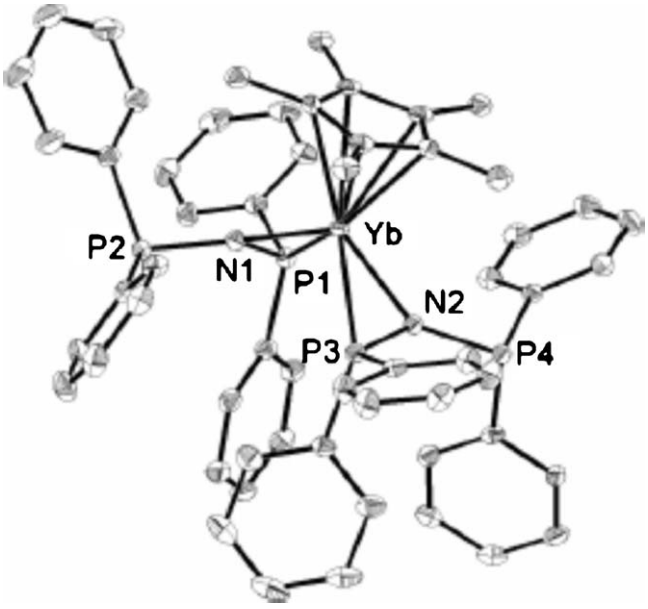

Fig. 19. Molecular structure of Cp*Yb[N(PPh$_2$)$_2$]$_2$ [72].

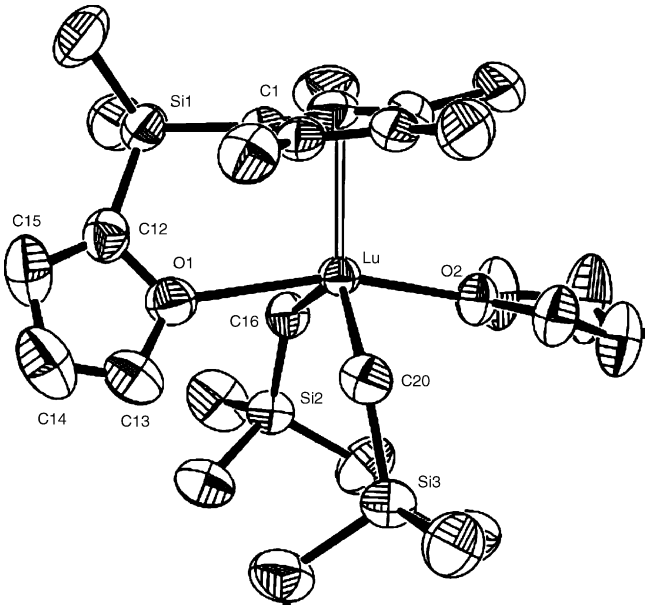

Fig. 20. Molecular structure of $[C_5Me_4SiMe_2(C_4H_3O\text{-}2)]Lu(CH_2SiMe_3)_2(THF)$ [74].

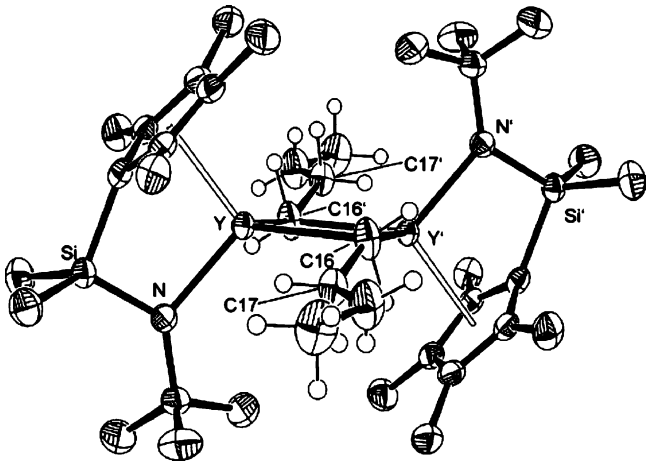

Fig. 21. Molecular structure of $[(\eta^5{:}\eta^1\text{-}C_5Me_4SiMe_2NBu^t)Y(\mu\text{-}CH_2CH_2CH_2CH_3)]_2$ [76].

been reported. Reactions of Cp_3Ln (Cp = Cp; Ln = Ho, Dy, Yb, Sm) with 2 equiv. of $HPzMe_2$ ($HPzMe_2$ = 3,5-dimethylpyrazole) in THF at room temperature yield complexes of the type $CpLn(PzMe_2)_2$ (Ln = Ho, Dy) and $Cp_2Yb(PzMe_2)(HpzMe_2)$ and $Sm(PzMe_2)_3$, respectively. Similar reactions have been carried out with the methylcyclopentadienyl lanthanide precursors $(C_5H_4Me)_3Ln$ (Ln = Nd, Gd, Dy) [73].

Rare earth metal bis(alkyls) of the type $[C_5Me_4SiMe_2(C_4H_3O\text{-}2)]Ln(CH_2SiMe_3)_2(THF)$ (Ln = Y, Lu; Fig. 20) have been prepared by σ-bond metathesis of $Ln(CH_2SiMe_3)_3(THF)$ with the 2-furyl-substituted tetramethylcyclopentadiene $(C_5Me_4H)SiMe_2(C_4H_3O\text{-}2)$ [74].

Similar *ortho*-metalation products have been obtained from reactions of $(\eta^5{:}\eta^1\text{-}C_5Me_4SiMe_2NBu^t)Y(CH_2SiMe_3)(THF)$ with anisole and 3- and 4-methylanisole [75]. Both the lutetium and ytterbium alkyl complexes were subjected to hydrogenolysis with dihydrogen or with phenylsilane in pentane at room temperature to give the dimeric hydrides $[(\eta^5{:}\eta^1\text{-}C_5Me_4SiMe_2NCMe_2R)Ln(THF)(\mu\text{-}H)]_2$ (Ln = Lu, Yb, Y) (Scheme 14). Because of the thermal instability of the alkyl complexes of lutetium and ytterbium, it proved advantageous to prepare the hydride complexes in a one-pot procedure without isolating the alkyl complexes [76].

The hydrido complex $[(\eta^5{:}\eta^1\text{-}C_5Me_4SiMe_2NBu^t)Y(THF)(\mu\text{-}H)]_2$ smoothly reacts with stoichiometric amounts of olefinic substrates such as ethylene, α-olefins, butadiene, and styrenes to give the corresponding alkyl or allyl complexes, respectively (Scheme 15). The molecular structure of the *n*-butyl-bridged dimer $[(\eta^5{:}\eta^1\text{-}C_5Me_4SiMe_2NBu^t)Y(\mu\text{-}CH_2CH_2CH_2CH_3)]_2$, prepared from *n*-butene, is shown in Fig. 21 [76].

This chemistry has also been extended to yttrium alkyl and hydrido complexes stabilized by tridentate-linked amidocyclopentadienyl ligands. A typical synthetic route is illustrated in Scheme 16. The molecular structures of both products are highlighted in Figs. 22 and 23. Especially remarkable is the isolation of a pure THF-free hydrido complex, which could be achieved by recrystallization of the crude product from heptane [77].

Synthetic routes leading to tetranuclear yttrium and lutetium hydride clusters have been worked out. The complexes are accessible by reacting precursors of the type $(C_5Me_4SiMe_2R)Ln(CH_2SiMe_3)_2(THF)$ (R = Me, Ph; Ln = Y, Lu) with either H_2 (Scheme 17) [78,79] or $PhSiH_3$ [80], and their reactivity has been studied [79,81,82]. This includes for example hydrogenation of carbon dioxide and aryl isocyanates [82]. The effective group potentials (EGP) method has been used for predicting the properties of the trinuclear hydride clusters $Cp_6Lu_3H_3$ and $Cp_6Lu_3H_4^-$ [83]. Related compounds have also been synthesized with the use of the $(C_5Me_4Pr^n)^-$ ligand [84].

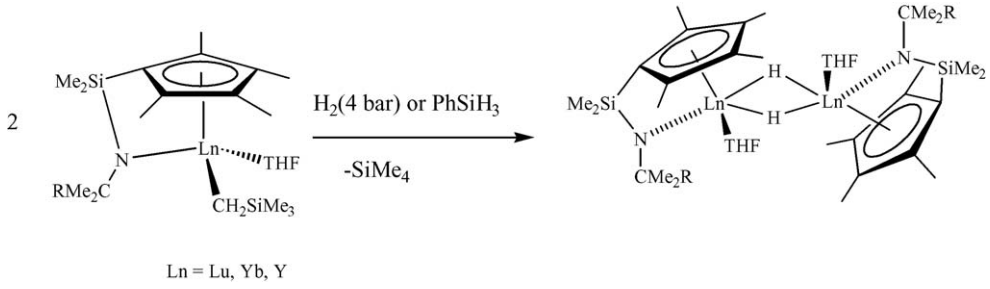

Ln = Lu, Yb, Y

Scheme 14.

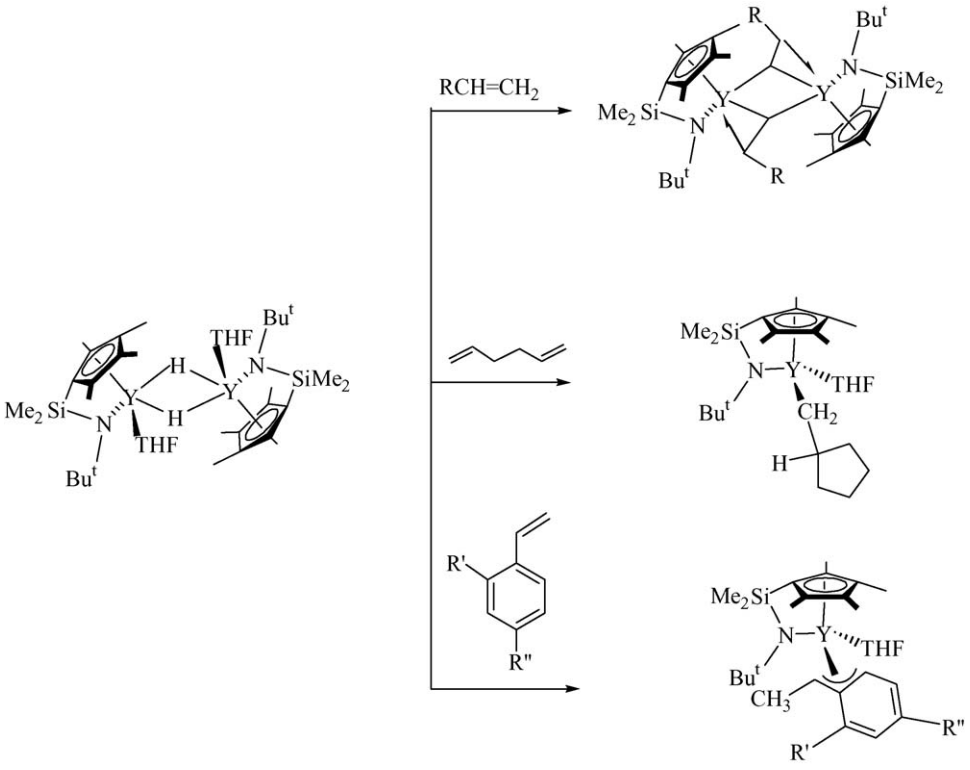

Scheme 15.

Fig. 24 shows an ORTEP-drawing of the overall molecular structure of the yttrium hydride cluster $(C_5H_5SiMe_3)_4Y_4(\mu\text{-}H)_4(\mu_3\text{-}H)_4(THF)_2$, while the Y_4H_8 core in this complex is highlighted in Fig. 25. The X-ray crystal structure determination revealed the presence of an unsymmetrical tetrahedral configuration of four $[Y(C_5H_5SiMe_3)]$ units, two of which contain each one molecule of THF. Each yttrium atom is bonded to two μ_2-bridging as well as three μ_3-bridging hydrido ligands [78].

The scandium 2,3-dimethyl-1,3-butadiene complex $[\eta^5{:}\eta^1\text{-}C_5H_4(CH_2)_2NMe_2]Sc(C_6H_{10})$ has been obtained as red crystals in 48% yield by the two-step procedure outlined in Scheme 18. Fig. 26 clearly shows that the prone-oriented butadiene fragment has considerable 2-ene-1,4-diyl character, as indicated by the relatively short central C–C bond of 1.386(3) Å and relatively long C–CH_2 bonds of 1.455(3) and 1.464(3) Å [85].

The scandium diene complex reacts with PhCN via initial nitrile insertion into the Sc-diene bond to give a dimeric η^2-imido species, but with a 2,2′-bipyridine via the elimination of the free diene (Scheme 19). The latter reaction shows that $[\eta^5{:}\eta^1\text{-}C_5H_4(CH_2)_2NMe_2]Sc(C_6H_{10})$ can be used to generate the reactive fragment $[\eta^5{:}\eta^1\text{-}C_5H_4(CH_2)_2NMe_2]Sc^{I}$. The molecular structure of the black crystalline bis(2,2′-bipyridine) product is depicted in Fig. 27 [85].

The mono(cyclopentadienyl)lutetium complex $CpLu(2\eta^1{:}\eta^2\text{-guaiazulene})(DME)$ has been prepared in the form of blue crystals by reduction of guaiazulene with the naphthalene–lutetium complex $CpLu(\eta^1{:}\eta^2\text{-}C_{10}H_8)(DME)$ in DME (Scheme 20). According to an X-ray analysis, the molecule has a skewed *pseudo*-sandwich structure in which the Lu atom is $2\eta^1{:}\eta^2$-coordinated by the seven-membered ring of the guaiazulene dianion ligand [86].

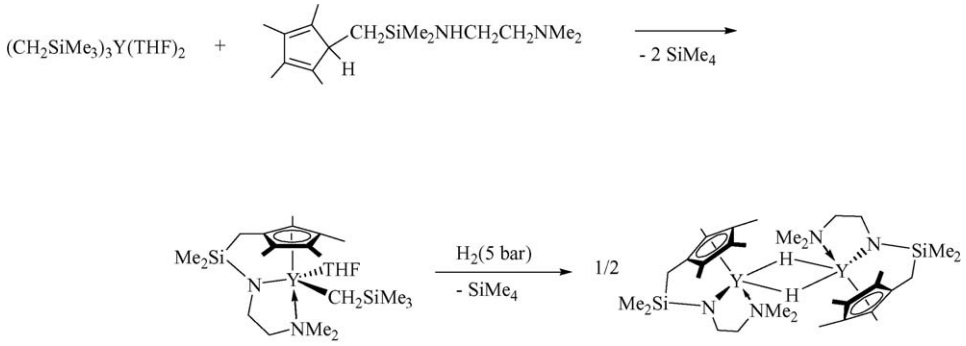

Scheme 16.

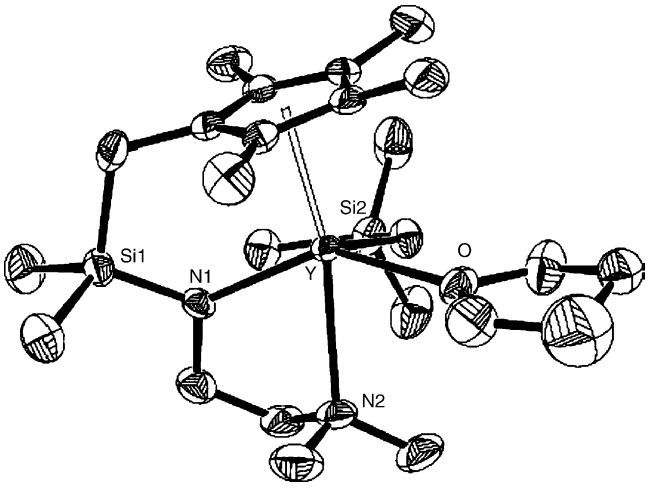

Fig. 22. Molecular structure of (η^5:η^1-$C_5Me_4CH_2SiMe_2NCH_2CH_2NMe_2$)$Y(CH_2SiMe_3)$(THF) [77].

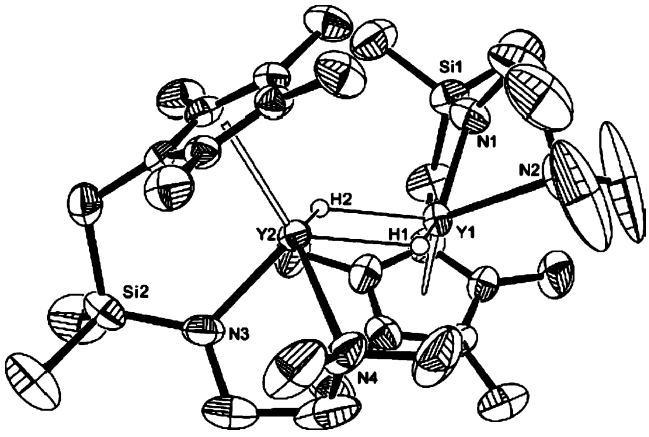

Fig. 23. Molecular structure of [(η^5:η^1-$C_5Me_4CH_2SiMe_2NCH_2CH_2NMe_2$)$Y(\mu\text{-}H)]_2$ [77].

2.5.4. Cp_2LnX compounds

Density functional studies have been carried out on the complexes Cp_2LnCl and $Cp_2LnX(THF)$ (Ln = La–Lu; X = F, Cl, Br, I). In these mixed-ligand complexes, Ln–Cp and Ln–THF bonds are more covalent as compared to Ln–X [87,88]. Density functional theory (DFT) calculations have been performed on the lanthanidocene complexes $Cp_2LnX(THF)$ (Ln = La, Gd, Lu; X = F, Cl, Br, I), and the calculated geometries were in good agreement with the available experimental data [89]. DFT calculations have also been carried out to elucidate the coordination geometry in the olefin-pendant-arm cyclopentadienyl scandium complexes $CpSc[C_5H_4SMe_2(CH_2\text{-}\eta^2\text{-}CH{=}CH_2)](CH_2Ph)$ [90]. The reaction of CF_4 with Cp_2LnH has been studied with DFT(B3PW91) calculations for the entire lanthanide series. The reaction paths for H/F exchange (formation of CF_3H and Cp_2LnF) and alkylation (formation of Cp_2LnCF_3 and HF) have been determined. Even though a transition state for formation of Cp_2LnCF_3 has been located, Cp_2LnCF_3 reacts with no energy barrier with HF to give Cp_2LnF and CF_3H [91].

Mixed-ring bis(cyclopentadienyl)lanthanide complexes of the type $Cp(C_5H_4Me)LnCl$ (Ln = Y, Gd, Er, Yb) have been synthesized by reacting $LnCl_3$ with $Na(C_5H_4Me)$ followed by

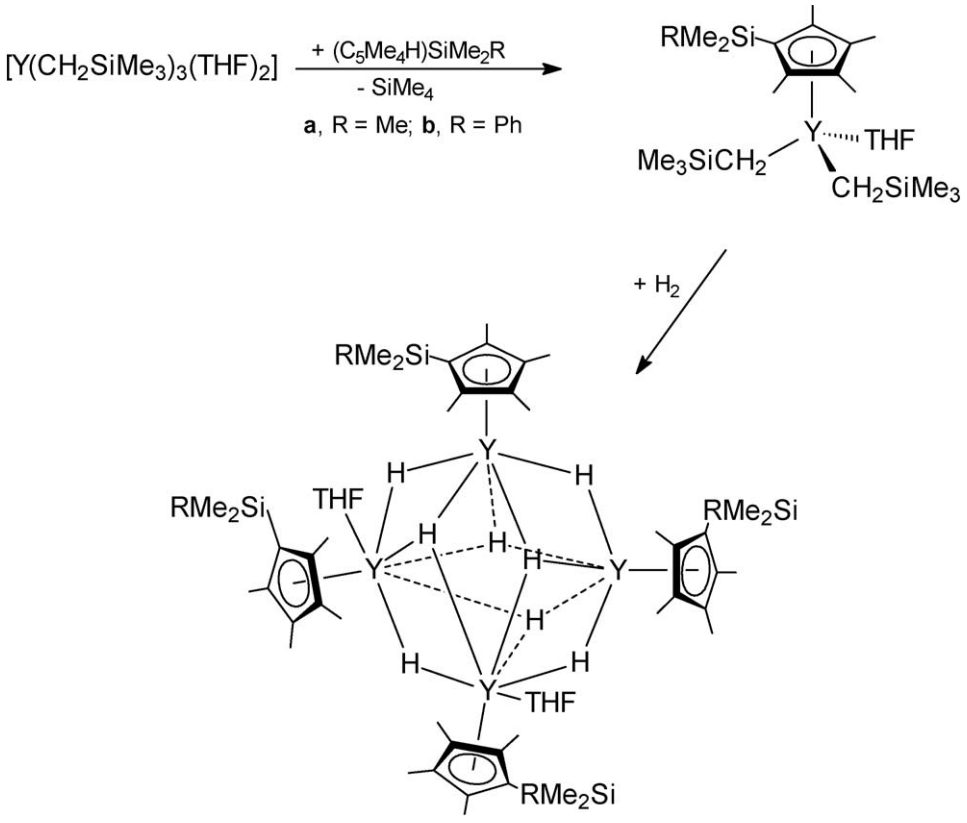

Scheme 17.

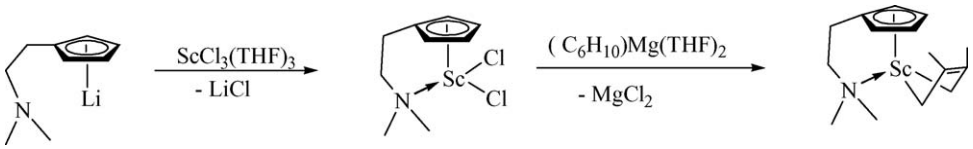

Scheme 18.

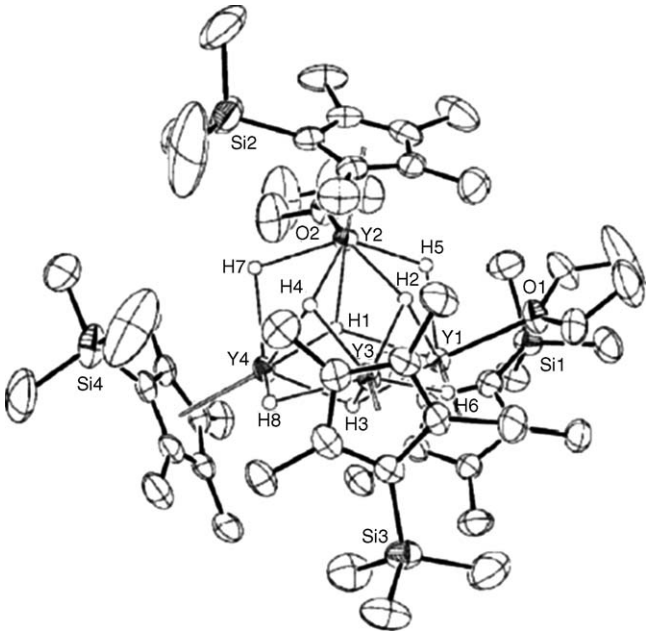

Fig. 24. Molecular structure of $(C_5H_5SiMe_3)_4Y_4(\mu\text{-}H)_4(\mu_3\text{-}H)_4(THF)_2$ [78].

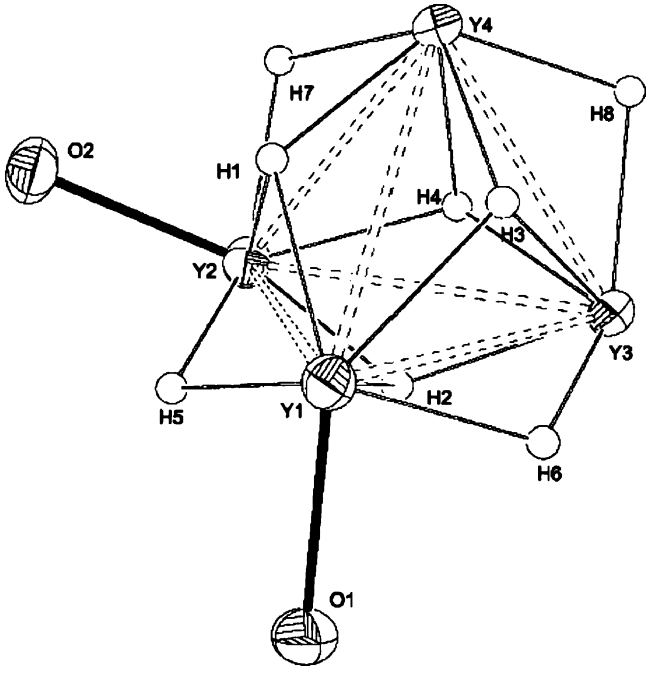

Fig. 25. Structure of the Y_4H_8 core in $(C_5H_5SiMe_3)_4Y_4(\mu\text{-}H)_4(\mu_3\text{-}H)_4(THF)_2$ (THF ligands denoted only by their oxygen atoms) [78].

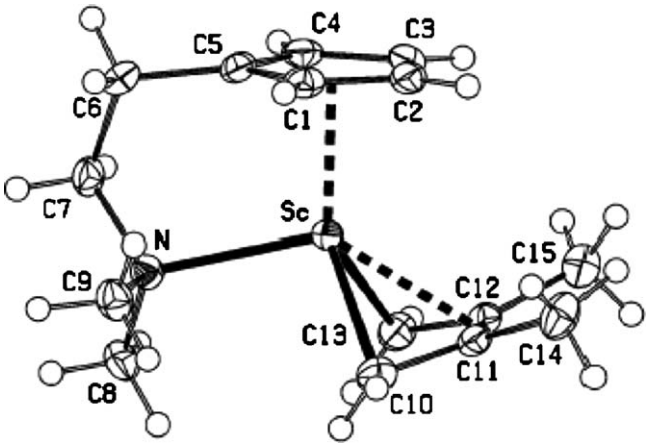

Fig. 26. Molecular structure of $[\eta^5\text{:}\eta^1\text{-}C_5H_4(CH_2)_2NMe_2]Sc(C_6H_{10})$ [85].

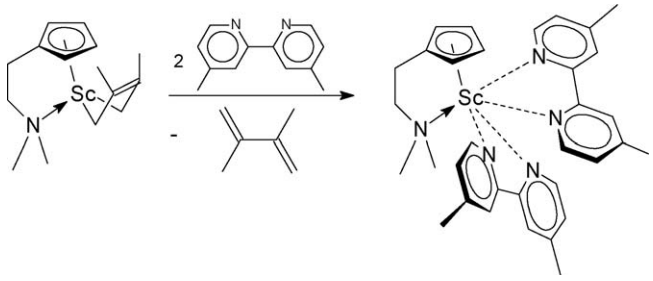

Scheme 19.

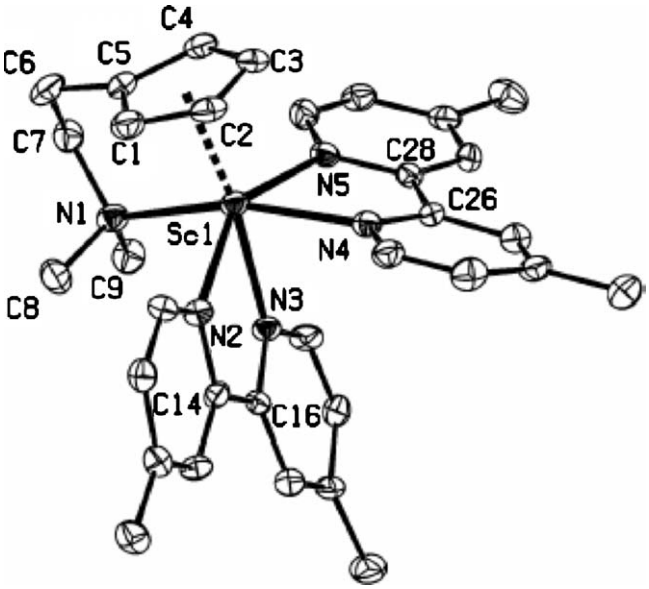

Fig. 27. Molecular structure of $[C_5H_4(CH_2)_2NMe_2]Sc(\eta^2\text{-}N_2C_{12}H_{12})_2$ [85].

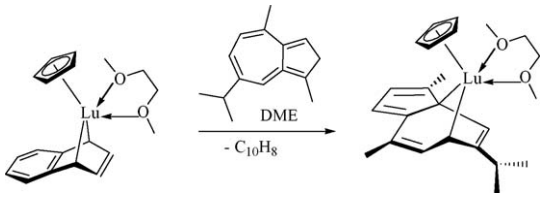

Scheme 20.

addition of 1 equiv. of NaCp. Further reaction of the Yb derivative with excess HCp led to ring displacement and formation of $Cp_2YbCl(THF)$ [92]. The chemistry of organolanthanide complexes containing the bulky vinyltetramethylcyclopentadienyl ligand and its homologues has been thoroughly investigated [93]. Complexes of the type Cp_2LnCl have been isolated with the very bulky tetraisopropylcyclopentadienyl ligand. Fig. 28 shows a structurally characterized unsolvated neodymium derivative. Substitution reactions leading to the corresponding lanthanide silylamide complexes have also been described [94].

The use of the *N*-functionalized cyclopentadienyl ligand $[(S)\text{-}C_5H_4CH(Ph)CH_2NMe_2]^-$ has been investigated [95]. Several lanthanide complexes (Ln = Y, Sm, Yb, Lu) containing sulfur functionalized cyclopentadienyl ligands have been reported. For example, yttrium trichloride reacted with 2 equiv. of $Na(C_5H_4CH_2CH_2SEt)$ in THF to form $(C_5H_4CH_2CH_2SEt)_2YCl$ (Scheme 21). The stepwise reaction of lutetium trichloride with 1 equiv. of $Na(C_5H_4CH_2CH_2SEt)$ and 1 equiv. of $NaCp^*$ yielded $Cp^*(C_5H_4CH_2CH_2SEt)LuCl$. Alkylation of $(C_5H_4CH_2CH_2SEt)_2YCl$ and $Cp^*(C_5H_4CH_2CH_2SEt)LuCl$ with MeLi in toluene gave the lanthanide alkyls $(C_5H_4CH_2CH_2SEt)_2YMe$ and $Cp^*(C_5H_4CH_2CH_2SEt)LuMe$, respectively [96,97].

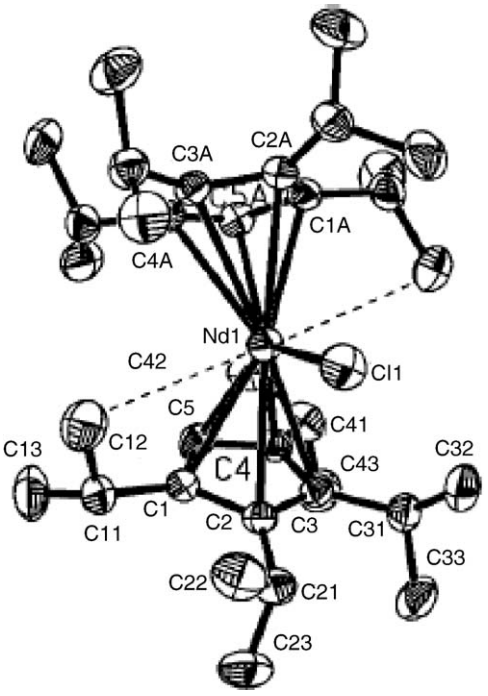

Fig. 28. Molecular structure of $(C_5HPr^i_4)_2NdCl$ [94].

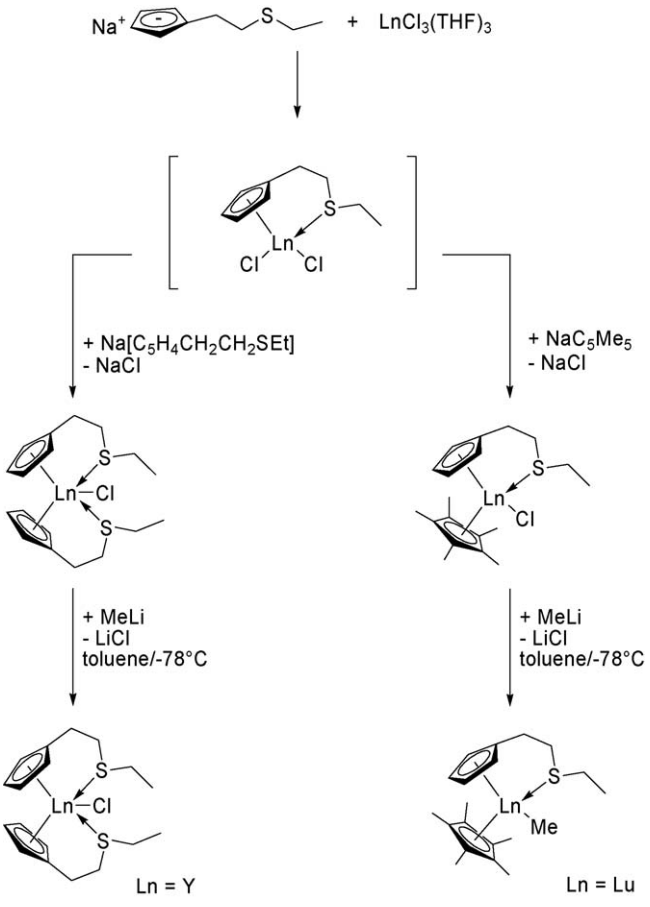

Scheme 21.

Dimeric bis(cyclopentadienyl)lanthanide complexes containing μ-alkoxide ligands form a large and well-investigated class of organolanthanide complexes. A review article on "Unusually structured organolanthanoid(III) dimers with two chiral, but not strictly equivalent, nitrogen-functionalized alkoxide bridges" has been published by Fischer and co-workers [98]. Reaction of Cp_3Ln (Ln = Sm, Yb) with cyclohexanol in a 1:1 molar ratio afforded the dimeric alkoxide complexes $[Cp_2Ln(\mu\text{-}OC_6H_{11})]_2$, of which the Yb derivative was structurally characterized [99]. Analogous dimeric alkoxides containing *N*-functionalized μ-alkoxide ligands have been prepared from $(C_5H_4Me)_3Ln$ or $Cp_3Yb(THF)$ and $HOCH_2CH_2NR_2$ (R = Me, Et) in THF [100,101].

A dimeric structure has been determined for the ytterbium benzoate complexes $[(C_5H_4Me)_2Yb(\mu\text{-}O_2CC_6F_5)]_2$ (orange plates) and $[(C_5H_4Me)_2Yb(\mu\text{-}O_2CC_6F_4H\text{-}o)]_2$ (orange plates) [102]. The complexes $[(C_5H_4SiMe_3)Ln(\mu_3\text{-}NCH_2R)]_4$ (Ln = Y, Lu) were made by reacting the tetranuclear lanthanide polyhydrido complexes $[(C_5H_4SiMe_3)Ln(\mu\text{-}H)_2]_4(THF)$ with nitriles RCN. This reaction involves double addition of the Ln–H units across the C≡N bond [81].

Lanthanocene guanidinate complexes of the type $Cp_2Ln[Pr^iNC(NPr^i_2)NPr^i]$ have also been obtained by insertion of *N*,*N*′-diisopropylcarbodiimide into the Ln–N bond of $Cp_2Ln(NPr^i_2)$ [103,104] and $Cp_2Yb(Cbz)(THF)$ (Cbz = carbazolate) [105]. The first examples of ketene inser-

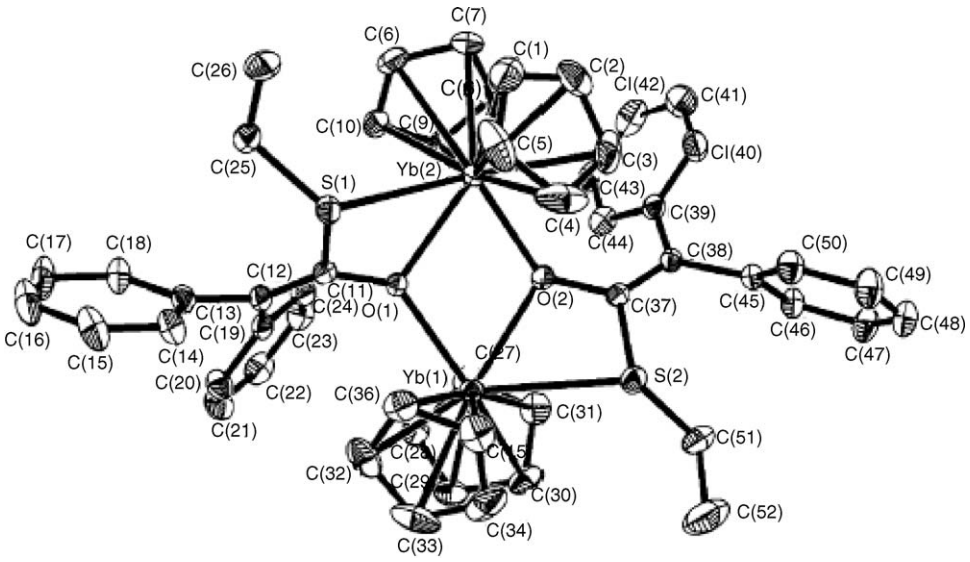

Fig. 29. Molecular structure of $[Cp_2Yb(\mu\text{-}\eta^1{:}\eta^2\text{-}OC(SEt){=}CPh_2)]_2$ [106].

tion into an Ln–S bond have also been described. Fig. 29 illustrates the dimeric structure of the ytterbium complex $[Cp_2Yb(\mu\text{-}\eta^1{:}\eta^2\text{-}OC(SEt){=}CPh_2)]_2$ which has been prepared in the form of red crystals by reacting $[Cp_2Yb(\mu\text{-}SEt)]_2$ with diphenylketene [106].

2.5.5. Cp_3Ln compounds

Cp_3Gd has been reported to show a green luminescence in ether solution [107]. The absorption spectra of the *pseudo*-trigonal bipyramidally coordinated complexes $(C_5H_4CH_2CH_2OMe)_3Nd$ and $(C_5H_4CH_2CH_2PMe_2)_3Nd$ have been measured [108].

2.5.6. Cp_3LnL and Cp_3LnL_2 compounds

Absorption and magnetic circular dichroism spectra have been measured for the methyl-THF derivative $Cp_3Er(MeTHF)$ [109], the samarium tris(cyclopentadienyl) complexes $(C_5H_4Bu^t)_3Sm$, $(C_5H_4Bu^t)_3Sm(THF)$, and $Cp_3Sm(CNC_6H_{11})$ [110], $Cp_3Nd(methylacetate)$ [111], as well as $(C_5H_4Bu^t)_3Nd$, $(C_5H_4Bu^t)_3Nd(THF)$, and $(C_5H_4SiMe_3)_3Nd$ [112]. The cerium and neodymium derivatives $Cp_3Ln(NCMe)_2$ (Ln = Ce, Nd) were analyzed analogously. Large blue-purple crystals of the neodymium compound could be obtained by slow cooling of a solution of Cp_3Nd in acetonitrile [113]. Trialkylphosphate adducts of the type $Cp_3Ln[OP(OR)_3]$ (Ln = Pr, R = Me; Ln = La, Pr, R = Et) have been prepared and their electronic structure investigated [114].

A novel ring displacement reaction of $(C_5H_4Me)_3Ln(THF)$ (Ln = Sm, Tb, Ho, Yb) with cyclopentadiene has been reported to give the parent tris(cyclopentadienyls) $Cp_3Ln(THF)$ in high yields [115]. The crystal structure of $Cp_3Pr(THF)$ has been determined [116]. Numerous adducts of $(C_5H_4Bu^t)_3Ce$ with six-membered *N*-heterocycles have been prepared and structurally characterized. Fig. 30 shows the molecular structure of $(C_5H_4Bu^t)_3Ce(pyridazine)$ as a representative example [117].

2.5.7. Pentamethylcyclopentadienyl compounds

2.5.7.1. Cp^*MX compounds. Novel chemistry has been developed around binuclear samarium(II) complexes containing one pentamethylcyclopentadienyl ligand and bulky siloxide ligands. The reaction of $Cp^*_2Sm(THF)_2$ with 1.5 equiv. of $(Bu^tO)_3SiOH$ in toluene gave the unsymmetrical binuclear Sm(II) complex $Cp^*Sm[\mu\text{-}OSi(OBu^t)_3]_3Sm$ as green crystals in 93% yield (Scheme 22, Fig. 31) [118].

Addition of 4 equiv. of HMPA to a toluene solution of $Cp^*Sm[\mu\text{-}OSi(OBu^t)_3]_3Sm$ afforded purple $Cp^*Sm[OSi(OBu^t)_3](HMPA)_2$ as the only isolable product (Scheme 23) [118].

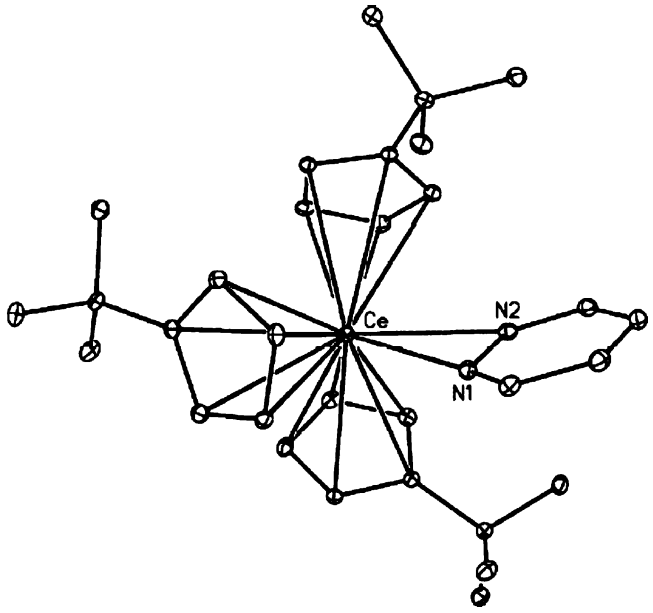

Fig. 30. Molecular structure of $(C_5H_4Bu^t)_3Ce(pyridazine)$ [117].

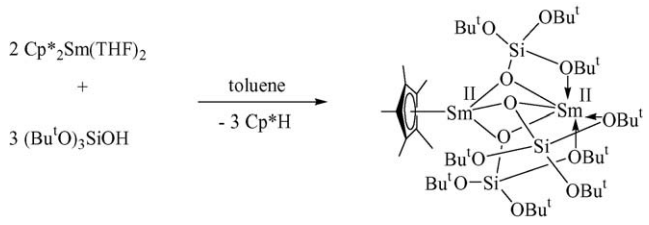

Scheme 22.

Other interesting reactions of $Cp^*Sm[\mu\text{-}OSi(OBu^t)_3]_3Sm$ led to novel samarium(III) species. For example, treatment with 1 equiv. of azobenzene in toluene gave the corresponding binuclear Sm(III) azobenzene–dianion complex as red-brown crystals in 64% yield (Scheme 24, Fig. 32). The azobenzene unit is oriented in a *cis*-fashion. One N atom (N1) bridges two Sm atoms, while the other N atom (N2) is bonded terminally to only one Sm atom (Sm1) [118].

A highly unusual trinuclear Sm(II)/Sm(III) mixed-valence "inverse sandwich" was obtained when $Cp^*Sm[\mu\text{-}OSi(OBu^t)_3]_3Sm$ was treated with either phenylacetylene or 4-Me-2,6-$Bu^t{}_2C_6H_2OH$ (=ArOH) in toluene (Scheme 25, Fig. 33). Most of the products were structurally characterized by X-ray analyses, and the reactions illustrated in Schemes 22–25 represent only part of the interesting chemistry discovered in this system [118].

Ytterbium metal reacts with $HgPh(C_6F_5)$ and HCp^* in THF to give the seven-coordinate monomeric perfluoroorganoytterbium(II) complex $Cp^*Yb(C_6F_5)(THF)_3$ (red-orange crystals, Fig. 34), which is presumably formed by protolysis of a transitory "$YbPh(C_6F_5)$" species with HCp^* [119].

2.5.7.2. $Cp^*{}_2M$ compounds. The results of DFT calculations have been used to define trends in the interactions of H_2, N_2, C_2H_4, and C_2Me_2 with the divalent lanthanide metallocenes Cp_2Ln and $Cp^*{}_2Ln$ (Ln = Sm, Eu, Yb) [120].

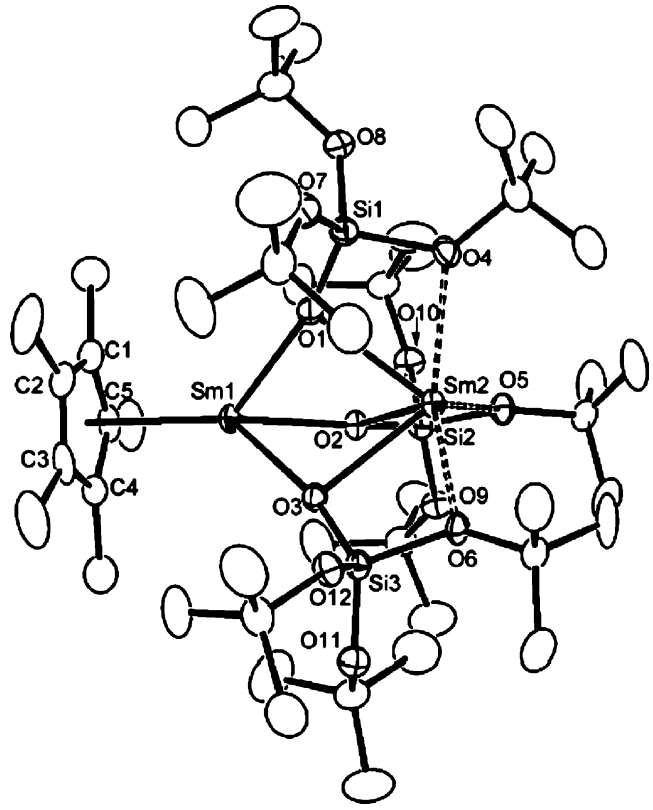

Fig. 31. Molecular structure of $Cp^*Sm[\mu\text{-}OSi(OBu^t)_3]_3Sm$ [118].

An $R_2Si \rightarrow Ln(II)$ complex, $Cp^*{}_2Sm[Si(Bu^tNCH)_2]$, has been synthesized as purple crystals in 90% yield by reaction of the free silylene with $Cp^*{}_2Sm$ in toluene (Scheme 26). As can be clearly seen in Fig. 35, the silylene ligand is located

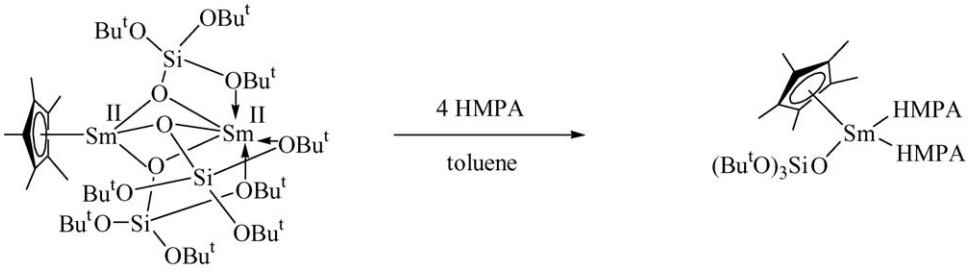

Scheme 23.

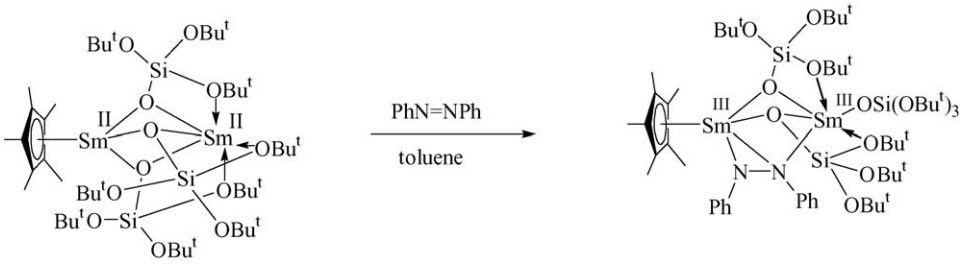

Scheme 24.

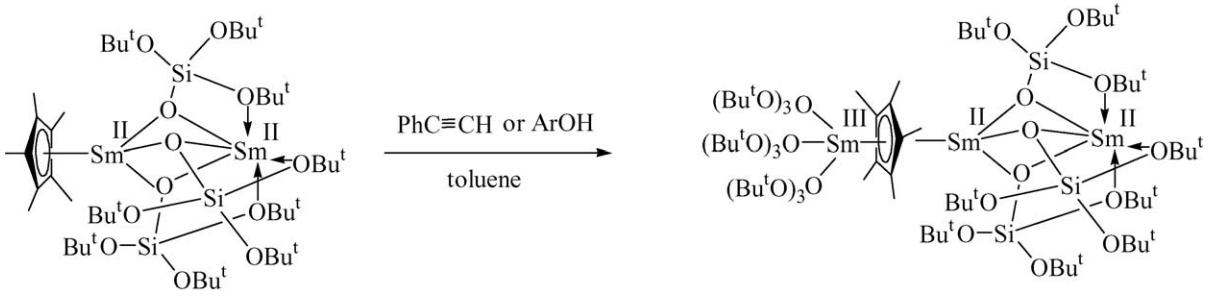

Scheme 25.

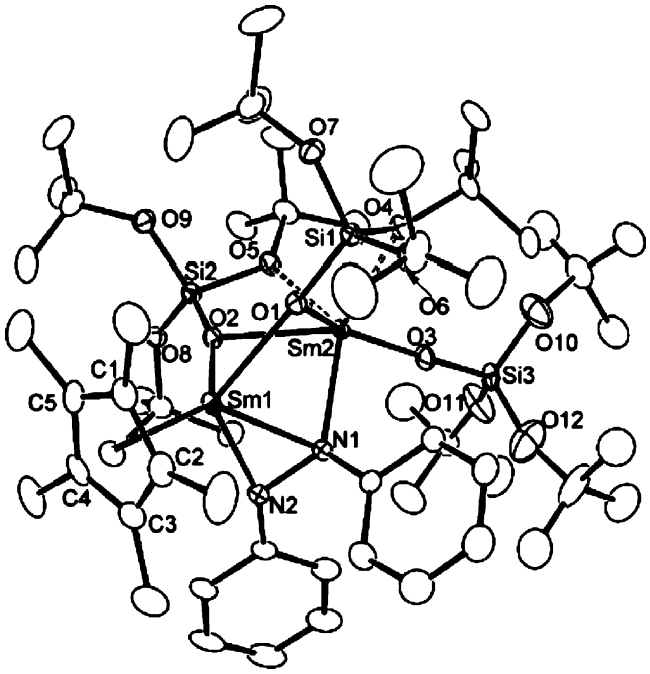

Fig. 32. Molecular structure of $Cp^*Sm[\mu\text{-}OSi(OBu^t)_3]_2(\mu\text{-}\eta^1{:}\eta^2\text{-}N_2Ph_2)SmOSi(OBu^t)_3$ [118].

asymmetrically in the metallocene wedge with one *t*-butyl group (Sm–C(Me) = 3.396(4) Å) much closer to the metal than the other (Sm–C(Me) = 4.741(4) Å). The Sm(II)–Si distance is 3.1910(1) Å [121].

Several Cp^*Ln^{II} alkyl and silyl complexes have also been prepared. Reactions of $Cp^*_2Ln(THF)_2$ with 1 equiv. of $KCH(SiMe_3)_2$ in THF afforded the corresponding Ln(II) alkyl complexes $[Cp^*Ln\{CH(SiMe_3)_2\}Cp^*K(THF)_2]_n$ (Ln = Sm (Fig. 36), Eu, Yb) in 90–92% isolated yields. In the presence of $PhSiH_3$ the reactions of $Cp^*_2Ln(THF)_2$ with an unidentified "$KH + H_3SiPh$" reaction product (presumably containing $KSiH_2Ph$ and $KSiH_3$) gave the Ln^{II}–SiH_3 complexes $[Cp^*Ln(SiH_3)(THF)Cp^*K(THF)]_n$ (Ln = Sm, Eu, Yb) in 81–85% yields. Fig. 37 shows the molecular structure of a monomeric unit of polymeric $[Cp^*Eu(SiH_3)(THF)Cp^*K(THF)]_n$, while the two-dimensional layer structure of this compound is illustrated in Fig. 38 [122].

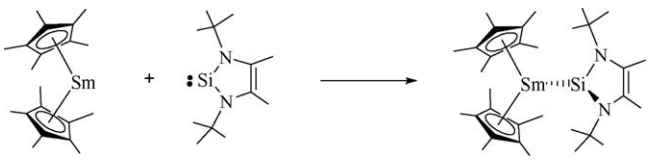

Scheme 26.

2.5.7.3. Mono(pentamethylcyclopentadienyl)lanthanide(III) compounds. Hydrated neodymium nitrates can be readily transformed to anhydrous ether solvates which react with cyclopentadienyl reagents to give organometallic nitrate complexes, e.g. $[Cp^*Nd(THF)(\mu\text{-}NO_3)_3Na(THF)_2]_x$ (Fig. 39) [123].

With $Cp^*Yb[N(PPh_2)_2]_2$ a mono-Cp^* lanthanide complex with two diphosphinoamide ligands has been synthesized and structurally characterized [72]. An unprecedented C–H activation of a 2,2′-bipyridine ligand has been found when $Cp^*Lu(bipy)(CH_2SiMe_3)(NHAr)$ (Ar = 2,6-$Pr^i{}_2C_6H_3$) was reacted with carbon monoxide [124].

The mono(pentamethylcyclopentadienyl)lutetium bis(alkyl) complex $Cp^*Lu(CH_2SiMe_3)_2(THF)$ (Fig. 40) has been synthesized from $Lu(CH_2SiMe_3)_3(THF)_2$ and HCp^*, and its derivative chemistry has been investigated. This includes reactions with 1,2-dimethoxyethane, 2,2′-bipyridine, 2,6-diisopropylaniline and phenylacetylene [125].

A new family of mono(cyclopentadienyl) organoscandium bis(alkyls) supported by a bulky trialkylphosphine oxide ancillary ligand have been reported. Treatment of the oligomeric precursor $[Cp^*{}_2ScCl]_n$ with tri-*t*-butylphosphine oxide in THF led to the mono(cyclopentadienyl)scandium dichloride $Cp^*ScCl_2(OPBu^t{}_3)$ as a monomeric, THF-free solid in 72% yield. Facile alkylation with MeLi gave the dimethyl derivative $Cp^*ScMe_2(OPBu^t{}_3)$ (Scheme 27) [126].

Treatment of $Cp^*ScMe_2(OPBu^t{}_3)$ with 1 equiv. of $B(C_6F_5)_3$ in toluene led to the soluble contact ion pair $[Cp^*ScMe(OPBu^t{}_3)][B(C_6F_5)_3]$ (Scheme 28), demonstrating that the $Cp^*/OPBu^t{}_3$ system can deliver a stable platform for organoscandium chemistry [126].

2.5.7.4. Bis(pentamethylcyclopentadienyl)lanthanide(III) compounds. The crystal structure of $Cp^*{}_2Sm(\mu\text{-}Cl)_2Li(Et_2O)_2$ was found to be isomorphous with its long-known Ce(III) and Yb(III) analogues [127]. The unsolvated salt-like species $[Cp^*{}_2Ln][B(C_6F_5)_4]$ (Ln = Pr, Nd, Gd) have become available by reacting the bimetallic precursors $[Cp^*{}_2Ln(\mu\text{-}Me)_2AlMe_2]_2$ with 2 equiv. of $[CPh_3][B(C_6F_5)_4]$ [128].

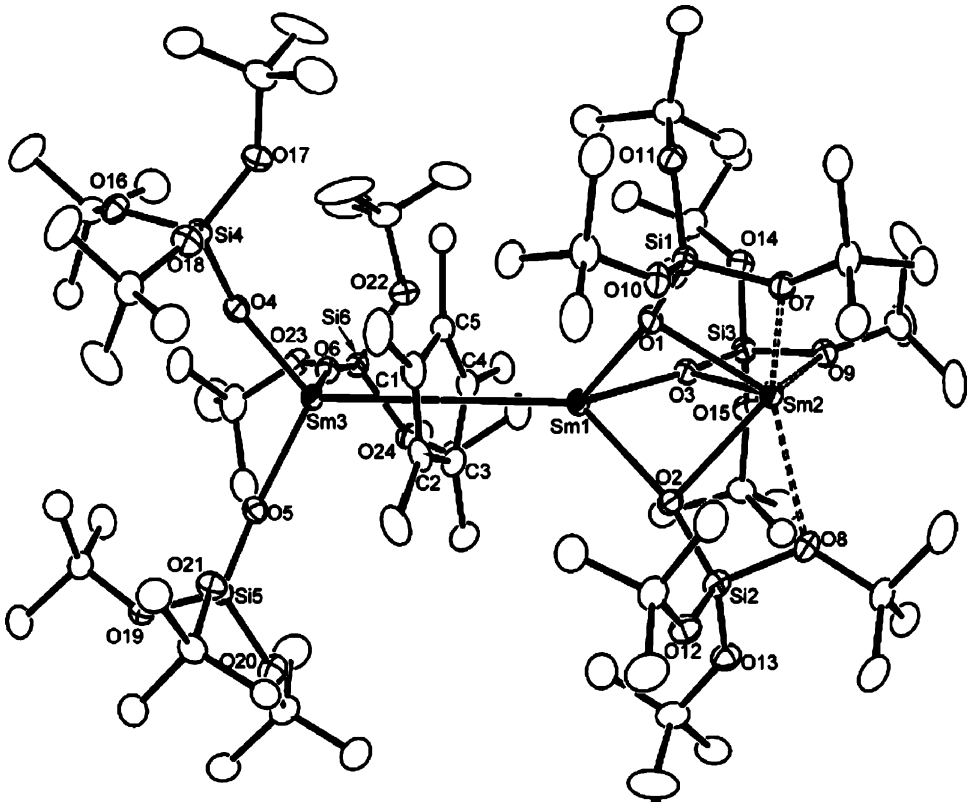

Fig. 33. Molecular structure of $[(Bu^tO)_3SiO]_3Sm^{III}(\mu\text{-}Cp^*)Sm^{II}[\mu\text{-}OSi(OBu^t)_3]_3Sm^{II}$ [118].

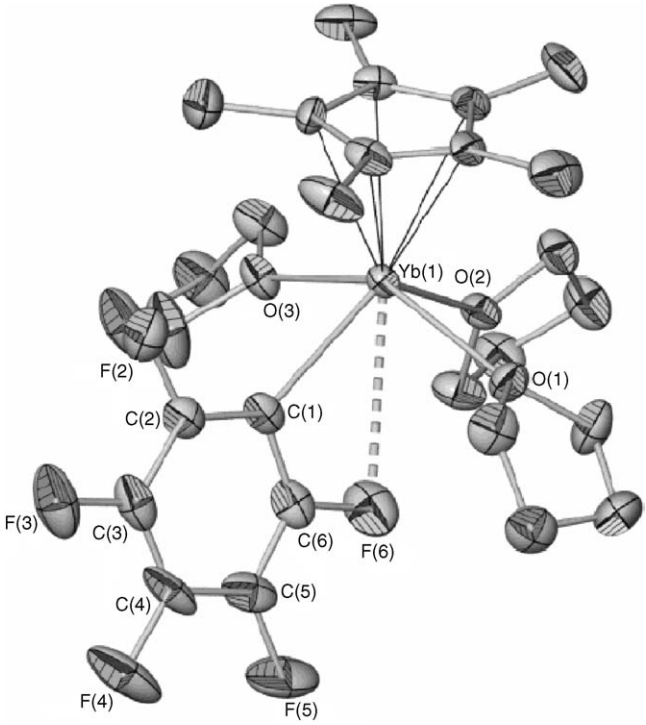

Fig. 34. Molecular structure of $Cp^*Yb(C_6F_5)(THF)_3$ [119].

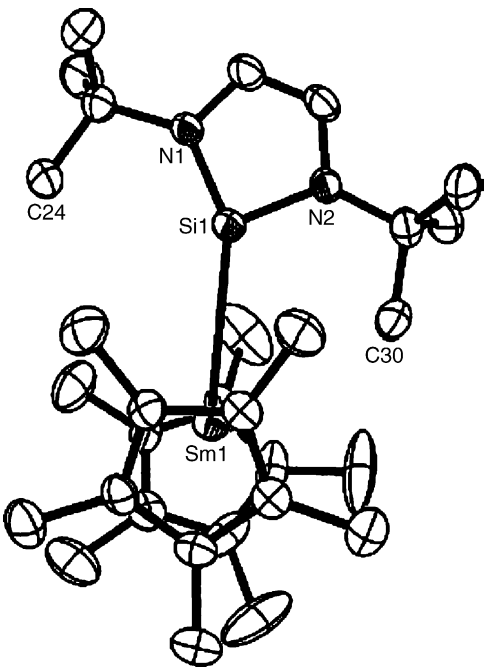

Fig. 35. Top view of the molecular structure of $Cp^*{}_2Sm[Si(Bu^tNCH)_2]$, oriented such that the widest part of the bent metallocene wedge is horizontal in the diagram [121].

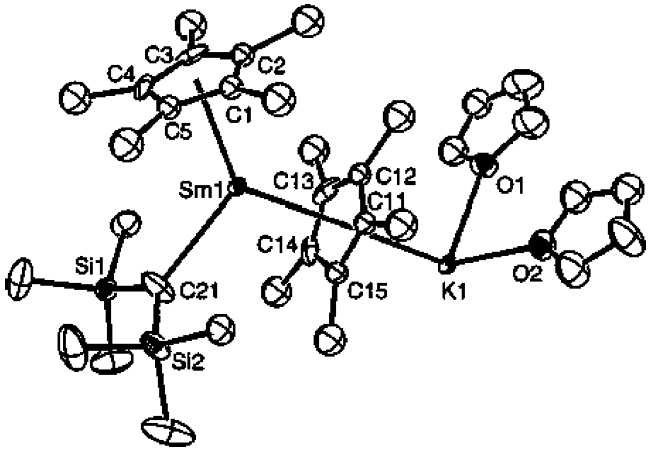

Fig. 36. Molecular structure of a monomeric unit of $[Cp^*Sm\{CH(SiMe_3)_2\}Cp^*K(THF)_2]_n$ [122].

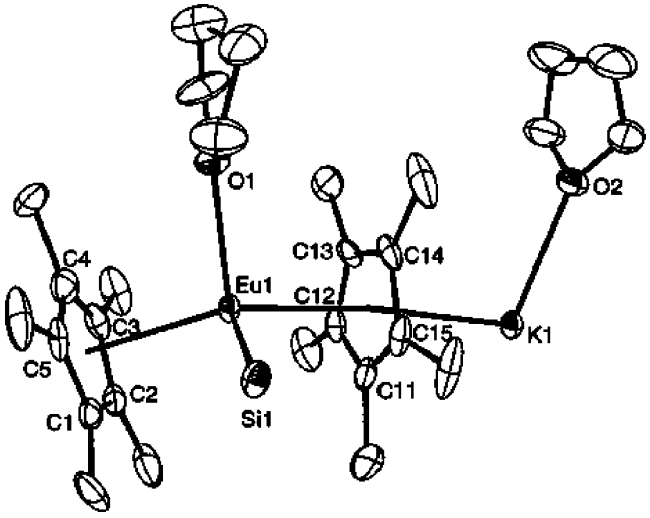

Fig. 37. Molecular structure of a monomeric unit of $[Cp^*Eu(SiH_3)(THF)Cp^*K(THF)]_n$ [12].

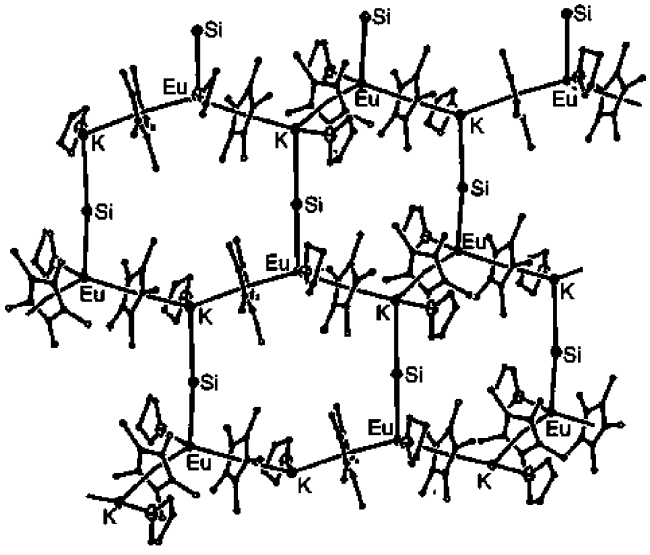

Fig. 38. Two-dimensional layer structure of $[Cp^*Eu(SiH_3)(THF)Cp^*K(THF)]_n$ [122].

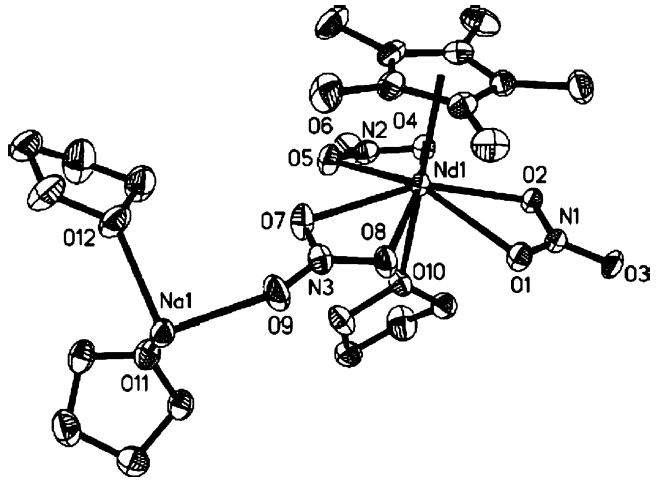

Fig. 39. Molecular structure of a repeat unit in polymeric $[Cp^*Nd(THF)(\mu\text{-}NO_3)_3Na(THF)_2]_x$ [123].

Examination of the chemistry of sterically crowded $(C_5Me_4R)_3Ln$ complexes has provided access to a series of $(\mu\text{-}O)[(C_5Me_4R)_2Ln]_2$ complexes: $(\mu\text{-}O)[Cp^*{}_2La]_2$, $(\mu\text{-}O)[Cp^*{}_2Nd(NC_5H_4NC_4H_8)]_2$, $(\mu\text{-}O)[(C_5Me_4Pr^i)_2Sm]_2$, $(\mu\text{-}O)[(C_5Me_4Et)_2Gd]_2$, and $(\mu\text{-}O)[Cp^*{}_2Gd(NC_5H_5)]_2$. X-ray crystallographic data on these complexes provided information on the effect of metal and cyclopentadienyl ring size on Ln–O bond lengths. As a representative example, the molecular structure of $(\mu\text{-}O)[Cp^*{}_2Sm(NC_5H_5)]_2$ is depicted in Fig. 41 [129a].

μ-Dinitrogen-bis(pentamethylcyclopentadienyl) complexes of lanthanum and neodymium have become readily accessible through the use of potassium graphite as reducing agent. The synthetic routes are illustrated in Scheme 29. The molecular structure of the La derivative is shown in Fig. 42 [129b].

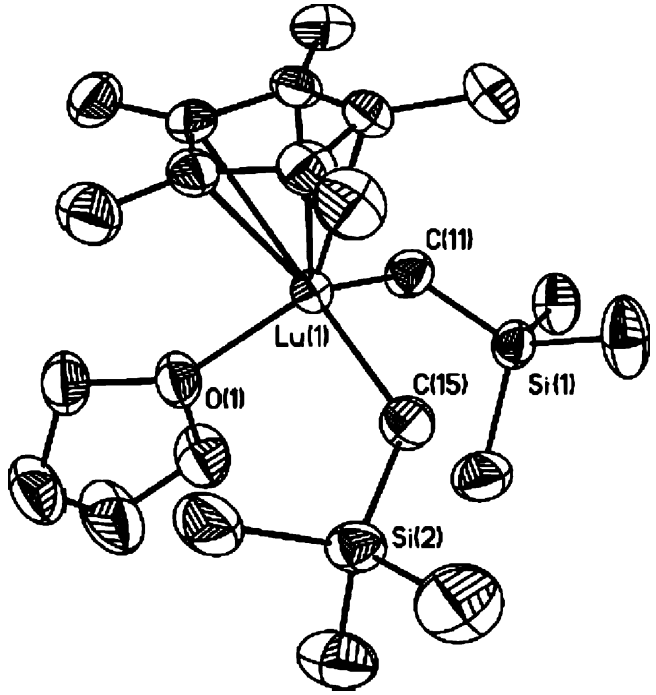

Fig. 40. Molecular structure of $Cp^*Lu(CH_2SiMe_3)_2(THF)$ [125].

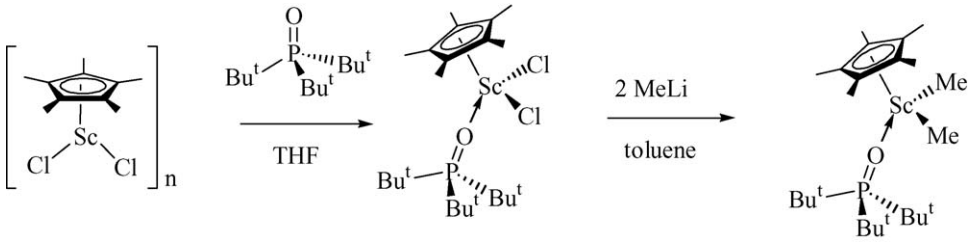

Scheme 27.

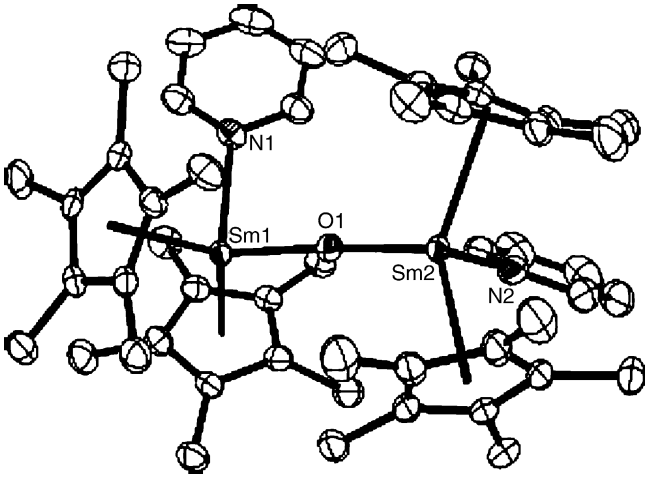

Fig. 41. Molecular structure of (μ-O)[Cp*2Sm(NC5H5)] [129a].

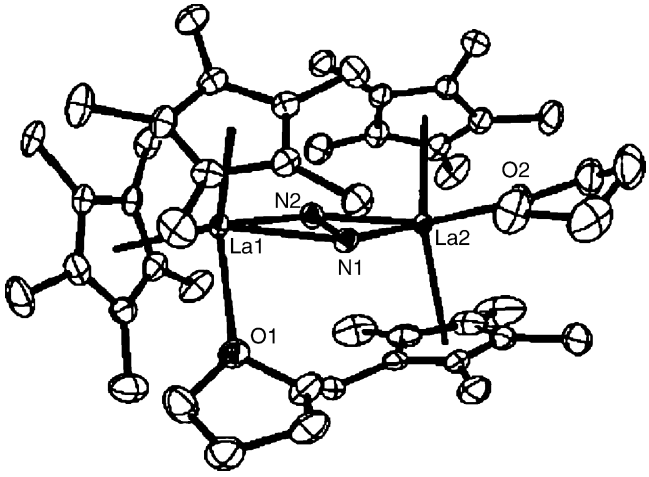

Fig. 42. Molecular structure of (μ-N2)[Cp*2La(THF)]2 [129b].

Oxidation of $Cp^*_2Yb(THF)_2$ with the diazadiene $Bu^tN{=}CHCH{=}NBu^t$ afforded a diazadiene complex, $Cp^*_2Yb(DAD)$, in 72% yield. An X-ray diffraction study confirmed the trivalent state of the ytterbium ion and the radical nature of the DAD ligand in this complex [130].

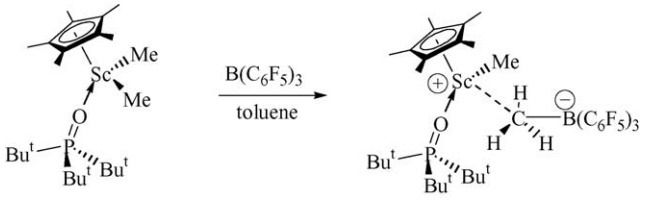

Scheme 28.

Adduct formation between $Cp^*_2Yb(THF)_2$ with 2,2′-bipyridine and 1,10-phenanthroline has been studied in detail [131]. In both cases deeply colored 1:1 adducts of the type $Cp^*_2Yb(L)$ were formed, which have to be formulated as $Cp^*_2YbIII(L^{\bullet-})$ ($L^{\bullet-}$ = radical anion). In a similar manner, $Cp^*_2Yb(Et_2O)$ reacts with terpyridine (Fig. 43) and tetrapyridinylpyrazine (Fig. 44) [132].

The first non-*ate* heteroleptic lanthanide complex containing a monoanionic 2-amidopyridine ligand has been reported for terbium (Scheme 30, Fig. 45). The monomeric complex $Cp^*_2Tb(amptms)$ (amptms = 2-(trimethylsilylamido)-6-methylpyridine) is the first structurally characterized terbium Cp^* compound [133].

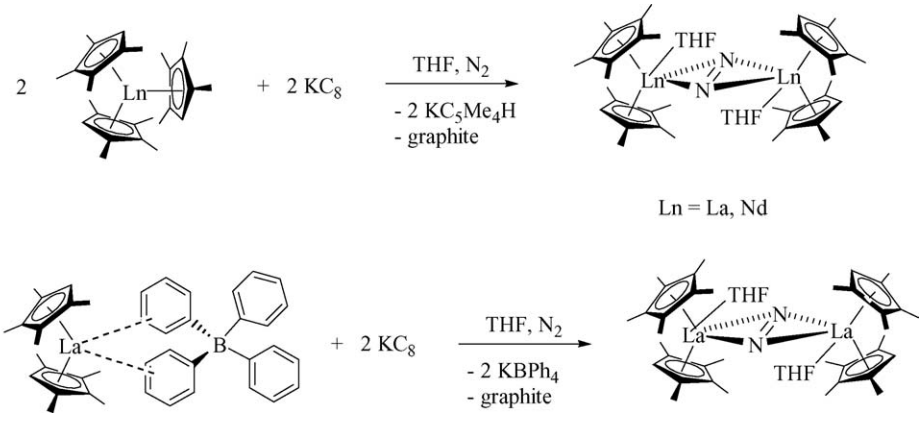

Scheme 29.

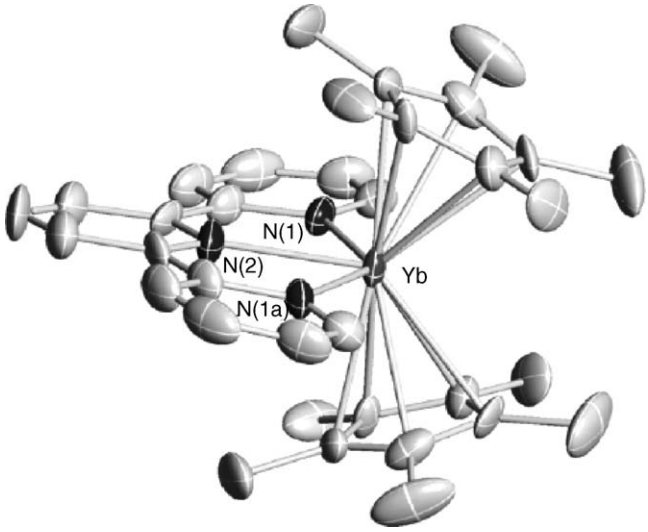

Fig. 43. Molecular structure of $Cp^*_2Yb(terpy)$ [132].

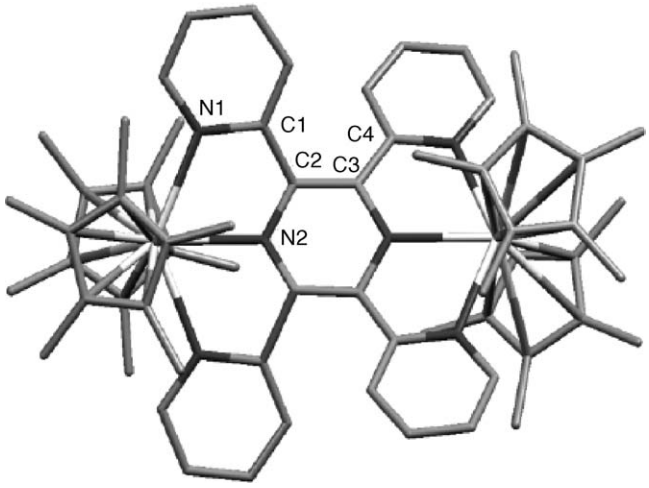

Fig. 44. Molecular structure of (μ-tetrapyridinylpyrazine)$[Cp^*_2Yb]_2$ [132].

Monoanionic phosphine(phosphinimino)methanide ligands have been introduced in organolanthanide chemistry. Scheme 31 illustrates the ligand synthesis and the preparation of a $Cp^*_2Sm(III)$ derivative, which is monomeric in the solid state and contains the ligand in η^3-heteroallylic fashion as shown in Fig. 46 [134].

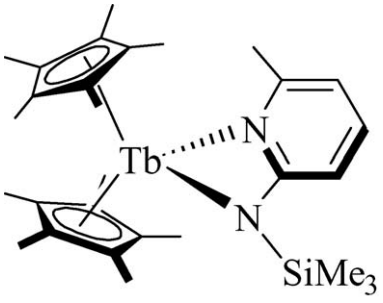

Scheme 30.

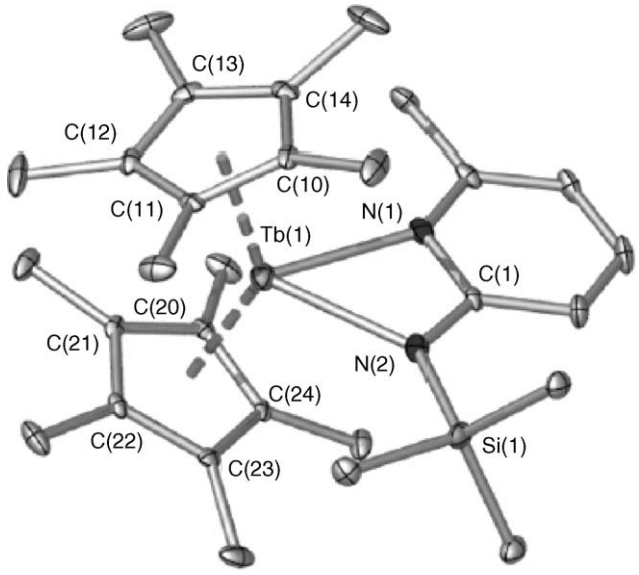

Fig. 45. Molecular structure of $Cp^*_2Tb(amptms)$ [133].

Agostic interactions in yttrium alkyls of the type Cp^*_2YR have been studied in detail [135]. DFT and QM/MM calculations have been carried out to model Cp^* for reactivity studies in Cp^*_2LnR complexes [136]. The precise mechanism of the reaction of butadiene with Cp^*_2SmH to give the known insertion product $Cp^*_2Sm(\eta^3\text{-}CH_2CHCHMe)$ has been investigated on the basis of DFT calculations [137]. The reaction of $Cp^*_2Sm(THF)_2$ with 2 equiv. of benzophenone imine ($Ph_2C{=}NH$) in THF at room temperature gave the samarocene(III) amine/ketimido complex $Cp^*_2Sm(N{=}CPh_2)(NH_2CHPh_2)$ (Scheme 32), while an excess of $Ph_2C{=}NH$ led to formation of the imine-coordinated complex $Cp^*_2Sm(N{=}CPh_2)(HN{=}CPh_2)$ [138].

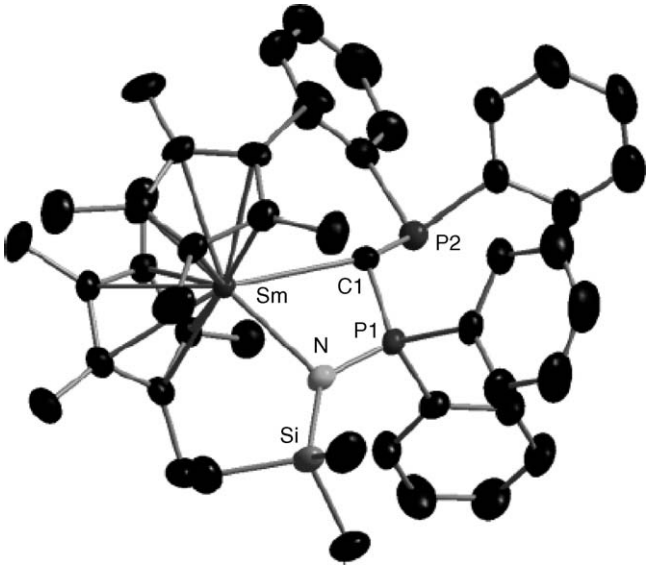

Fig. 46. Molecular structure of $Cp^*_2Sm(Ph_2PCHPPh_2NSiMe_3)$ [134].

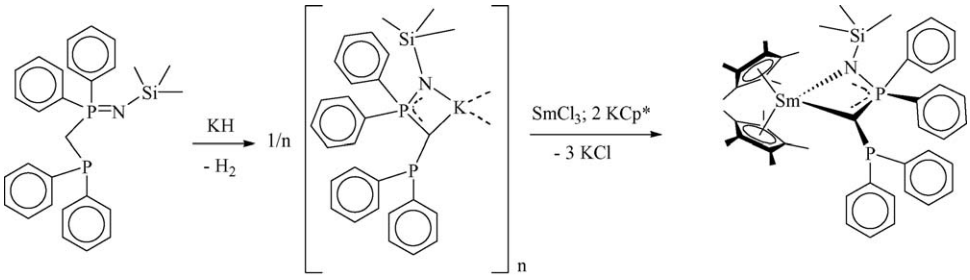

Scheme 31.

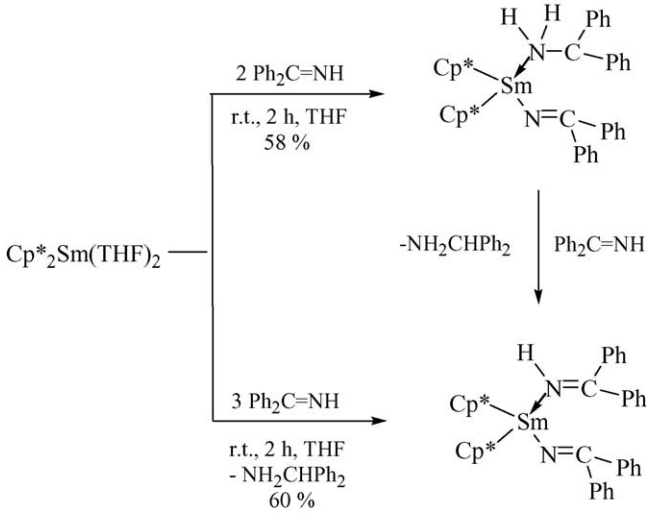

Scheme 32.

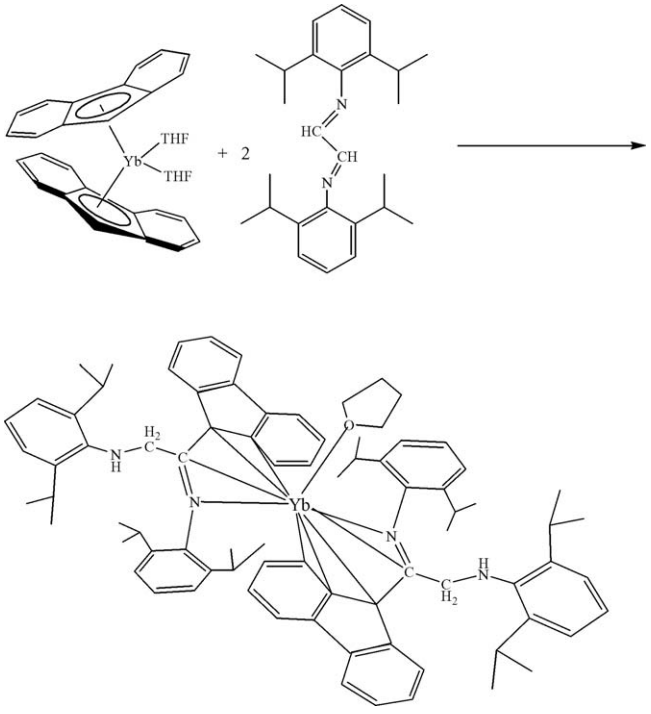

Scheme 33.

2.5.8. *Compounds with ring-bridged cyclopentadienyl ligands*

Guaiazulene reacts with ytterbium metal under reductive coupling to give an *ansa*-bis(guaiazulene)ytterbium(II) complex [139].

2.5.9. *Indenyl and fluorenyl compounds*

2.5.9.1. Lanthanide(II) compounds. Protonolysis of $(C_9H_7)_2Sm(THF)_3$ with $[NEt_3H][BPh_4]$ has been reported to yield the "inorganic" salt-like species $[Sm(THF)_7][BPh_4]_2$ [140].

Unexpected pathways including C–C coupling and C–H bond activation have been found for reactions of $(C_{13}H_9)_2Yb(THF)_2$ with sterically demanding diazadienes. Scheme 33 illustrates the formation of a novel multifunctional ligand system in the reaction with the bulky ligand (2,6-Pr^{i}C$_6$H$_3$)N=CHCH=N(2,6-Pr$^i_2$C$_6$H$_3$) (Fig. 47) [141].

It was found that replacement of the imino hydrogen atoms in the DAD ligand by methyl groups dramatically influenced the reaction pathway and led to formation of a totally different product (Scheme 34) which was isolated as a deep green crystalline solid in 64% yield. The novel ytterbium(II) complex (Fig. 48) contains a new ligand resulting from proton abstraction from a methyl substituent on the imino group [141].

A series of europium(II) and ytterbium(II) metallocenes containing methoxyethyl-functionalized indenyl ligands have been

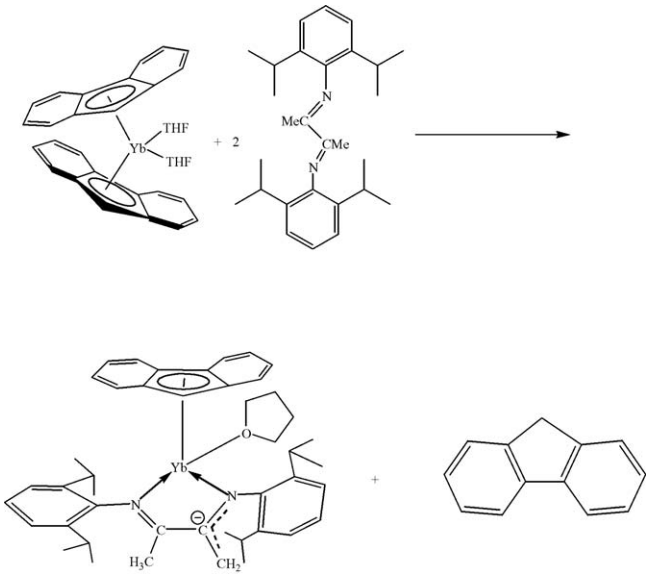

Scheme 34.

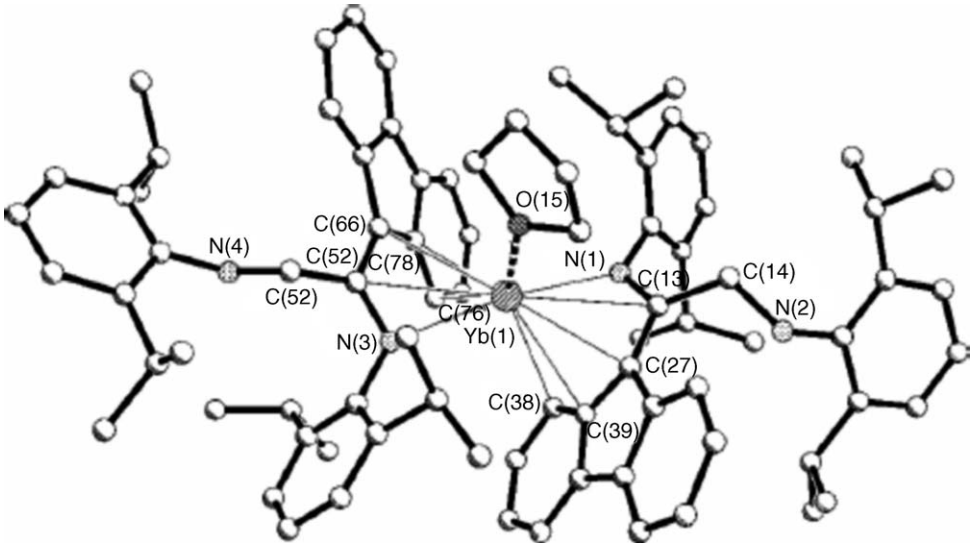

Fig. 47. Molecular structure of the reaction product of $(C_{13}H_9)_2Yb(THF)_2$ with (2,6-$Pr^iC_6H_3$)N=CHCH=N(2,6-$Pr^i{}_2C_6H_3$) [141].

synthesized by reacting suitable lanthanide silylamide precursors with the free ligands [142].

The first examples of unsolvated racemic bis(2-dimethylaminoethylindenyl) divalent organolanthanide complexes, $(Me_2NCH_2CH_2C_9H_6)_2Sm$ and $(Me_2NCH_2CH_2C_9H_6)_2Yb$, were synthesized according to Scheme 35 by the reaction of $K(Me_2NCH_2CH_2C_9H_6)$ with LnI_2 (Ln = Sm, Yb) in THF at room temperature or alternatively by reacting the Yb(III) silylamide $Yb[N(SiMe_3)_2]_3$ with 2 equiv. of the free ligand. Fig. 49 shows the molecular structure of the ytterbium derivative [143,144].

Divalent lanthanide metallocenes of Sm and Yb have also been prepared using the pendant-arm 3-(2-pyridylmethyl)indenyl ligand [145]. A novel europium(II) complex containing a pendant-arm pyrrolidinyl-indenyl ligand has been synthesized according to Scheme 36. The yellow compound was isolated in 75% yield. An X-ray diffraction analysis revealed its monomeric structure (Fig. 50) [146].

The reaction of $YbI_2(THF)_2$ with the aminosilylindene ligand $(C_9H_7)SiMe_2NHBu^t$ in the presence of potassium 1,2-diphenylethylenide took a different course and yielded a divalent ytterbocene complex with non-chelating aminosilyl indenyl ligands (Scheme 37) [147].

The corresponding 2,2′-bipyridine adduct has been prepared directly from the free ligand and ytterbium naphthalenide, followed by addition of 2,2′-bipyridine (Scheme 38). The black crystalline material has been structurally characterized by X-ray analysis (Fig. 51) [147].

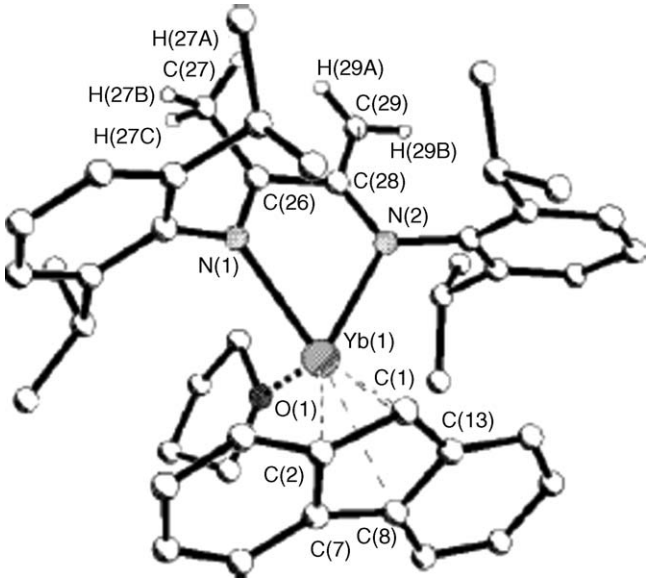

Fig. 48. Molecular structure of $(C_{13}H_9)Yb(THF)[(2,6\text{-}Pr^i{}_2C_6H_3)N{=}C(CH_3){-}C(CH_2){=}N(2,6\text{-}Pr^i{}_2C_6H_3)]$ [141].

2.5.9.2. Lanthanide(III) compounds. Interesting "constrained-geometry" lanthanide complexes have been synthesized with the use of the fluorenyl-based ligands $[(3,6\text{-}Bu^t{}_2Flu)SiR_2NBu^t]^{2-}$ (R = Me, Ph) (Scheme 39). Fig. 52 depicts the molecular structure of the dimethylsilyl-bridged derivative. This compound is thermally stable in toluene solution and shows a dynamic behavior connected to THF dissociation [148].

Reaction of pyridine with the corresponding fluorenyl-(hydrido)yttrium complex $[\{(3,6\text{-}Bu^t{}_2Flu)SiR_2NBu^t\}Y(\mu\text{-}H)(THF)]_2$ selectively gave the 1,4-addition product, which was characterized by single-crystal X-ray diffraction (Scheme 40, Fig. 53) [149].

The sterically demanding heptamethylindenyl ligand has been introduced in organolanthanide chemistry. The chloride complex $Ind^*{}_2YCl(THF)$ (Ind^* = heptamethylindenyl) (Fig. 54) was prepared according to Scheme 41 and served as valuable starting material for a series of new alkyl, silyl and hydride derivatives [150].

The cyclopentyl-substituted bis(indenyl)lanthanide complexes $(C_9H_6C_5H_9)_2Ln(\mu\text{-}Cl)_2Li(Et_2O)_2$ (Ln = Y, Yb) [151,152] and the bis[(tetrahydrofurfuryl)indenyl]lanthanide chlorides $(C_6H_6CH_2OC_4H_7)_2LnCl$ (Ln = Y, La, Pr, Gd, Lu) [153,154] have been prepared by standard methods. The

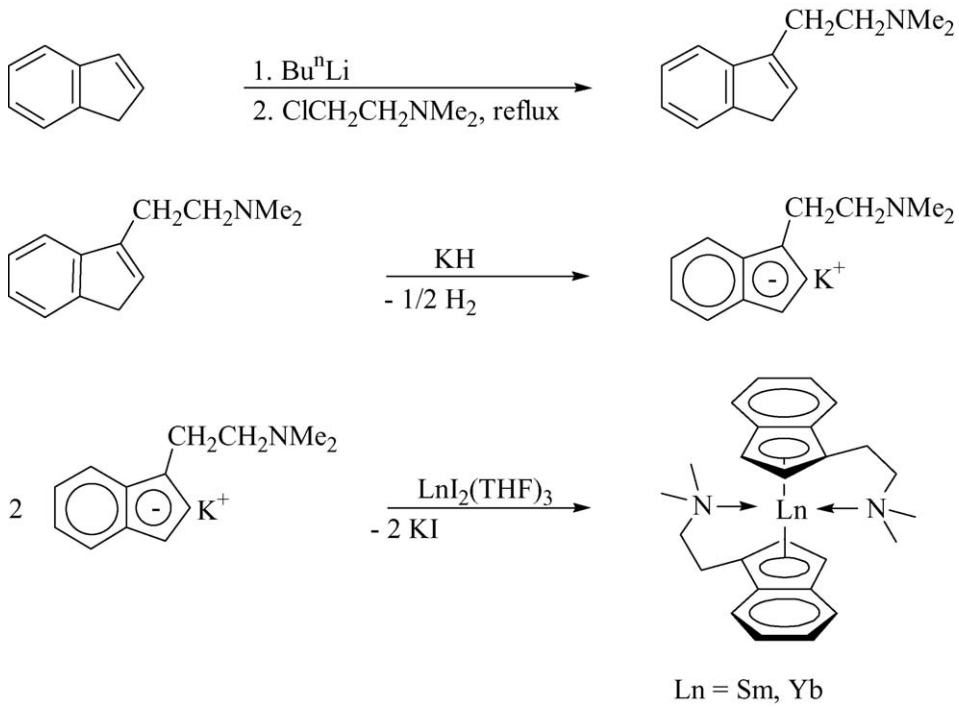

Scheme 35.

trialkylphosphate complex $(C_9H_7)_3Pr[OP(OEt)_3]$ has been synthesized [115]. The reaction of $(C_9H_7)_2LnCl(THF)$ with NaH in THF generated the dimeric bis(indenyl)lanthanide hydrides $[(C_9H_7)_2Ln(\mu\text{-}H)]_2{\cdot}4THF{\cdot}NaCl$ [155].

2.5.9.3. ansa-Indenyl and fluorenyl compounds. A series of chiral 1,1′-(3-oxapentamethylene)-bridged bis(indenyl) *ansa*-lanthanidocenes have been synthesized with high stereoselectivity. The synthetic routes are illustrated in Scheme 42. The molecular structure of the samarium chloro complex $[O(CH_2CH_2C_9H_6)_2]SmCl(THF)$ is illustrated in Fig. 55 [156].

An interesting η^3-coordination mode has been found in *ansa*-metallocenes of the general formula

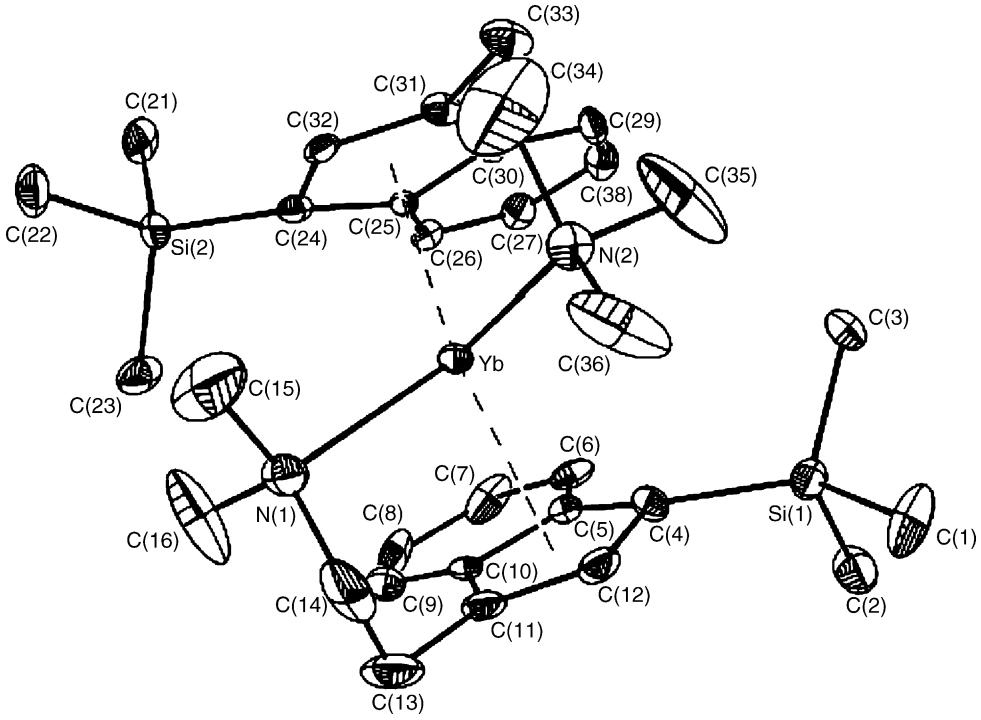

Fig. 49. Molecular structure of $(Me_2NCH_2CH_2C_9H_6)_2Yb$ [143].

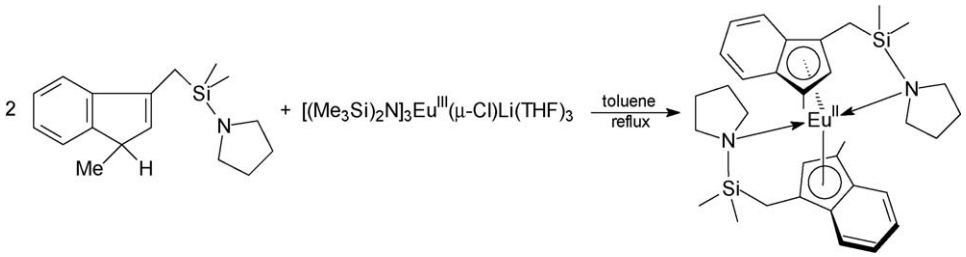

Scheme 36.

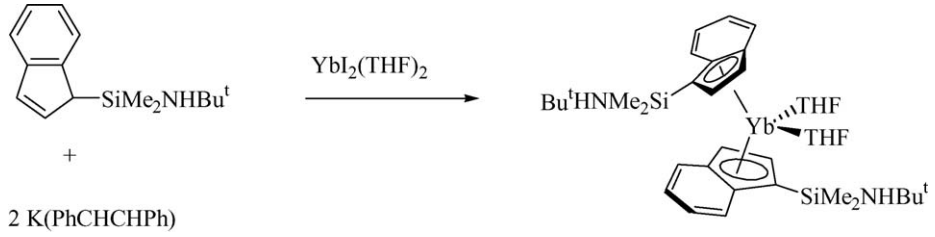

Scheme 37.

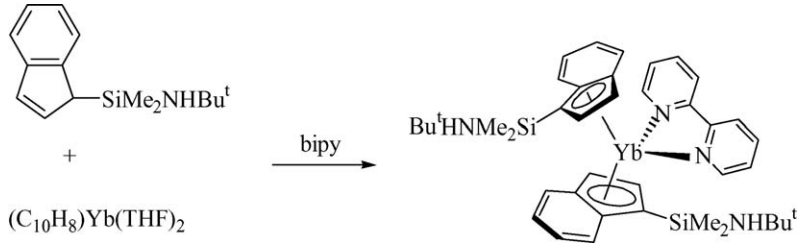

Scheme 38.

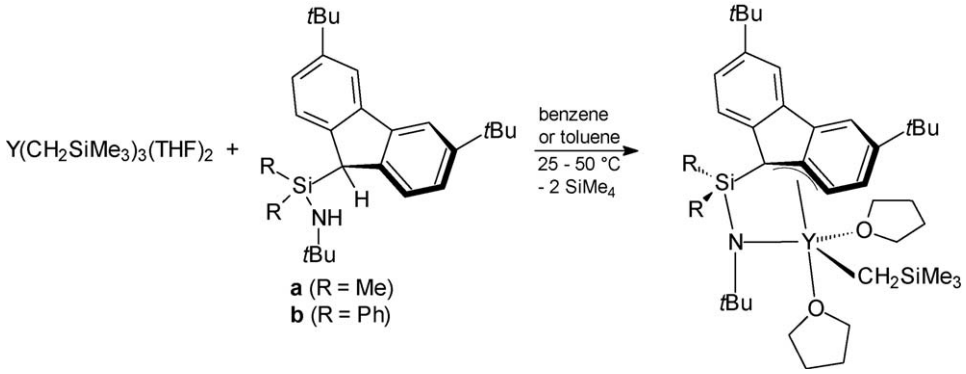

Scheme 39.

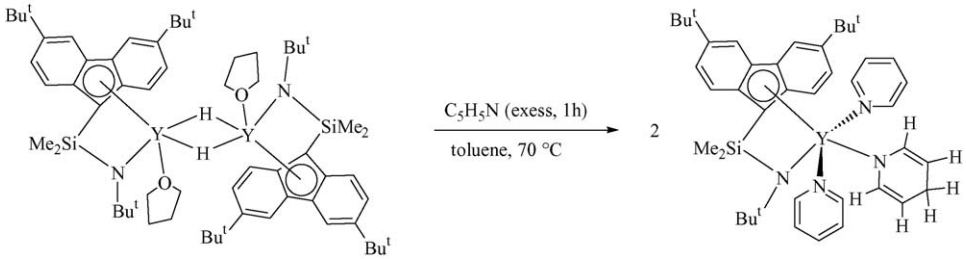

Scheme 40.

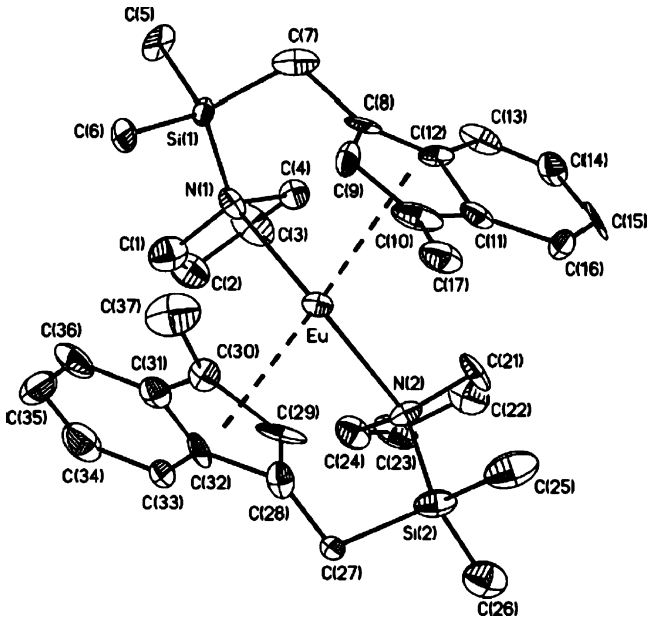

Fig. 50. Molecular structure of $(C_9H_5\text{-}1\text{-}Me\text{-}3\text{-}CH_2SiMe_2NC_4H_8)_2Eu$ [146].

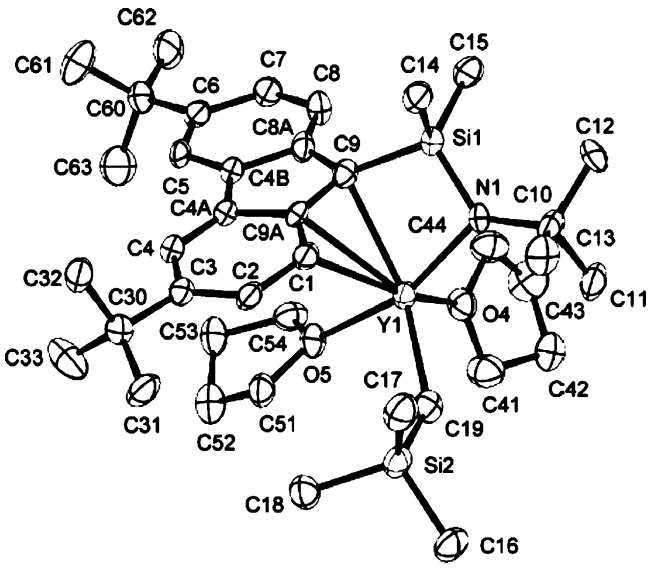

Fig. 52. Molecular structure of $[(3,6\text{-}Bu^t{}_2Flu)SiR_2NBu^t]Y(CH_2SiMe_3)(THF)_2$ [148].

$[Li(Et_2O)_2][Ln\{Me_2C(Flu)(C_5H_4)\}]$ (Ln = Y, La) (Scheme 43) [157,158].

The *ansa*-yttrocene complex $[(C_9H_5\text{-}2\text{-}Me)_2SiMe_2]YN(SiHMe_2)_2$, derived from a linked bis(indenyl) ligand, has been prepared by an amine elimination reaction as depicted in Scheme 44. Treatment of $[(\eta^5\text{-}C_9H_5\text{-}2\text{-}Me)_2SiMe_2]YN(SiHMe_2)_2$ with $AlHBu^i{}_2$ (=DIBAH) led to formation of a dimeric hydride species [159].

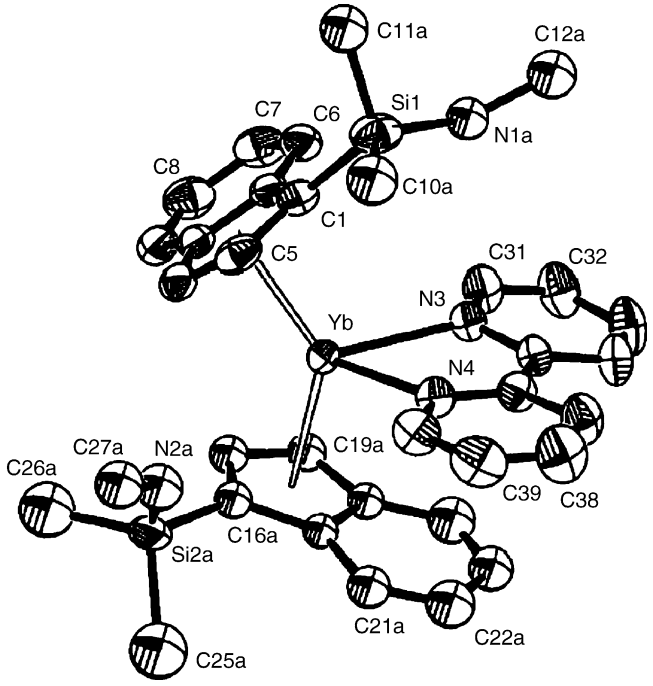

Fig. 51. Molecular structure of $[(C_9H_7)SiMe_2NHBu^t]_2Yb(bipy)$ [147].

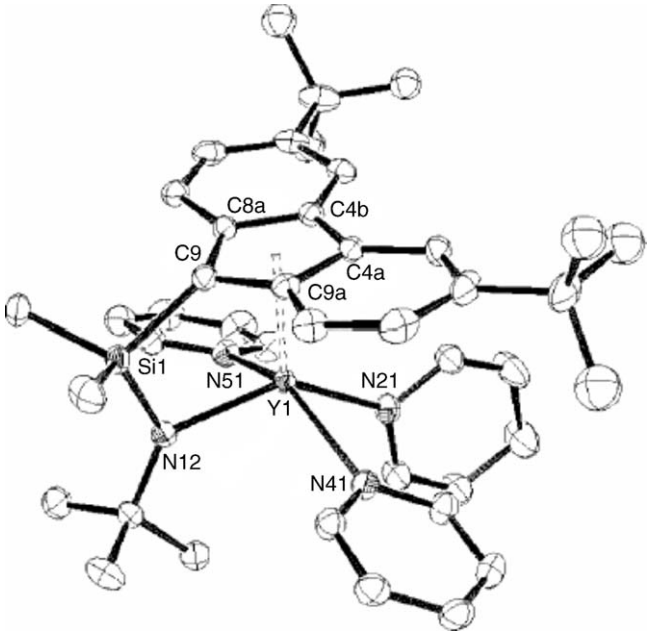

Fig. 53. Molecular structure of $[(3,6\text{-}Bu^t{}_2Flu)SiR_2NBu^t]Y(\eta^1\text{-}NC_5H_6)(py)_2$ [149].

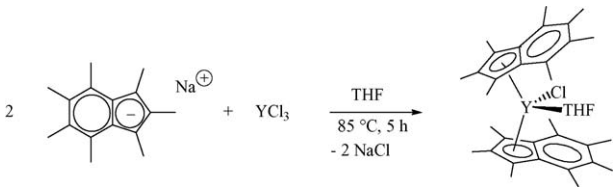

Scheme 41.

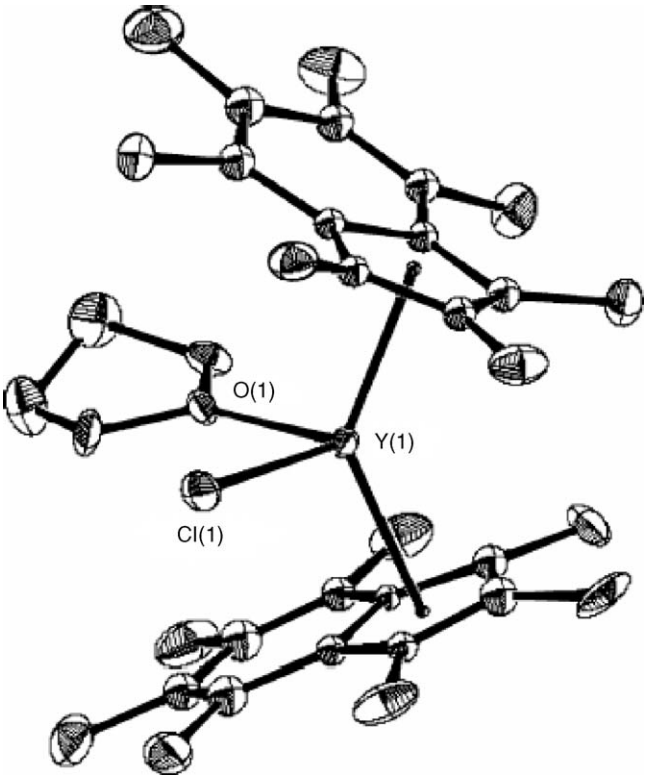

Fig. 54. Molecular structure of $Ind_2^*YCl(THF)$ [150].

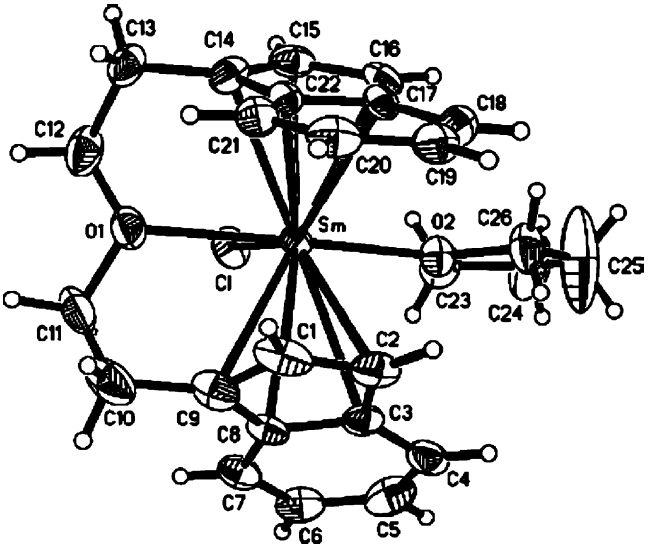

Fig. 55. Molecular structure of $[O(CH_2CH_2C_9H_6)_2]SmCl(THF)$ [156].

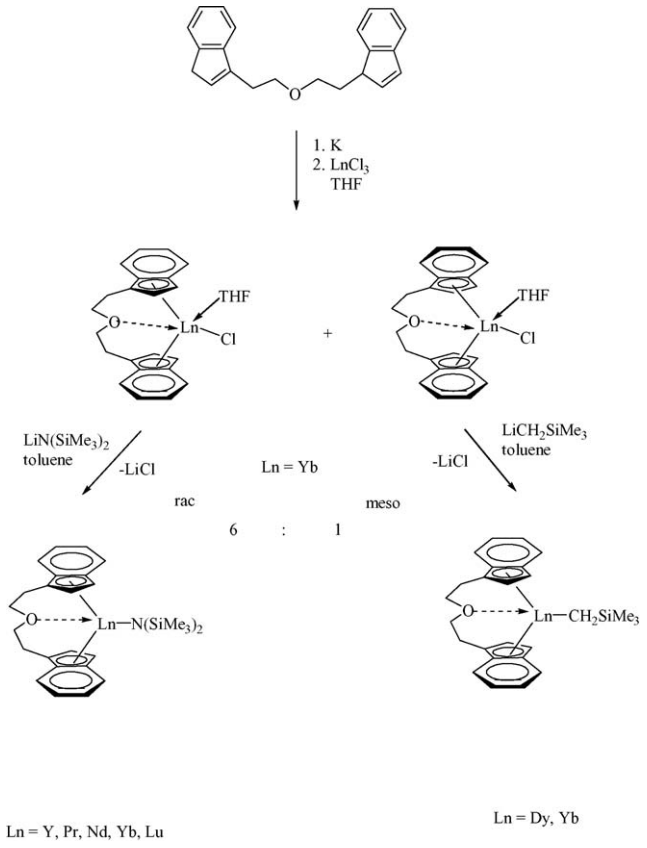

Scheme 42.

2.6. Organolanthanide complexes with cyclopentadienyl-like ligands

2.6.1. Compounds with heteroatom five-membered ring ligands

Samarium chemistry with polydentate pyrrolyl ligands is very diverse. Di- and trivalent dinuclear samarium complexes supported by pyrrole-based tetradentate Schiff bases [160] as well as Ln(II) and Ln(III) *meso*-octaethylporphyrinogen complexes [161] have been investigated, which all involve coordination of the pyrrolyl rings to the lanthanide metals. The same is true for a series of homoleptic lanthanide pyrazolates [162,163] and the europium indolate $Eu_2(Ind)_4(NH_3)_6$. The latter has a dimeric structure and contains divalent Eu. The coordination sphere around the europium atoms consists of five N atoms of two *cisoid* indolate anions and three NH_3 molecules as well as an

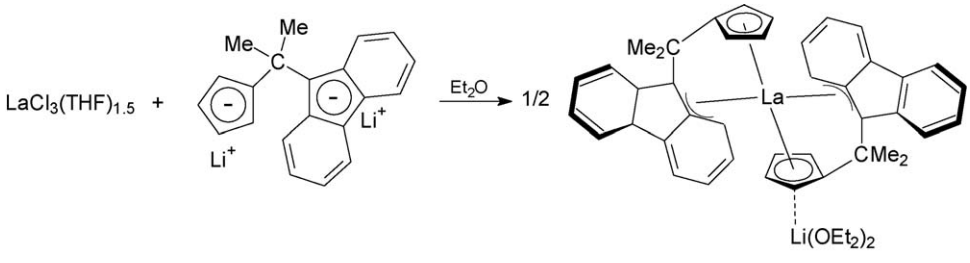

Scheme 43.

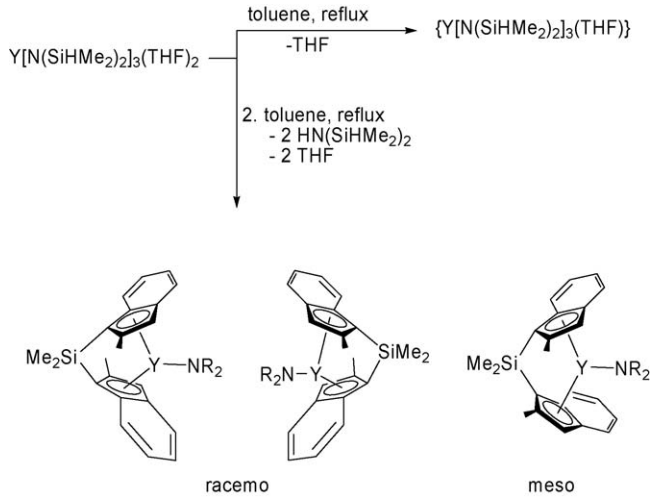

Scheme 44.

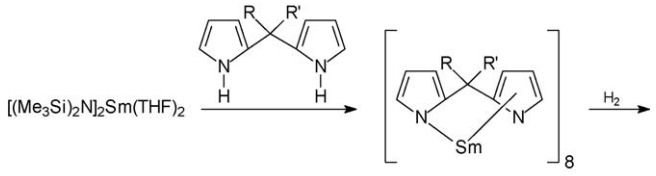

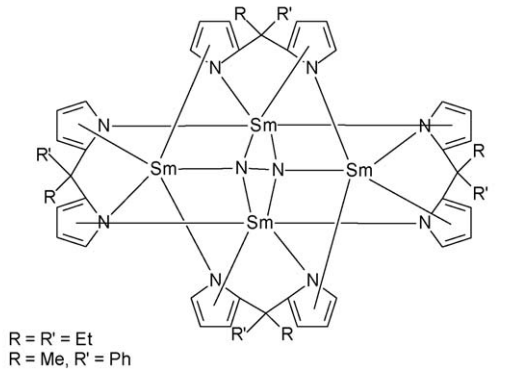

Scheme 45.

η^5-coordinating π-system of another indolate ligand, bridging to the next Eu atom with an sp^2-orbital [164]. Transamination reactions of $Sm[N(SiMe_3)_2]_2(THF)_2$ with dipyrrolylmethanes under nitrogen as illustrated in Scheme 45 produced unusual tetranuclear dinitrogen complexes in the form of red crystals. Fig. 56 highlights the molecular structure of the product with

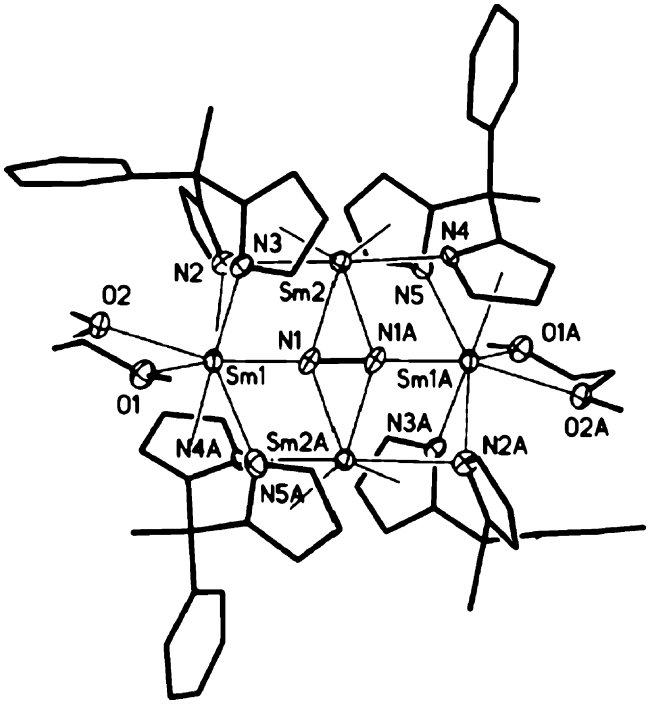

Fig. 56. Molecular structure of $(\mu\text{-}N_2)[\{PhMeC(C_4H_3N)_2Sm\}_4(DME)_2]$ [165].

R = Me and R′ = Ph. In these compounds the dinitrogen unit has undergone a four-electron reduction via cooperative attack of four divalent samarium atoms and remains coordinated both side-on and end-on between the four coplanar metal centers [165].

Several other homoleptic samarium(II) and thulium(II) phospholyl sandwich complexes containing the 2,5-di-*t*-butyl-3,4-dimethylphospholide (=dtp) or 2,5-bis(trimethylsilyl)-3,4-dimethylphospholide (=dsp) ligand have been synthesized (Scheme 46) and structurally characterized. X-ray studies revealed that $[Sm(dtp)_2]_2$ and $[Sm(dsp)_2]_2$ are both dimeric in the solid state due to coordination of the phosphorus lone pairs to samarium (Fig. 57) [166].

Quite in contrast to the centrosymmetric dimers $[Sm(dtp)_2]_2$ and $[Sm(dsp)_2]_2$, a crystal structure determination revealed that the emerald-green thulium derivative $(dtp)_2Tm$ is an unsolvated, monomeric complex und is thus the first homoleptic sandwich complex of thulium(II) (Fig. 58) [166].

Like the decamethyllanthanidocenes, the bis(phospholyl)-lanthanide(II) sandwich complexes exhibit an interesting derivative chemistry. For example, addition of azobenzene to the

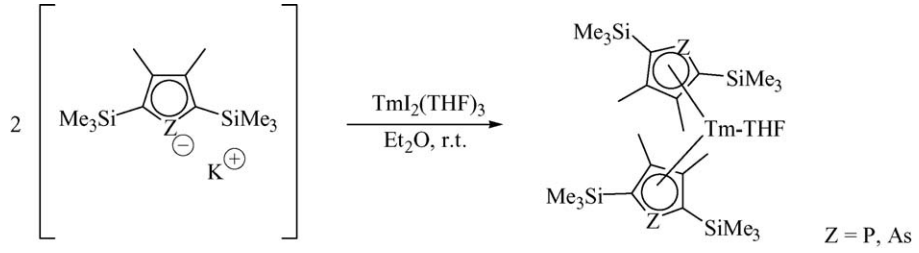

Scheme 46.

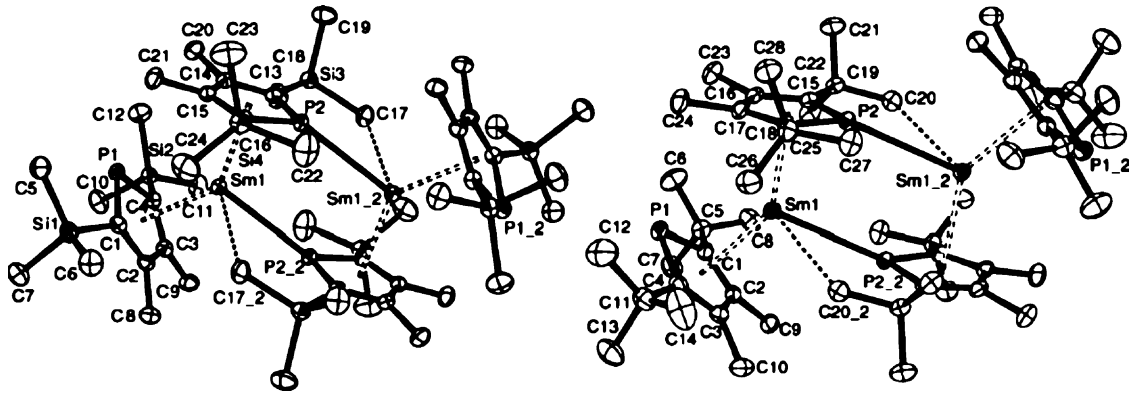

Fig. 57. Molecular structure of $[Sm(dtp)_2]_2$ and $[Sm(dsp)_2]_2$ [166].

samarium(II) and thulium(II) complexes resulted in the immediate formation of dark blue solutions from which the adducts $(dtp)_2Tm(N_2Ph_2)$ (Fig. 59), $(dsp)_2Sm(N_2Ph_2)$, and $(dtp)_2Sm(N_2Ph_2)$ could be isolated, in which the azobenzene is η^2-coordinated (Scheme 47). In these complexes the N–N bond is substantially elongated relative to free azobenzene and thus indicates reduction of the ligand so that the metal is in the trivalent state [166].

Triphenylphosphine sulfide reacts with $Tm(dtp)_2$ to give the sulfido-bridged binuclear complex $(\mu\text{-}S)[(dtp)_2Tm]_2$, whereas the samarium(II) phospholyl complexes have been found to be unreactive towards Ph_3PS (Scheme 48). The molecular structure of $(\mu\text{-}S)[(dtp)_2Tm]_2$ is shown in Fig. 60 [166].

Prolonged heating of base-free $K[P_3C_2Bu^t]$ and ScI_3 in toluene or mesitylene resulted in formation of a deep red solution from which red crystals of $Sc[P_3C_2Bu^t]_3$ could be isolated (Scheme 49, Fig. 61) [167].

Further treatment of $Sc[P_3C_2Bu^t]_3$ with KC_8 in toluene at low temperature (−78 °C) produced a very deep blue solution, whose color persisted at room temperature. Sublimation of the residue after removal of the volatiles gave very dark blue crystals of $[Sc(P_3C_2Bu^t)_2]_2$ containing formally divalent scandium. The complex is dimeric in the solid state and should best be described as a mixed-oxidation state complex containing both Sc^{I} and Sc^{III} centers (Fig. 62) [167].

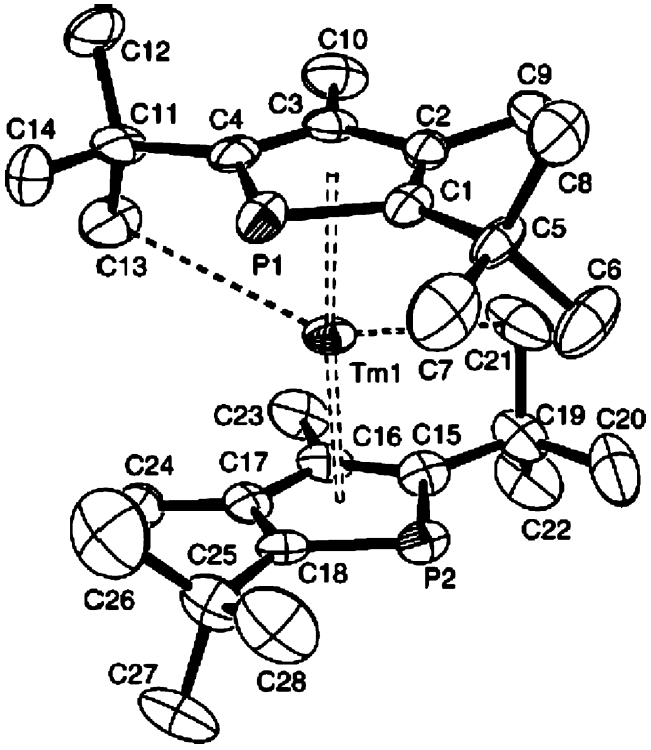

Fig. 58. Molecular structure of $(dtp)_2Tm$ [166].

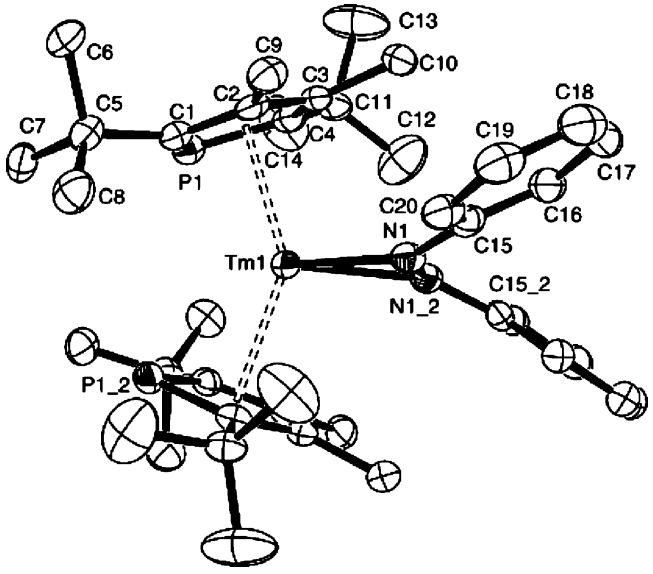

Fig. 59. Molecular structure of $(dtp)_2Tm(N_2Ph_2)$ [166].

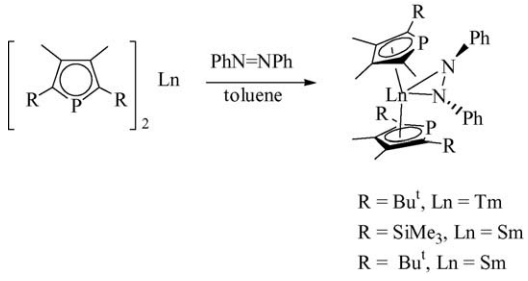

Scheme 47.

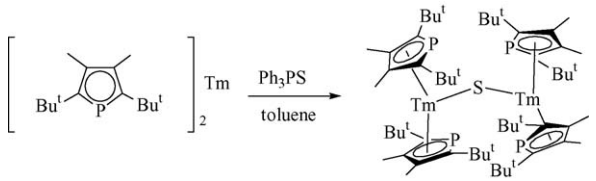

Scheme 48.

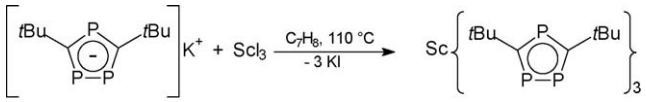

Scheme 49.

2.6.2. Compounds with carboranyl ligands

Reactions of *closo-exo*-5,6-Na(THF)$_2$-1-Na(THF)$_2$-2,4-(SiMe$_3$)$_2$-2,4-$C_2B_4H_4$ with anhydrous $LnCl_3$ (Ln = Dy, Er) at carborane to Ln molar ratios of 3:1 in dry benzene at 60 °C produced novel metallacarboranes, analogues of Cp_3Ln, with the formula [Na$_3$][1,1′-[5,6-(μ-H)$_2$-*nido*-2,4-(SiMe$_3$)$_2$-2,4-$C_2B_4H_4$]-2,2′,4,4′-(SiMe$_3$)$_4$-1,1′-*commo*-Ln-(2,4-$C_2B_4H_4$)$_2$] as yellow crystalline solids in 78 and 82% yields, respectively (Scheme 50, Fig. 63) [168,169], while in the case Ln = La, Nd, Gd, Tb, Ho, and Lu oxide ion-encapsulating tetralanthanide clusters have also been isolated (Figs. 64 and 65 show the holmium derivative) [170,171], and with neodymium an unsolvated "carbons apart" neodymacarborane sandwich stabilized by bis(η^6-benzene) potassium cation has been obtained [172]. For terbium and erbium novel sandwich complexes derived from mixed η^5-pentadienyl and C_2B_4 carborane ligands have been described [173].

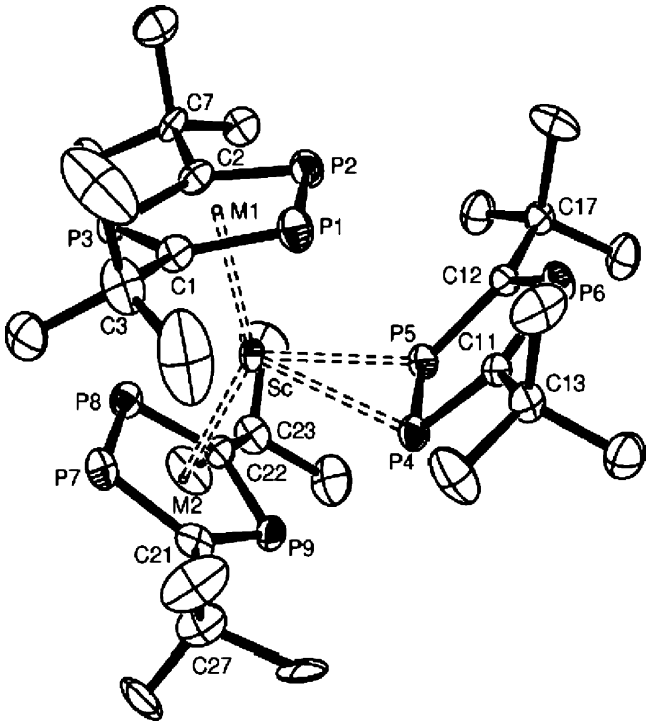

Fig. 61. Molecular structure of Sc[P$_3$C$_2$Bu^t]$_3$ [167].

Among the new classes of lanthanide metallacarboranes are several examples containing η^7-carboranyl ligands. As a typical representative of these unusual compounds, Fig. 66 illustrates the molecular structure of the anion in the erbium derivative [{η^5:η^7-[Me$_2$Si(C$_9$H$_6$)(C$_2$B$_{10}$H$_{11}$)]Er}$_2${Na$_4$(THF)$_8$}]$_n$ containing a Me$_2$Si-bridged indenyl/carborane ligand [174].

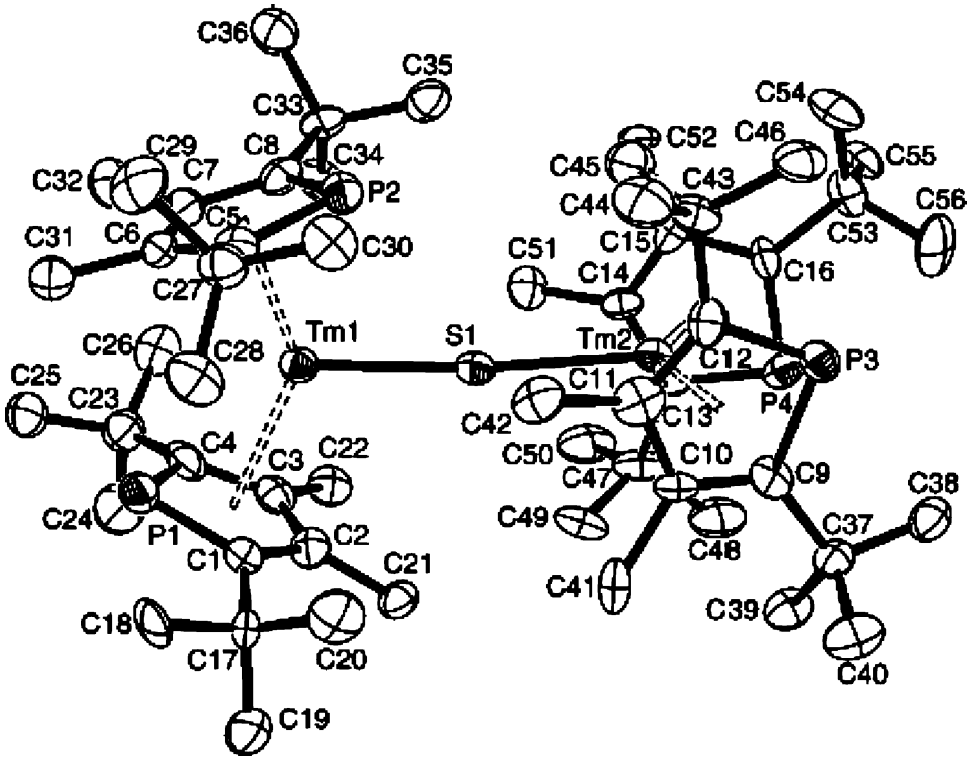

Fig. 60. Molecular structure of (μ-S)[(dtp)$_2$Tm]$_2$ [166].

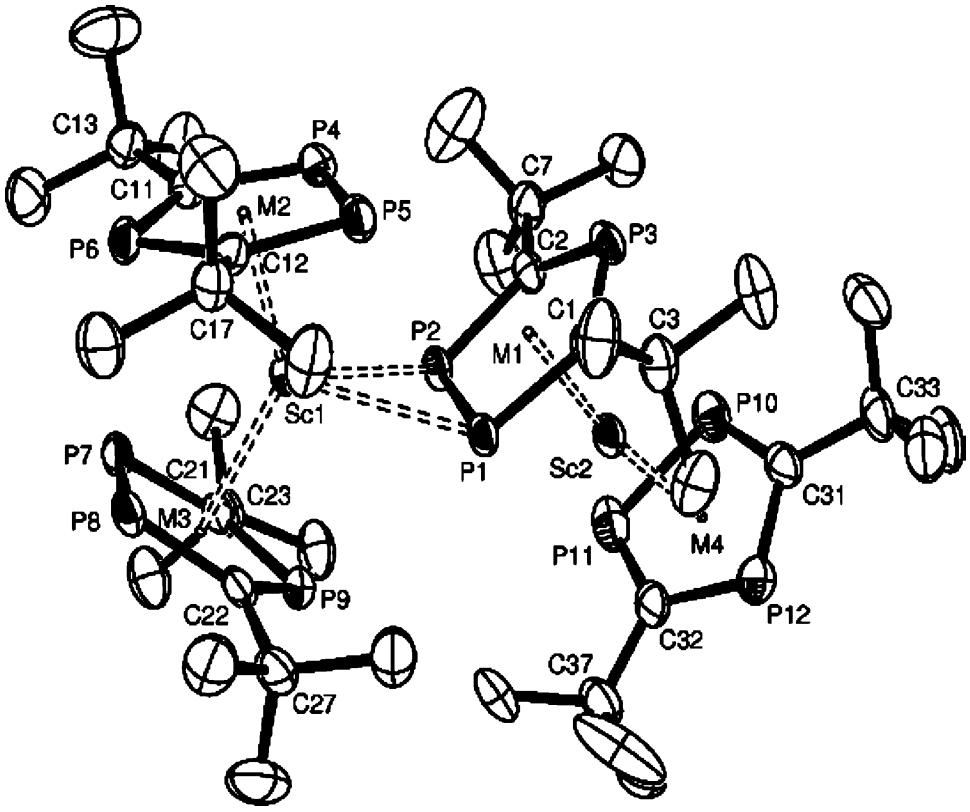

Fig. 62. Molecular structure of $[Sc(P_3C_2Bu^t)_2]_2$ [167].

An interesting variation of the indenyl/carborane ligand system is the introduction of additional donor-functionalized side-chains. New metallacarboranes bearing a (*nido*-$RC_2B_{10}H_{10})_2^{4-}$ ligand, $[\{\eta^5{:}\eta^1{:}\eta^6\text{-}Me_2Si(C_9H_5CH_2CH_2G)(C_2B_{10}H_{10})Sm\}_2(\mu\text{-}Cl)][Li(THF)_4]$ (G = NMe_2, OMe), have been prepared and structurally characterized by treatment of $SmI_2(THF)_x$ with the lithium salt of the ligand via an unexpected samarium-mediated ligand coupling reaction (Scheme 51) [175,176].

A recent addition to organolanthanide carborane chemistry is the use of hydroxyethyl- and alkoxyethyl-*o*-carborane ligands. Scheme 52 illustrates a typical synthetic route leading to an erbium derivative of such ligand system, while Fig. 67 shows the molecular structure of the anionic part of this compound [177].

Numerous organolanthanide complexes derived from the new versatile phosphorus-bridged ligand $Pr^i_2NP(C_9H_7)(C_2B_{10}H_{11})$ have been synthesized [178].

2.7. Arene complexes

The scandium benzene complexes $ScC_6H_6^-$, ScC_6H_6, and $Sc_n(C_6H_6)_m$ (n = 1–3, m = 2–4) have been successfully synthesized using a laser vaporization method [179,180]. Codeposition of a monoatomic lanthanide vapor (Sm, Eu, Tm, Yb) and tri-*t*-butylbenzene, 1,3,5-$Bu^t_3C_6H_3$, onto a cold (77 K) surface afforded matrices that contained zerovalent bis(η^6-arene)lanthanide complexes of the form Ln(η^6-$C_6H_3Bu^t_3$-1,3,5)$_2$ as formed in macroscale co-condensation reactions using metal vapor synthetic (MVS) techniques. Holmium capor reacts

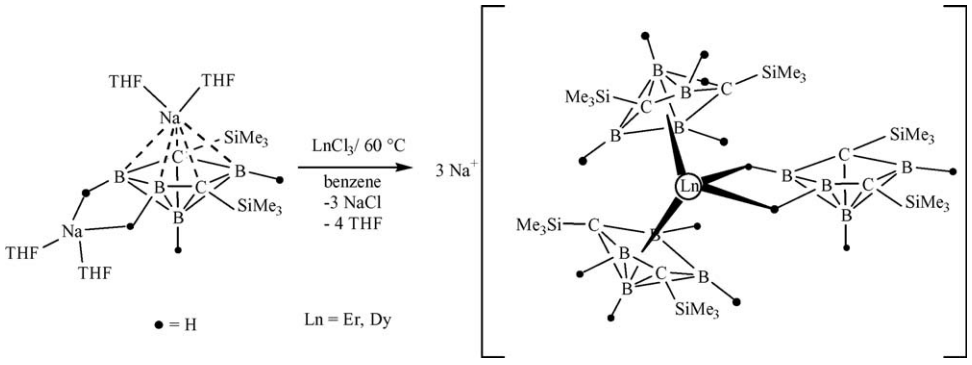

Scheme 50.

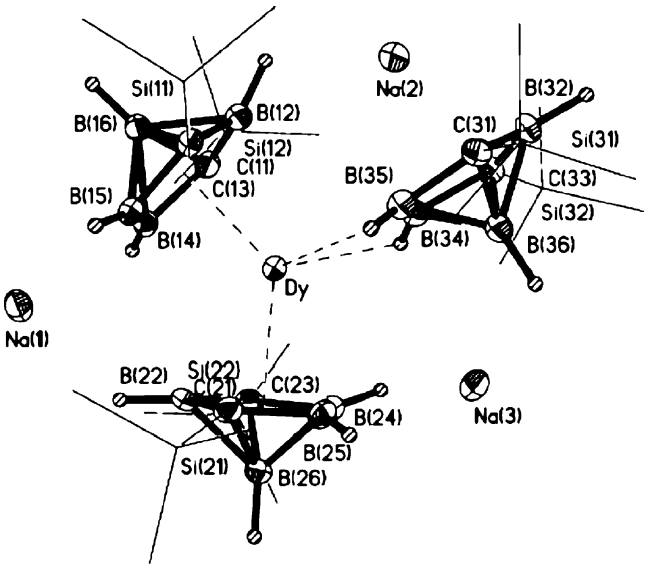

Fig. 63. Molecular structure of $[Na_3][1,1'$-$[5,6$-$(\mu$-$H)_2$-*nido*-2,4-$(SiMe_3)_2$-2,4-$C_2B_4H_4]$-2,2′,4,4′-$(SiMe_3)_4$-1,1′-*commo*-Dy-$(2,4$-$C_2B_4H_4)_2]$ [168].

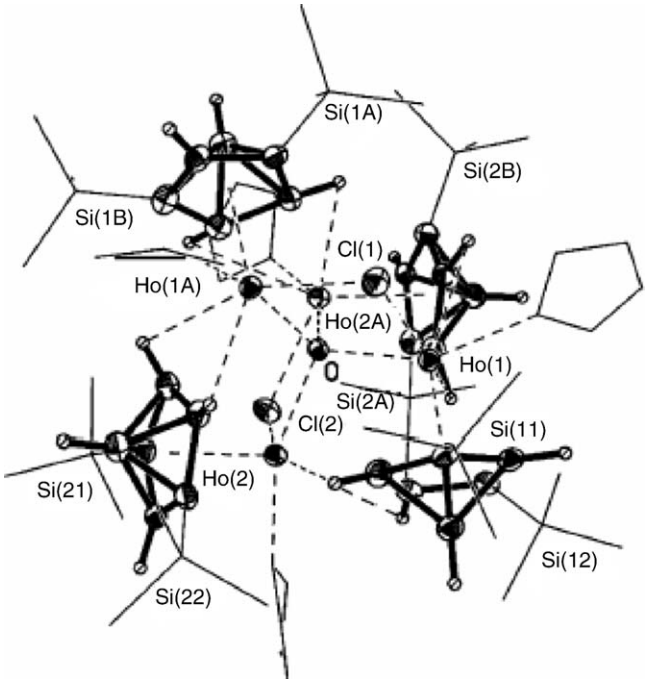

Fig. 64. Molecular structure of $(\mu$-Cl$)(\mu_4$-O$)[1$-Ho-(THF)-2,3-$(SiMe_3)_2$-2,3-$C_2B_4H_4]_4$ [170].

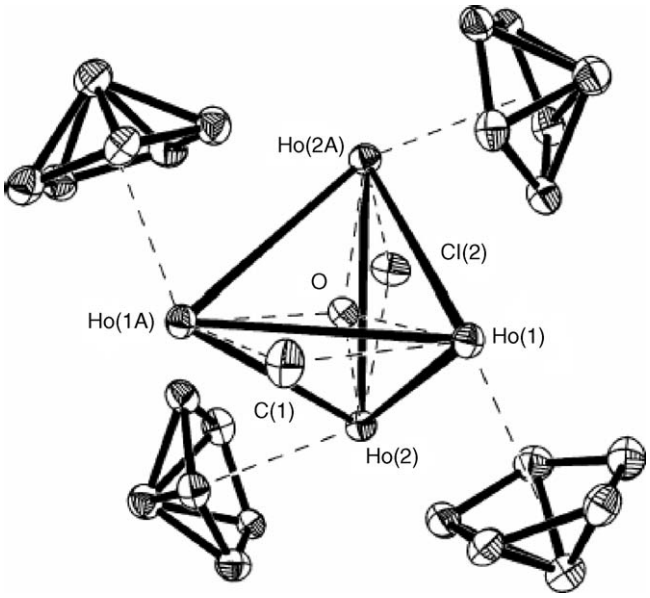

Fig. 65. Molecular structure of the $[(C_2B_4Ho)_4Cl_2O]$ cluster core in $(\mu$-Cl$)(\mu_4$-O$)[1$-Ho-(THF)-2,3-$(SiMe_3)_2$-2,3-$C_2B_4H_4]_4$ [170].

with 2,4,6-tri-*t*-butylphosphorin to afford the zerovalent heteroarene lanthanide complex $Ho(\eta^6$-$PC_5H_2Bu^t{}_3$-2,4,6$)_2$, the first structurally characterized complex of this class. Gram quantities of the compound are formed in 45% yield as extremely air- and moisture-sensitive, purple iridescent crystals, which can be recrystallized from pentane. The novel sandwich complex sublimes at 160 °C (10^{-5} mbar) with 90% recovery [181].

Bridging acenaphthylene was found in the binuclear lanthanum complex $(\mu$-$C_{12}H_8)[LaI_2(THF)_3]_2$ [182]. η^6-Arene coordination has been reported for a series of cationic scandium complexes containing β-diketiminato ligands [183].

2.8. Lanthanide cyclooctatetraenyl compounds

2.8.1. Mono(cyclooctatetraenyl) lanthanide(III) compounds

The dimeric mono(cyclooctatetraenyl)lanthanide chlorides $[(COT)Ln(\mu$-Cl$)(THF)_2]_2$ are long known and still represent the most useful precursor in (COT)Ln chemistry. An alternative preparation of the Sm derivative involves the reaction of samarium metal with cyclooctatetraene in THF in the presence of a small amount of $HgCl_2$. The molecular structure of $[(COT)Sm(\mu$-Cl$)(THF)_2]_2$ has been determined [184].

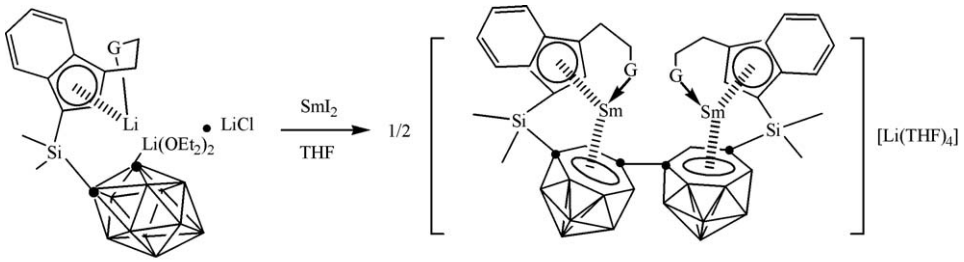

G = NMe_2, OMe

Scheme 51.

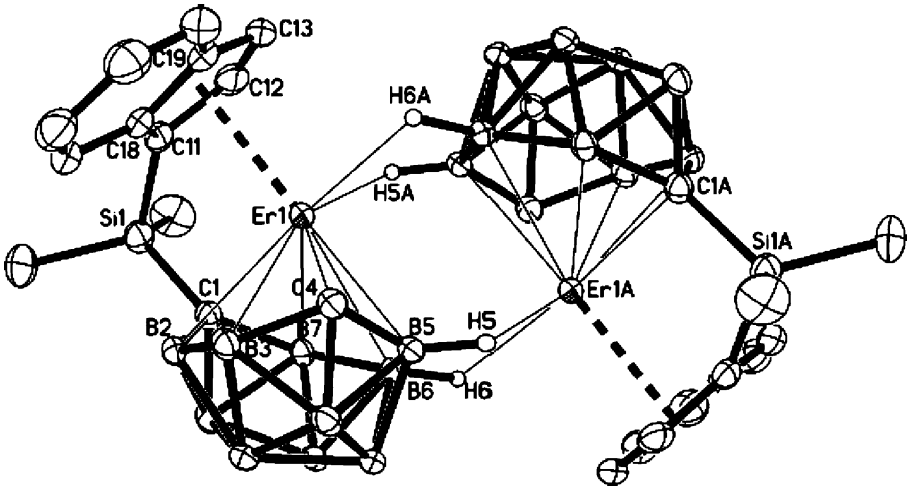

Fig. 66. Molecular structure of the anion in $[\{\eta^5{:}\eta^7\text{-}[Me_2Si(C_9H_6)(C_2B_{10}H_{11})]Er\}_2\{Na_4(THF)_8\}]_n$ [174].

Diphoshinoamide complexes of the type (COT)Ln[N(PPh_2)$_2$](THF) have been prepared with Ln = La and Sm, and both complexes have been structurally characterized [185]. Terphenyl cyclooctatetraenyl samarium complexes of the type (COT)Sm(Dpp)(μ-Cl)Li(THF)$_3$, (COT)Sm(Dmp)(THF), and (COT)Sm(Danip)(THF) (Dpp = 2,6-diphenylphenyl; Dmp = 2,6-dimesitylphenyl; Danip = 2,6-di(*o*-anisyl)phenyl) have been synthesized in a one-pot reaction from $SmCl_3$, K_2COT and the corresponding terphenyllithium derivative [20]. (COT)Tm(Dmp)(THF) displays an analogous molecular structure [186].

2.8.2. *Bis(cyclooctatetraenyl) lanthanide(III) compounds*

Structural investigations have been carried out on the anionic sandwich complexes [Li(THF)$_3$][Tm(COT)$_2$] [187] and [Li(THF)$_2$][Sc(COT)$_2$] [188].

2.8.3. *Cerocenes*

An efficiently modified synthesis for the long-known parent cerocene has been published, which involves oxidation of K[Ce(COT)$_2$] with allyl bromide. An electrochemical study of cerocene showed redox with the cerate ion [Ce(COT)$_2$]$^-$ to be reversible with a relatively low reduction potential (−0.6 V versus NHE). The corresponding praseodymium salt, K[Pr(COT)$_2$] does not undergo comparable reversible oxidation [189].

2.9. *Lanthanide metallofullerenes*

Three isomers of $Y_2C_2@C_{82}$ have been synthesized and chromatographically isolated (Fig. 68) [190].

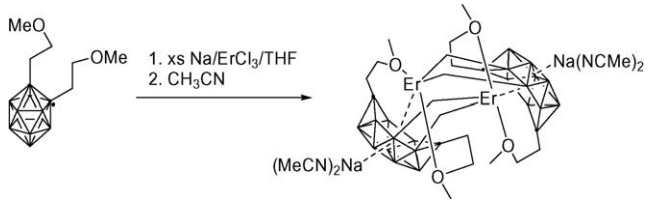

Scheme 52.

Quantized rotational states of a diatomic C_2 unit have been observed in the solid endohedral metallofullerene $C_2Sc_2@C_{84}$ [191]. A photofragmentation study of metal fullerides $C_{60}Ln_x$ (Ln = Y, La, Sm) by excimer laser ablation-TOF mass spectrometry showed that various kinds of metallofullerenes are observed in both the positive and negative ionic modes. For $C_{60}Sm_x$, the metal atom is incorporated into the network of the fullerene cage to replace one carbon atom of the cage forming substitutional metallofullerenes. In the case of the metal fullerides $C_{60}Ln_x$ (Ln = Y, La), evidence for encapsulation of Y and La atoms in the fullerene cages forming endohedral fullerenes has been observed [192]. The configuration of the La ions of $La_2@C_{80}$ in the [80]fullerene cage has been investigated by use of quantum-chemical calculations [193].

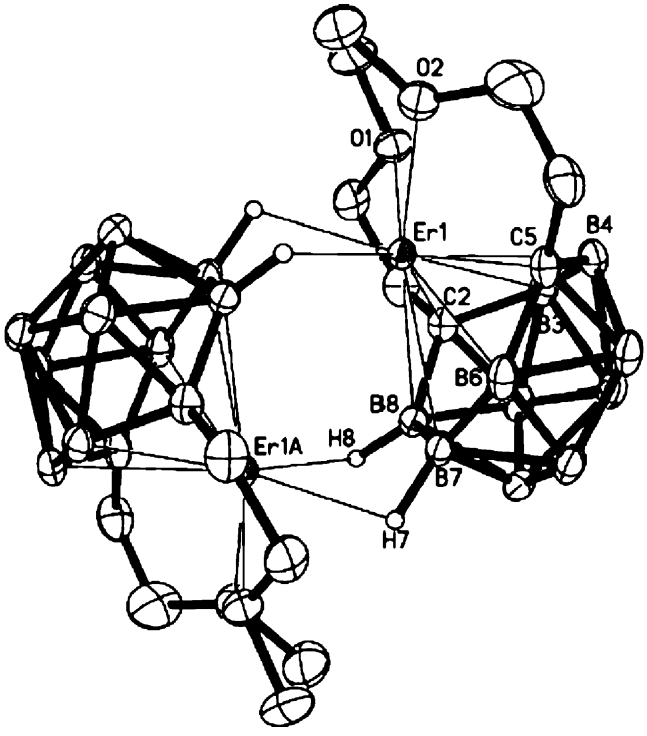

Fig. 67. Molecular structure of the $\{\eta^7\text{-}[(CH_3OCH_2CH_2)_2C_2B_{10}H_{10}]Er\}_2^{2-}$-anion [177].

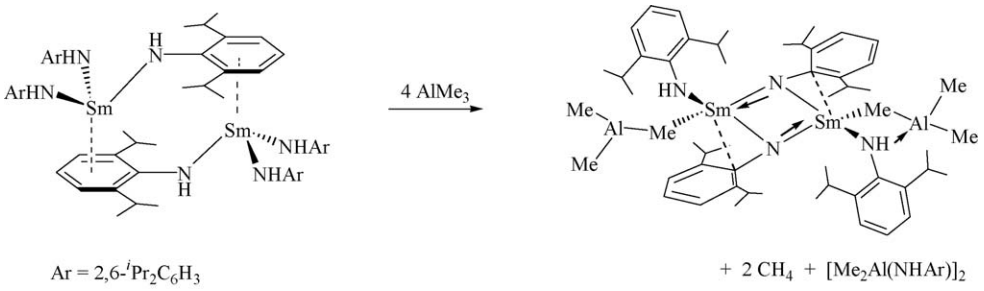

Scheme 53.

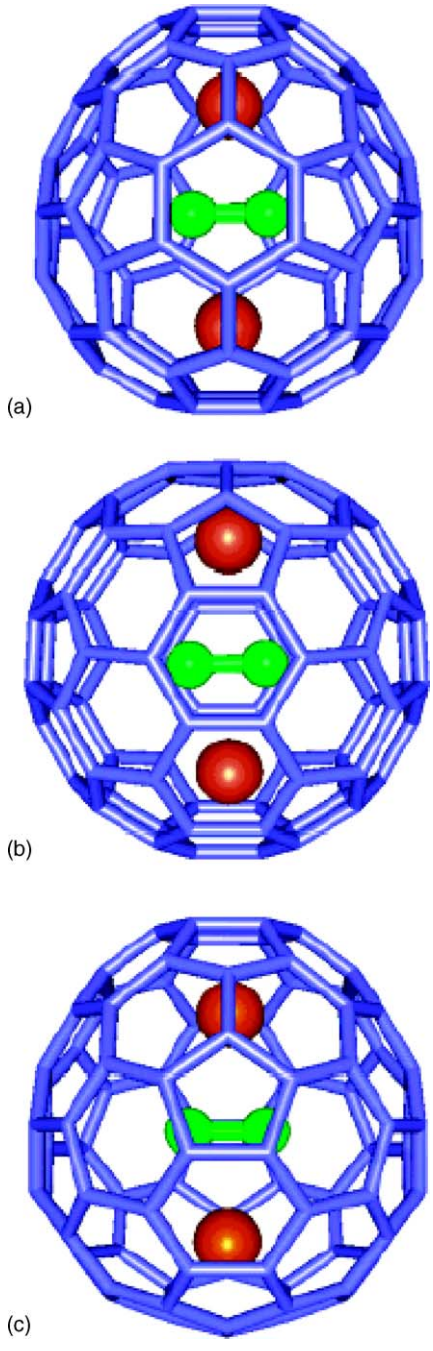

Fig. 68. Molecular structure of the three isomers of $Y_2C_2@C_{82}$ consistent with the ^{13}C NMR results [190].

2.10. Heterobimetallic organolanthanide complexes

Synthetic routes to the Yb/Al complexes $Cp^*_2Yb(AlMe_4)$ and $[Cp^*_2Yb(ER)(AlMe_3)_2]_2$ (ER = OBu^t, SPh, SC_6H_4Me-*p*, TePh) have been developed [194]. Treatment of the dimeric arylimido complex $[Sm(NHAr)_3]_2$ (Ar = 2,6-$Pr^i_2C_6H_3$) with trimethylaluminum resulted in formation of an unusual imido-bridged heterobimetallic samarium–aluminum complex (Scheme 53) [195].

A novel type of metallotropic tautomerism, i.e. reversible and equilibrium isomerization of η^5-bis(Me_3Si-fluorenyl)–rare earth metal complexes to η^6-bis(Me_3Si-fluorene-AlR_3)–rare earth metal complexes, has been reported (Scheme 54). This metallotropic tautomerism was realized by the addition of AlR_3 to the former complexes. η^6-Bis(Me_3Si-fluorenyl-$AlMe_3$)Sm was synthesized by the reaction of η^5-bis(Me_3Si-fluorenyl)Sm$(THF)_2$ with excess $AlMe_3$. The corresponding reaction of excess $AlEt_3$ with η^5-bis(Me_3Si-fluorenyl)Sm$(THF)_2$ gave η^6-bis(Me_3Si-fluorenyl-$AlEt_3$)Sm [196].

The reaction of $[(COT)Sm(\mu\text{-}Cl)(THF)_2]_2$ with $Na[CpCo\{P(O)(OEt)_2\}_3]$ in a molar ratio of 1:2 in THF solution afforded orange $(COT)Sm[CpCo\{P(O)(OEt)_2\}_3]$ as the first organolanthanide containing Kläui's tripod ligand (Scheme 55) [197].

2.11. Organolanthanide catalysis

2.11.1. Organolanthanide-catalyzed oligomerization reactions

Different types of organolanthanide complexes have been found to catalyze the oligomerization of phenylisocyanate [198]. A novel *Z*-selective head-to-head dimerization of termi-

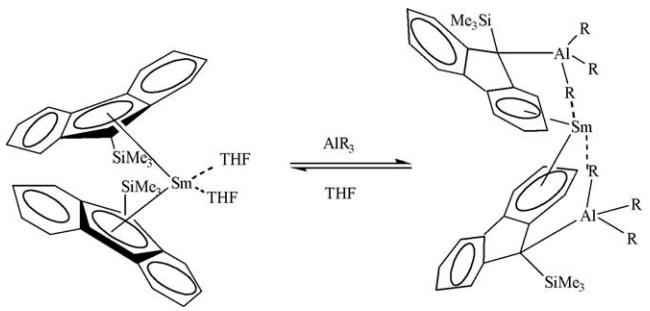

Scheme 54.

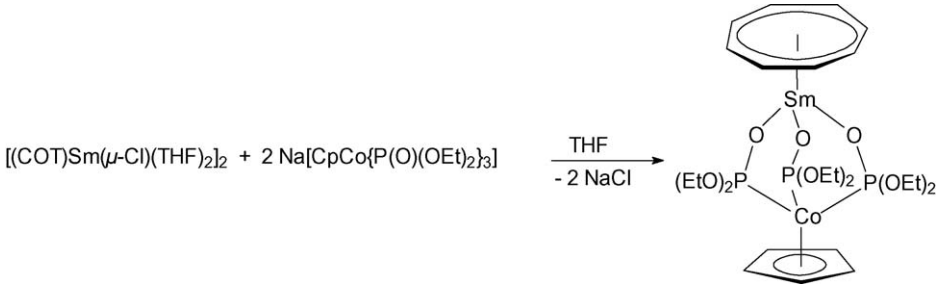

Scheme 55.

nal alkynes has been achieved with the use of "constrained-geometry" lanthanide half-sandwich complexes as catalysts [199].

2.11.2. Organolanthanide-catalyzed polymerization reactions

2.11.2.1. Review. "Developments of rare earth metal catalysts for olefin polymerization" have been highlighted by Yasuda et al. [196].

2.11.2.2. Monoolefins (ethylene, propene, styrene, etc.). A series of lanthanide metallocene catalysts are active in the regioselective ring-opening polymerization of strained *exo*-methylenecycloalkanes to yield *exo*-methylene-functionalized polyethylenes [200–202]. A quantum-chemical molecular dynamics simulation study of the ring opening of methylenecyclopropane catalyzed by the lanthanocene Cp_2LaH has been published [203].

Highly syndiospecific polymerization has also been achieved by allyl lanthanide complexes of the type $[Me_2C(Flu)(C_5H_4)]Ln(\eta^3\text{-}C_3H_5)$ (Ln = Y, La, Sm) [204] and with scandium half-metallocenes such as $(C_5Me_4SiMe_3)Sc(CH_2SiMe_3)_2(THF)$ [205]. Diphenylphosphine has been shown to be an efficient chain transfer agent in organolanthanide-catalyzed ethylene polymerization, yielding phosphine-terminated polyethylenes. This reaction is a versatile, efficient way of incorporating an electron-rich functional group into an otherwise inert polymer [206]. A similar strategy has been followed to synthesize polyolefins end-functionalized with nitroxide derivatives [207].

2.11.2.3. Dienes (butadiene, isoprene, etc.). The stereospecific polymerization of butadiene with $Li[Nd(\eta^3\text{-}C_3H_5)_4]\cdot 1.5$dioxane, $Li[CpNd(\eta^3\text{-}C_3H_5)_3]\cdot 2THF$, $Li[Cp^*Nd(\eta^3\text{-}C_3H_5)_3]\cdot 3DME$ and $(\eta^3\text{-}C_3H_5)_2Nd(\mu\text{-}Cl)_2MgCl(THF)$ as catalysts has been reported [208,209]. The same authors also published the synthesis of neutral tris(allyl)-lanthanide complexes $La(\eta^3\text{-}C_3H_5)_3\cdot 1.5$dioxane and $Nd(\eta^3\text{-}C_3H_5)_3\cdot$dioxane and their test as "single site" catalysts for the stereospecific polymerization of butadiene. The title complexes were obtained by reaction of tetrakis(allyl)lanthanide(III) complexes $Li[Ln(C_3H_5)_4]\cdot 1.5$dioxane (Ln = La or Nd) with BEt_3 in dioxane. The compounds catalyzed the 1,4-*trans*-polymerization of butadiene in toluene with high selectivity. By addition of proper Lewis acids, such as Et_2AlCl, $EtAlCl_2$ or $(MeAlO)_x$, catalysts for the 1,4-*cis*-polymerization are obtainable. The results allowed first conclusions on the mechanism of the lanthanide-complex-catalyzed butadiene polymerization [210]. Various supported La and Nd allyl complexes have also been investigated as highly active single-site catalysts for the 1,4-*cis*-polymerization of butadiene [211]. (Allyl)neodymium intermediates have been discussed for the butadiene polymerization and copolymerization of butadiene with styrene and glydidyl methacrylate using well-defined neodymium alkoxides/aryloxides in combination with dialkylmagnesium reagents as catalysts [212], while the *ansa*-metallocenes $[Me_2Si(C_5H_3SiMe_3\text{-}3)_2]NdCl$ or $[Me_2Si(C_{13}H_8)_2]NdCl$ in combination with Bu^nLi and $AlHBu^i_2$ have been found to be efficient and unique catalysts for the copolymerization of ethylene with butadiene [213,214].

Addition of appropriate co-catalysts such as MMAO (=modified methylaluminoxane) or $AlR_3/[Ph_3C][B(C_6F_5)_4]$ to the samarocene complexes $Cp^*_2Sm(THF)_2$ or $Cp^*_2Sm(\mu\text{-}Me)_2AlMe_2$ also afforded catalytic systems for stereospecific 1,4-*cis*-living polymerization of butadiene and copolymerization of butadiene with styrene [215]. Stereospecific polymerization of isoprene with molecular and MCM-48-grafted lanthanide(III) tetraalkylaluminates such as $Ln[(\mu\text{-}Me)_2AlMe_2]_3$ has been reported [216,217]. The novel complexes $[Cp^*_2Ln][B(C_6F_5)_4]$ (Ln = Pr, Nd, Gd) in combination with $AlBu^i_3$ efficiently induce highly 1,4-*cis*-specific polymerization of butadiene. The activity of the Gd complex/$AlBu^i_3$ system is high enough to exhibit good catalytic activity even at low temperature. Polymerization at −78 °C gave polybutadiene with nearly perfect 1,4-*cis*-microstructure (>99.9%) with a sharp molecular weight distribution ($M_w/M_n = 1.45$) and in reasonable yield [129]. Other organolanthanide complexes which have been reported to effectively catalyze diene polymerization include the new divalent samarocenes $(C_5Me_4Pr^n)_2Sm(THF)$ and $(C_5H_2Ph_2\text{-}1,2,4)_2Sm(THF)$ [218], mixed cyclopentadienyl/β-diketiminate complexes of Sm and Nd [219], and Nd complexes supported by a dianionic modification of the 2,6-diiminopyridine ligand [220].

2.11.2.4. Cyclic esters and amides (ε-caprolactone, L-lactide, etc.). Ring-opening polymerization and block copolymerization of L-lactide has also been achieved with the divalent samarocene complexes $(C_5H_4C_5H_9)_2Sm(THF)_2$ as catalyst [221], while D,L-lactide is effectively polymerized using $Cp^*_2SmMe(THF)$ [222]. The complexes $[(C_5H_4SiMe_3)_2Sm(\mu\text{-}$

Me)]$_2$ and [{$C_5H_3(SiMe_3)_2$-1,3}$_2$Ln(μ-Me)]$_2$ (Ln = Nd, Sm) perform the block copolymerization of L-lactide with ε-caprolactone in high yields in the absence of any co-catalysts [223]. The guanidinate lanthanide methyl complexes [$(Me_3Si)_2NC(NPr^i)_2$]$_2$Ln(μ-Me)$_2$Li(TMEDA) (Ln = Nd, Yb) have been established as effective single-component initiators for ε-caprolactone polymerization [27]. Other organolanthanide complexes which have been reported to catalyze the (co-)polymerization of ε-caprolactone and/or ethylenecarbonate include homoleptic lanthanide guanidinate complexes [224], $Cp^*_2Sm(BH_4)(THF)$ [225], and sterically hindered lanthanide allyl complexes [56].

2.11.2.5. Acrylic monomers (methylmethacrylate (MMA), acrylonitrile, etc.). Block copolymerizations of higher 1-olefins with traditional polar monomers have been achieved using metallocene-type single-component lanthanide initiators [226]. The polymerization of acrylate-based macromonomers to cylindrical brushes initiated by organolanthanides has been reported [227,228]. Other complexes which have been found to exhibit high catalytic activity in the polymerization of MMA include the samarocene derivative $Cp^*_2SmMe(THF)$ supported on mesoporous silicates [229], Yb[$C(SiMe_3)_3$]$_2$ [230], bis(pyrrolylaldiminato)samarium hydrocarbyl complexes [43], divalent ytterbium complexes containing β-diketiminate ligands [70], a Sm(II) allyl complex [54], *ansa*-bis(allyl) lanthanide complexes [58], bis- and tetrakis(trimethylsilyl)-substituted lanthanocene methyl complexes such as [$(C_5H_4SiMe_3)_2$Sm(μ-Me)]$_2$ and [{$C_5H_3(SiMe_3)_2$-1,3}$_2$Ln(μ-Me)]$_2$ (Ln = Nd, Sm) [223], guanidinate lanthanide methyl complexes of the type [$(Me_3Si)_2NC(NPr^i)_2$]$_2$Ln(μ-Me)$_2$Li(TMEDA) (Ln = Nd, Yb) [27], bis(arylamido)lanthanide methyl complexes [141], Cp_2Ln complexes containing piperonaldimethylacetal as ligand [231], silylene-bridged *ansa*-bis(fluorenyl)lanthanide complexes [232], pendant phenylcyclopentadienyl lanthanide complexes [233], sterically hindered allyl lanthanide complexes [56], and benzyl-substituted cyclopentadienyl lanthanide complexes [234].

2.11.2.6. Other monomers. The regio- and stereoselective polymerization of aromatic diynes catalyzed by lanthanide metallocenes such as $Cp^*_2PrCH(SiMe_3)_2$ has been investigated [235].

2.11.3. Organolanthanide-catalyzed hydrosilylation reactions

Commercially available lanthanum-tris[bis(trimethylsilyl)amide] has been shown to be a very effective catalyst for the hydrosilylation of representative alkenes and dienes in the presence of $PhSiH_3$ [236]. Dimeric yttrium hydrido complexes containing the pendant-arm cyclopentadienyl ligand $[C_5Me_4CH_2SiMe_2NBu^t]^-$ have been found to catalyze the hydrosilylation of 1,5-hexadiene, 1,7-octadiene and vinylcyclohexene by $PhSiH_3$ [237].

Lanthanide(II)–imine complexes, obtained by reduction of aromatic ketimines with samarium and ytterbium metal, effectively catalyze the hydrosilylation of imines. The proposed catalytic cycle for the imine hydrosilylation is outlined in Scheme 56 [238].

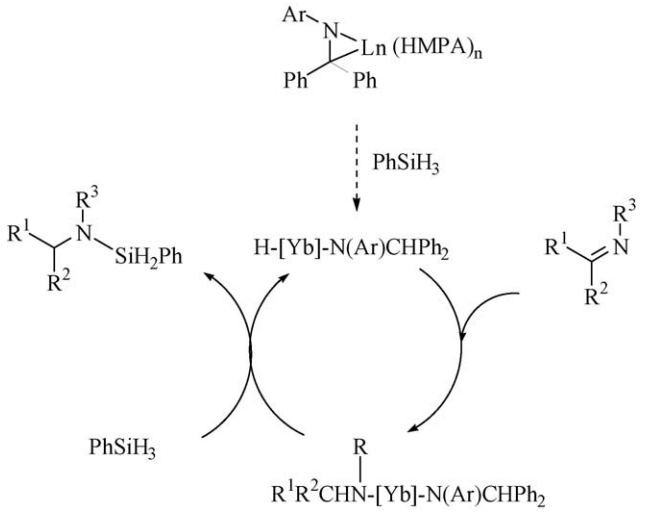

Scheme 56.

2.11.4. Organolanthanide-catalyzed hydroamination reactions

Organo-*f*-element-catalyzed hydroamination has been continuously investigated in 2003 and 2004 [239–241]. The organolanthanide-catalyzed hydroamination/cyclization has also been extended to conjugated aminodienes [242] and amine-tethered unactivated 1,2-disubstituted alkenes (Scheme 57) [243].

The scope of the lanthanide-mediated, intramolecular amination/cyclization reaction has been determined for the formation of substituted quinolizidines, indolizidines, and pyrrolizidines [244], as well as tricyclic and tetracyclic aromatic nitrogen heterocycles [245]. Novel C_2-symmetric bis(oxazolinato)lanthanide catalysts have been introduced as precatalysts for the efficient enantioselective intramolecular hydroamination/cyclization of aminoalkenes and aminodienes [246]. Chiral binaphtholate yttrium aryl complexes have been reported to be highly active and enantioselective catalysts for the asymmetric hydroamination of aminoalkenes, as well as the kinetic resolution of α-substituted 1-aminopent-4-enes to give *trans*-2,5-disubstituted pyrrolidines with good enantiomeric excess and high k_{rel} [247]. Intramolecular hydroamination of alkenes and alkynes has also been reported for yttrium catalysts bearing diamidoamine lig-

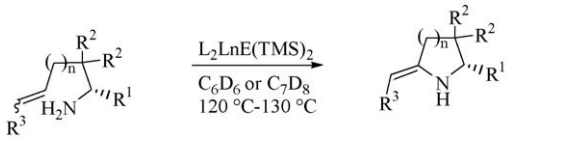

R^1, R^2 = H, Me
R^3 = Me, Et
n = 1, 2

yield : up to 95 %
dr: *trans*/*cis* = 11/1-16/1

Scheme 57.

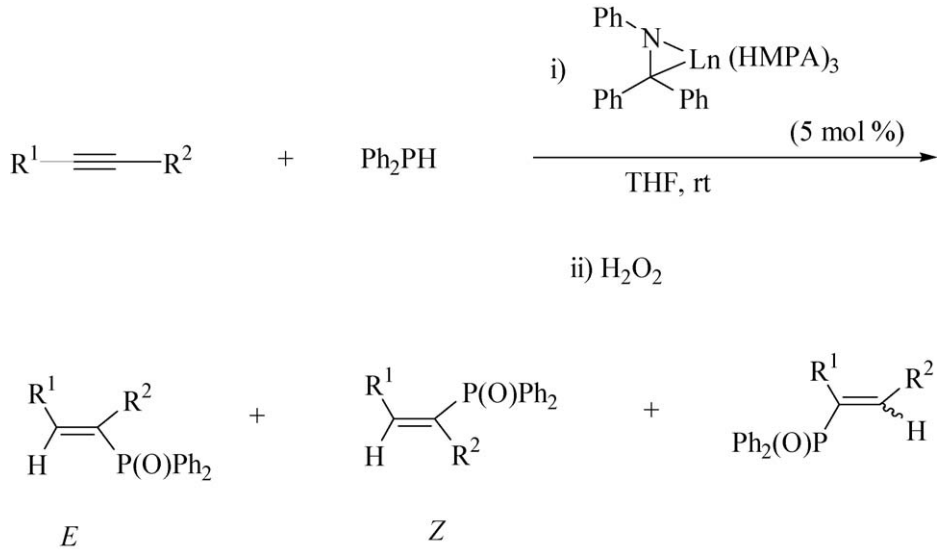

Scheme 58.

ands [39] and a cationic β-diketiminato scandium alkyl complex [248].

Homoleptic lanthanide alkyls of the form $Ln[CH(SiMe_3)_2]_3$ (Ln = Y, La, Nd, Sm, Lu) have been reported to serve as efficient precatalysts for intramolecular homogeneous hydrophosphination reactions. Both phosphinoalkenes and phosphinoalkynes undergo cyclization to the corresponding heterocyclic structures [249]. Intermolecular hydrophosphination of alkynes with diphenylphosphine is catalyzed by a Yb–imine complex, $Yb(\eta^2\text{-}Ph_2CNPh)(HMPA)_3$, to give alkenylphosphines and phosphine oxides after oxidative workup in good yields under mild conditions (Scheme 58). This reaction is also applicable to various carbon–carbon multiple bonds such as conjugated diynes and dienes, allenes, and styrene derivatives. The reaction takes place through insertion of alkynes to a Yb-PPh_2 species, followed by protonation [250].

2.11.5. Other organolanthanide-catalyzed reactions

An exciting new approach for the selective, catalytic conversion of methane has been described. Heating a cyclohexane solution of Ph_2SiH_2 and Cp^*_2ScMe to 80 °C under 150 atm of methane produced 5 equiv. of Ph_2MeSiH after 1 week, 1 equiv. of which was derived directly from Cp^*_2ScMe [251]. The related scandium alkyl $Cp^*_2ScCH_2Bu^t$ was synthesized by the addition of a pentane solution of $LiCH_2Bu^t$ to Cp^*_2ScCl at low temperature. $Cp^*_2ScCH_2Bu^t$ reacts with the C–H bonds of hydrocarbons including methane, benzene, and cyclopropane to yield the corresponding hydrocarbyl complex and CMe_4. High selectivity toward methane activation suggested the participation of this chemistry in a catalytic hydromethylation, which was observed in the slow, Cp^*_2ScMe-catalyzed addition of methane across the double bond of propene to form isobutene [252].

Dimeric bis(indenyl)lanthanide hydrides $[(C_9H_7)_2Ln(\mu\text{-}H)]_2{\cdot}4THF{\cdot}NaCl$ have been found to promote the Claisen rearrangement and selectively reduce carbonyl functions. For example, organolanthanide-catalyzed Claisen rearrangement of $PhCH_2C(O)OCH_2CH{=}CH_2$ in THF gave $PhCH(CHO)(CH_2CH{=}CH_2)$ in 61% yield [155]. Cross-silyl benzoin additions have been reported to be catalyzed by an in situ prepared "$LaBu^n_3/Me_3SiCN$" catalyst system [253].

2.12. Organolanthanides in organic synthesis

A computational study of cyclopropanation reactions of the divalent samarium carbenoid $ISmCH_2I$ with ethylene has been presented. The $ISmCH_2I$ species was found to have a "samarium carbene complex" character with properties similar to previously investigated lithium carbenoids $LiCH_2X$ (X = Cl, Br, I). The $ISmCH_2I$ carbenoid was found to be noticeably different in structure with more electrophilic character and higher chemical reactivity than the closely related classical Simmons–Smith carbenoid $IZnCH_2I$ [254,255]. Organocerium reagents have been employed in the preparation of trisubstituted allylphosphine boranes [256] and in other alkylation reactions [257]. The allylcerium reagent $(CH_2{=}CHCH_2)CeCl_2$ has been prepared in situ by stirring allylmagnesium chloride with cerium trichloride, and used for allylation reactions [258]. The in situ preparation of $Me_3SiC{\equiv}CCeCl_2$ and its reactions with aldehydes have been described [192,259].

Allylsamarium bromide reacts with acyl azides to give the corresponding *gem*-diallylation products, 4-alkyl-1,6-heptadiene-4-ol derivatives, in good to excellent yields. This novel reaction has been described to proceed within a few minutes at room temperature [260]. The nucleophilic substitution of the benzotriazolyl group in the *N*-(α-benzotriazol-1-ylalkyl)amides and *N*-(α-benzotriazol-1-ylalkyl)sulfonamides with allylsamarium bromide has been investigated, and the corresponding homoallylamides or homoallylsulfonamides have been obtained in good to excellent yields [261].

An alkenylcerium reagents (Scheme 59) has been utilized in the total synthesis of sesterpenic acids [262].

Ytterbium and samarium metals reduce aromatic ketimines to give directly divalent azalanthanacyclopropane complexes in quantitative yields (Scheme 60) [238].

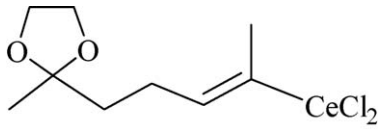

Scheme 59.

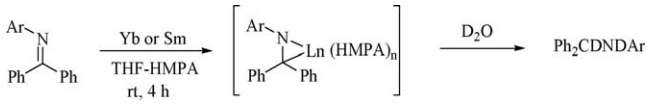

Scheme 60.

The imine complexes have been found to catalyze dehydrogenative silylation of terminal alkynes, hydrosilylation of imines and alkenes, and intermolecular hydrophosphination of alkynes. Moreover, dehydrogenative double silylation of conjugated dienes was achieved with these reagents [238]. Metalation of 1,3-diphenyl-2-benzylpropene by diphenylytterbium followed by addition of Ph_3SnCl afforded $(PhCHSnPh_3)_2C{=}CHPh$ [263].

2.13. Organolanthanides in materials science

Mesoporous niobium oxide with a pore size of 22 Å was treated with excess $Cp^*_2Sm(THF)_2$ in THF to give a new mesoporous niobium oxide composite with a mixed-oxidation state organosamarium phase in the pores [264,265].

Rare earth oxides could represent a valuable alternative to SiO_2 in complementary metal-oxide-semiconductor devices. In this context, the growth of lutetium oxide (Lu_2O_3) films by atomic-layer deposition using the dimeric $[(C_5H_4SiMe_3)_2Lu(\mu\text{-}Cl)]_2$ precursor complex and H_2O has been described. The films were found to be stoichiometric, with Lu_2O_3 composition, and amorphous. Annealing in nitrogen at 950 °C led to crystallization in the cubic bixbyite structure [266].

Rare earth (RE)-group V (RE-V) compounds are of great interest in realizing new functions of high-speed magneto-electronic, magneto-optical devices, semi-metal-base transistors, etc. Erbium phosphide, ErP, has been grown on In(0 0 1) substrates by organometallic vapor phase epitaxy (OMVPE) using the new liquid organolanthanide precursor tris(ethylcyclopentadienyl)erbium, $(C_5H_4Et)_3Er$ [267].

3. Actinides

In 2003 Dormond et al. published a comprehensive review under the title: "Product class 23: organometallic complexes of the actinides" [268].

3.1. Actinide carbonyls

While stable binary actinide carbonyls are still unknown, research in this area focusses mainly on the detection and theoretical investigation of unstable molecules such as the monocarbonyl complexes of thorium and uranium. CUO has been produced experimentally by reaction of laser-ablated U atoms with CO in excess argon and trapped in a triplet state in solid argon at 7 K [269].

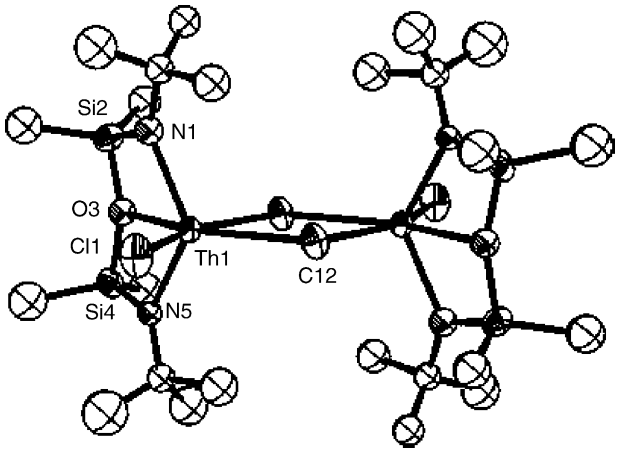

Fig. 69. Molecular structure of $\{[Bu^tNON]Th(\mu\text{-}Cl)\}_2$ [270].

3.2. Actinide hydrocarbyls

The doubly deprotonated diamidosilyl ether ligand $(Bu^tNHSiMe_2)_2O^{2-}$ ($[Bu^tNON]^{2-}$) has been successfully employed in the stabilization of heteroleptic organoactinide complexes. Scheme 61 depicts the preparation of the dimeric halide precursors, which have subsequently been treated with C_3H_5MgCl or $LiCH_2SiMe_3$ to afford stable disubstituted diallyl and dialkyl complexes. The molecular structure of $\{[Bu^tNON]Th(\mu\text{-}Cl)\}_2$ is shown in Fig. 69 [270].

The first examples of compounds with an *N*-heterocyclic carbene ligand coordinated to a low-valent uranium center have been reported in 2004. The synthetic procedures are illustrated in Schemes 62 and 63. Notably, the silylamide derivative (Scheme 63) was isolated in the form of dark blue crystals in excellent yield (>90%). DFT studies indicated a significant degree of π-bonding in the U(III) carbene entity. The solid-state structures of both complexes are depicted in Figs. 70 and 71 [271].

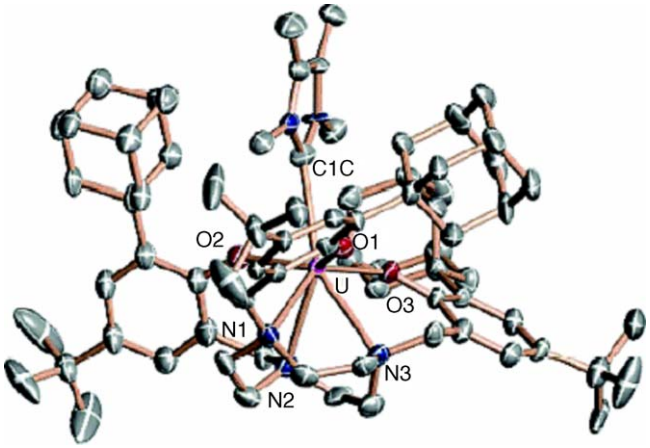

Fig. 70. Molecular structure of $[(^{Ad}ArO)_3tacn]U^{III}(Me_4MC)$ [271].

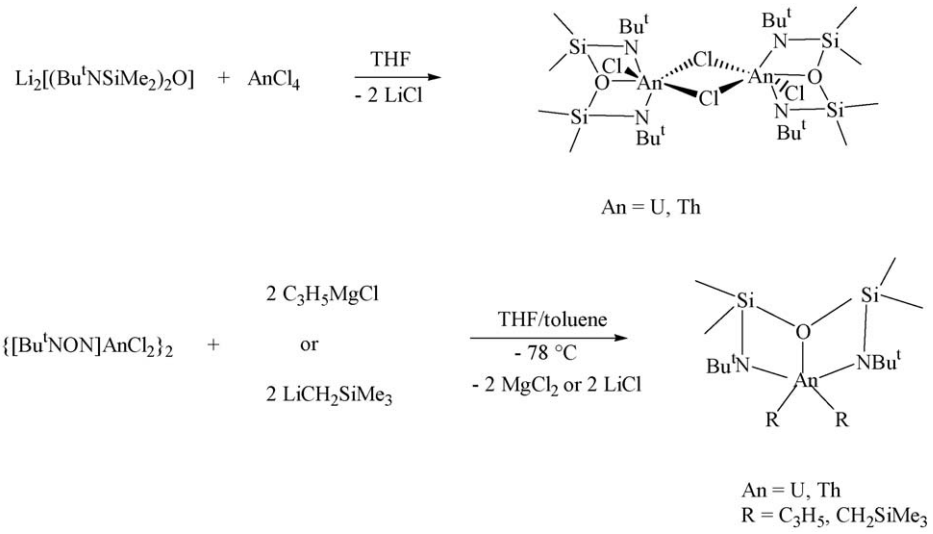

Scheme 61.

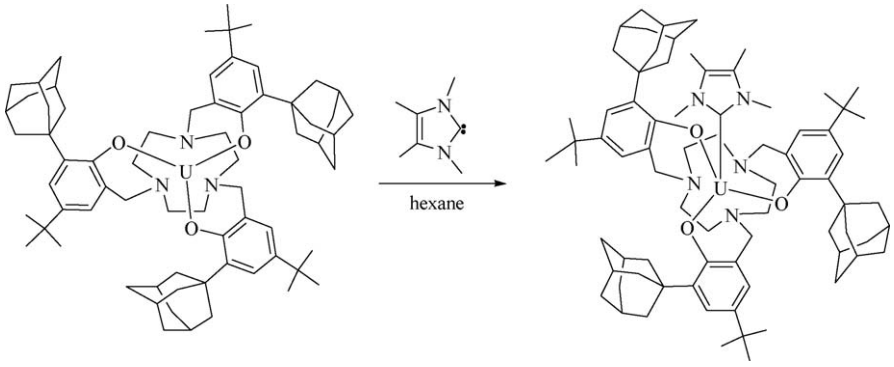

Scheme 62.

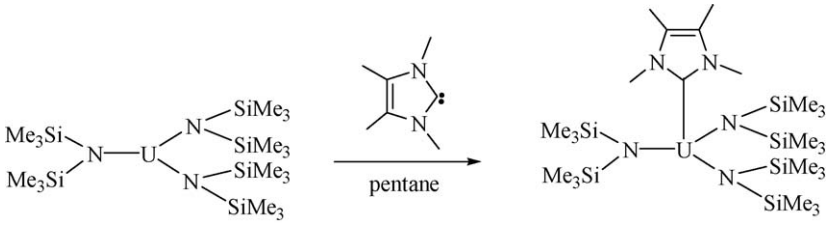

Scheme 63.

A uranyl-carbon bond is also present in the adduct of $[PhC(NSiMe_3)_2]_2UO_2$ with *t*-butylisonitrile. Treatment of a toluene solution of the precursor with Bu^tNC cleanly formed $[PhC(NSiMe_3)_2]_2UO_2(CNBu^t)$ as the first uranyl complex containing a coordinated isonitrile [272].

3.3. Actinide allyls

Significant progress in actinide allyl chemistry has been made through the use of bulky silyl-substituted allyl ligands. Reactions of 4 equiv. of $K[C_3H_4SiMe_3\text{-}1]$ or $K[C_3H_3(SiMe_3)_2\text{-}1,3]$ with $ThBr_4(THF)_4$ in THF at −78 °C cleanly produced the bright yellow complexes $[C_3H_4SiMe_3\text{-}1]_4Th$ (Fig. 72) and $[C_3H_3(SiMe_3)_2\text{-}1,3]_4Th$, respectively, in high yields. In both complexes the central Th atom is tetrahedrally coordinated by four η^3-allyl ligands. In view of the thermal fragility of parent $(C_3H_5)_4Th$ (rapid decomposition at ca. 0 °C) the properties of its counterparts containing trimethylsilylated allyl ligands are striking. For example, bright yellow $[C_3H_3(SiMe_3)_2\text{-}1,3]_4Th$ is indefinitely stable at room temperature in the solid state and in solution under an inert atmosphere. It melts at 122–124 °C (dec.) and tolerates brief (<5 min) exposure to air without noticeable decomposition [273].

Bis(allyl)actinide complexes containing the doubly deprotonated diamidosilyl ether ligand $(Bu^tNHSiMe_2)_2O^{2-}$ ($[Bu^tNON]^{2-}$) have been mentioned in the preceding section [270]. An uncommon η^3-(*N*,*C*,*C*′)-1-azaallyl bonding mode for a β-diketiminato ligand has been

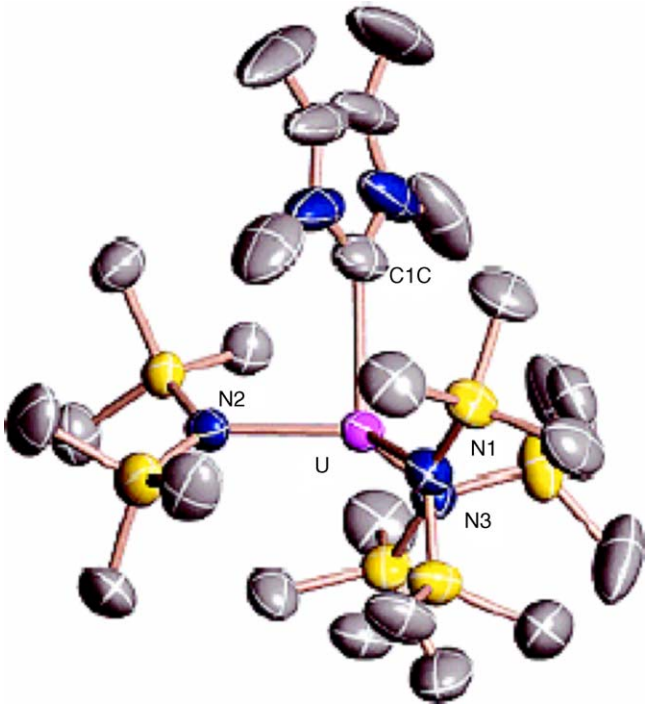

Fig. 71. Molecular structure of $[(Me_3Si)_2N]_3U^{III}(Me_4IMC)$ [271].

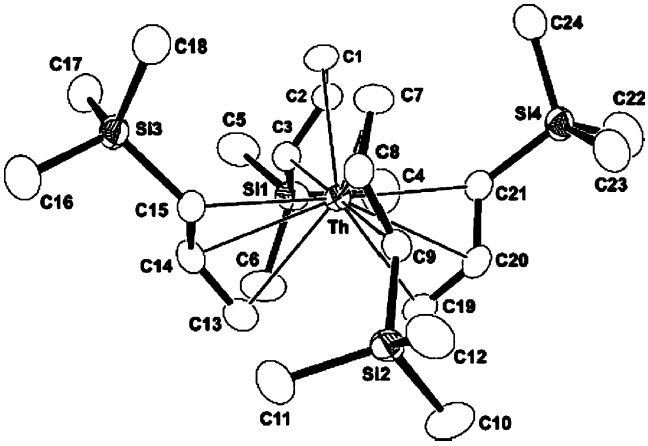

Fig. 72. Molecular structure of $[C_3H_4SiMe_3\text{-}1]_4Th$ [273].

reported for a bis(β-diketiminato)uranium(III) iodide complex. As shown in Scheme 64, reaction of $UI_3(THF)_4$ with 2 equiv. of the sterically demanding K(Nacnac) ($Nacnac^- = [Ar]NC(Me)CHC(Me)N[Ar]$, $Ar = 2,6\text{-}Pr^i{}_2C_6H_3$) in toluene solution at room temperature afforded a bis(β-diketiminato)uranium(III) complex as a dark blue crystalline solid in 42% isolated yield. The molecule features one β-diketiminato ligand bound to the U(III) center in an unusual

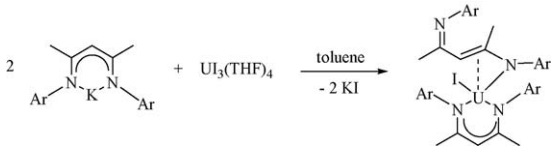

Scheme 64.

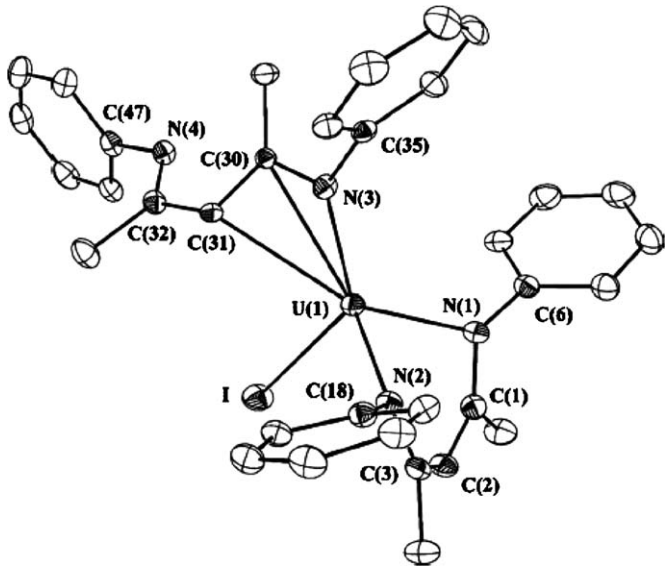

Fig. 73. Molecular structure of the reaction product of $UI_3(THF)_4$ with K(Nacnac) ($Nacnac^- = [Ar]NC(Me)CHC(Me)N[Ar]$, $Ar = 2,6\text{-}Pr^i{}_2C_6H_3$) [274].

η^3-(*N*,*C*,*C*′)-1-azaallyl mode and possesses close $U\cdots C_{alkene}$ contacts (Fig. 73) [274].

3.4. Actinide cyclopentadienyl compounds

3.4.1. Cp_3An and Cp_3AnL compounds

Numerous adducts of $(C_5H_4Bu^t)_3U$ with pyridine derivatives and other six-membered *N*-heterocycles have been prepared and structurally characterized [275]. This reaction also allowed a clear lanthanide(III)/actinide(III) differentiation between $(C_5H_4Bu^t)_3Ce$ and $(C_5H_4Bu^t)_3U$. In contrast to $(C_5H_4Bu^t)_3Ce$, which reacts with pyrazine to give the Lewis-base adduct $(C_5H_4Bu^t)_3Ce$(pyrazine), the uranium analogue was oxidized by the azine molecule to the binuclear U(IV) complex (μ-pyrazine)$[(C_5H_4Bu^t)_3U]_2$ [276].

3.4.2. $CpAnX_3$ and Cp_2AnX_2 compounds

Novel constrained-geometry monocyclopentadienyl actinide complexes have been reported. The complexes $[Me_2Si(C_5Me_4)(NBu^t)]An(NRR')_2$ (Scheme 65, An = Th, U; R = R′ = Me; R = Me, R = Et; R = R′ = Et)

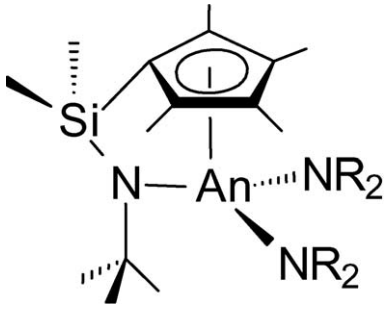

Scheme 65.

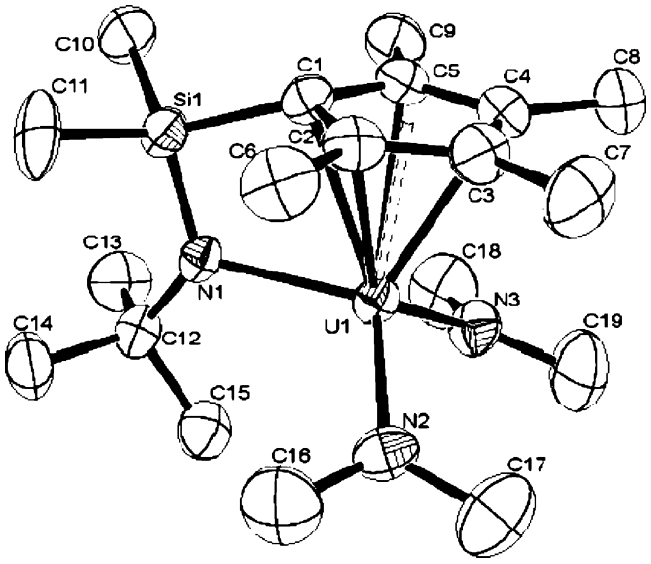

Fig. 74. Molecular structure of $[Me_2Si(C_5Me_4)(NBu^t)]U(NMe_2)_2$ [277].

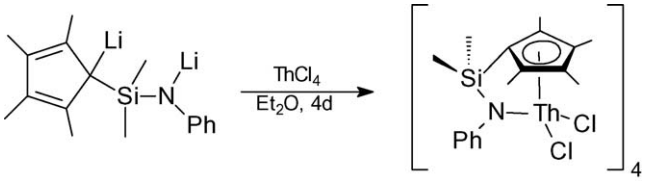

Scheme 66.

were synthesized in high yields and excellent purity, and $[Me_2Si(C_5Me_4)(NBu^t)]U(NMe_2)_2$ was structurally characterized by an X-ray analysis (Fig. 74) [277].

Starting from $ThCl_4$, two new thorium complexes, a tetramer of $[Me_2Si(C_5Me_4)(NPh)]ThCl$ (Scheme 66) and a dimer of $[Li(Et_2O)_2][\{Me_2Si(C_5Me_4)(NBu^t)\}ThCl_3]$ (Scheme 67) have been synthesized and structurally characterized. The tetrameric structure of $\{[Me_2Si(C_5Me_4)(NPh)]ThCl\}_4$ is illustrated in Fig. 75, while Fig. 76 depicts the solid-state structure of the dimer $[Li(Et_2O)_2][\{Me_2Si(C_5Me_4)(NBu^t)\}ThCl_3]_2$ [278].

3.4.3. Pentamethylcyclopentadienyl compounds

The pentamethylcyclopentadienyl ligand remains *the* most important ligand in organoactinide chemistry. It has been very successfully employed in the stabilization of novel organoactinide complexes and in organoactinide catalysis.

3.4.3.1. Cp^*AnX_2 and $Cp^*{}_2AnX$ compounds. Oxidation of the sterically crowded complex $Cp^*{}_3U$ provided access to $(\mu\text{-}O)[Cp^*{}_2U]_2$ as the first molecular trivalent uranium oxide. The U–O–U angle in this molecule is 171.5(6)° (Fig. 77) [279].

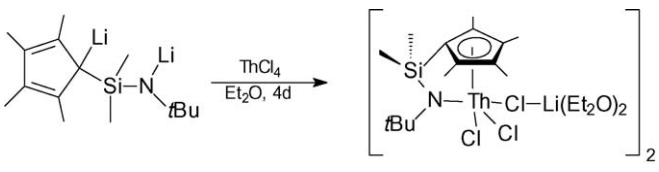

Scheme 67.

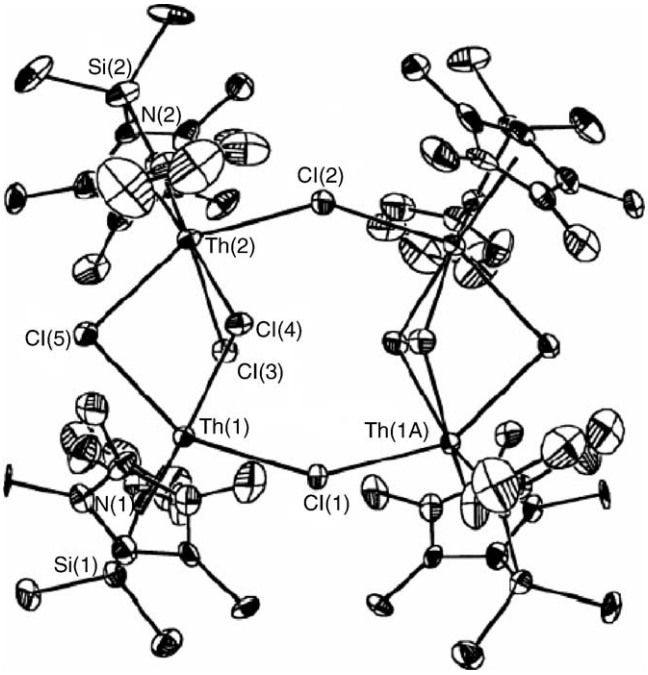

Fig. 75. Molecular structure of $\{[Me_2Si(C_5Me_4)(NPh)]ThCl\}_4$ [278].

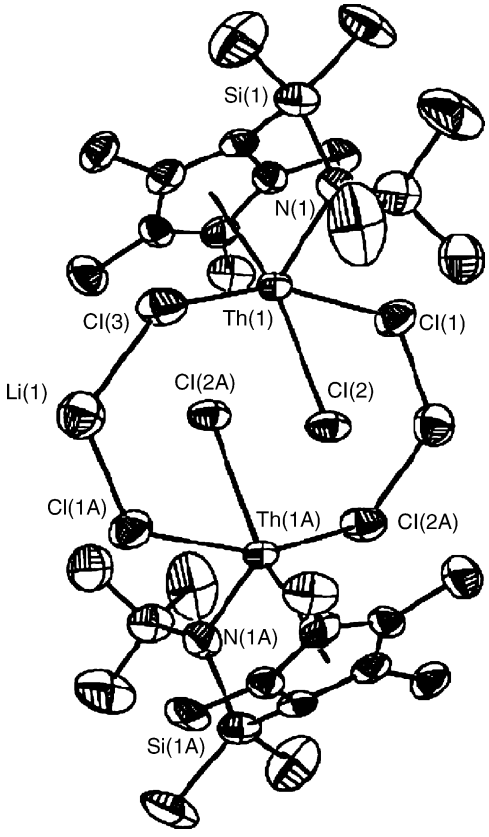

Fig. 76. Molecular structure of $[Li(Et_2O)_2][\{Me_2Si(C_5Me_4)(NBu^t)\}ThCl_3]_2$ [278].

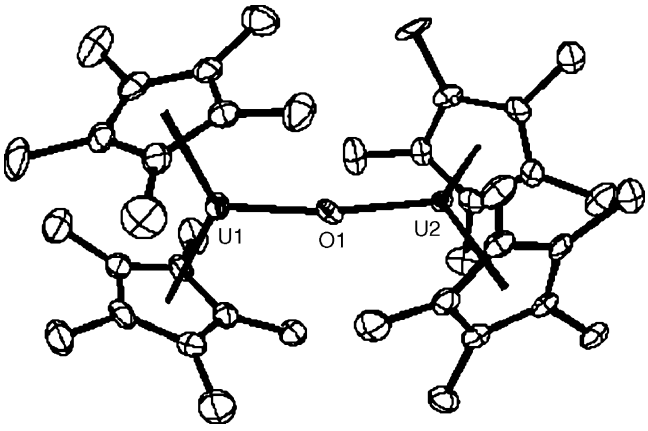

Fig. 77. Molecular structure of (μ-O)[Cp*$_2$U]$_2$ [279].

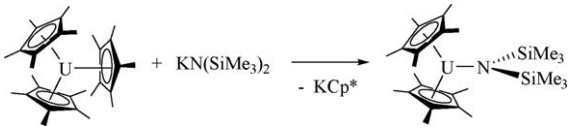

Scheme 68.

Cp*$_2$U[N(SiMe$_3$)$_2$] has been obtained in nearly quantitative yield by reacting sterically crowded Cp*$_3$U with KN(SiMe$_3$)$_2$ (Scheme 68) [280].

3.4.3.2. Cp$_3$An compounds.* Starting from sterically crowded Cp*$_3$U the synthesis of the first *f*-element complex binding a formally neutral N_2 ligand end-on has been achieved. It was found that solutions of Cp*$_3$U under N_2 at 80 psi slightly darken and produce hexagonal crystals of Cp*$_3$U(η^1-N$_2$). The U–N(N$_2$) bond length in this spectacular molecule is 2.492(10) Å (Fig. 78) [281].

In a similar manner, Cp*$_3$U reacts with CO to form a 1:1 adduct. The rare uranium carbonyl complex Cp*$_3$U(CO) has $\nu_{CO} = 1922\ cm^{-1}$ and a U–C(CO) distance of 2.485(9) Å. Fig. 79 shows two orientations of Cp*$_3$U(CO) [282].

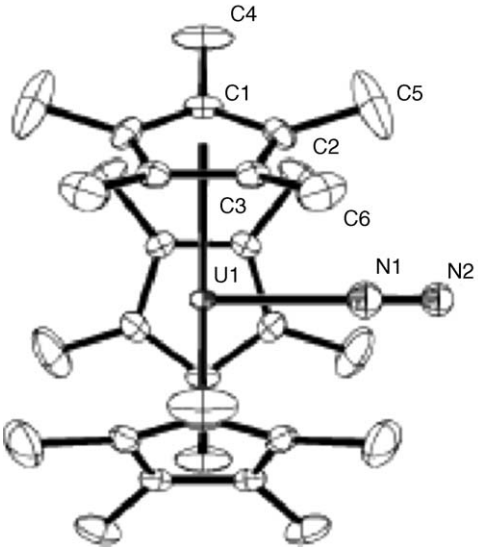

Fig. 78. Molecular structure of Cp*$_3$U(η^1-N$_2$) [281].

3.4.3.3. Mono(pentamethylcyclopentadienyl) actinide(IV)-compounds. Unusual mono(pentamethylcyclopentadienyl)actinide complexes containing a 15-membered trianionic hexaoxo-ligand built from catechol and catecholborate have been prepared and structurally characterized. As depicted in Scheme 69, the synthesis of these complexes has been achieved by reacting Cp*$_2$AnMe$_2$ (An = Th, U) with an excess of catecholborane that contains 5% dimethylsulfide (DMS) in benzene at room temperature for 24 h. The DMS ligand could be replaced by THF [283].

Mono(pentamethylcyclopentadienyl)actinide complexes containing the doubly deprotonated diamidosilyl ether ligand (Bu^{t}NHSiMe$_2$)$_2$O^{2-} ([Bu^{t}NON]$^{2-}$) have been prepared according to Scheme 70 [270].

3.4.3.4. Bis(pentamethylcyclopentadienyl) actinide(IV)-, (V)-, and (VI)-compounds. Detailed cyclic voltammetric and UV–vis–near-infrared electronic absorption spectral data have been published for a series of Cp*$_2$An (An = Th, U) complexes

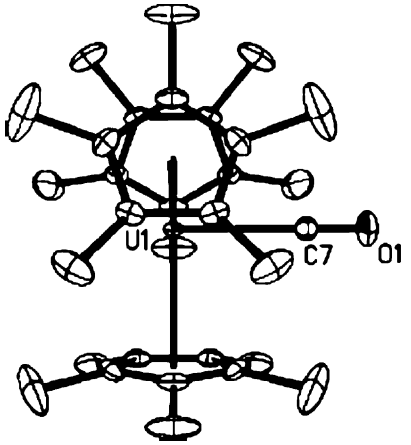

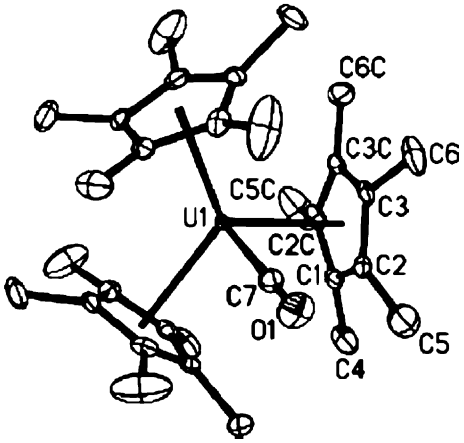

Fig. 79. Molecular structure of Cp*$_3$U(CO) [282].

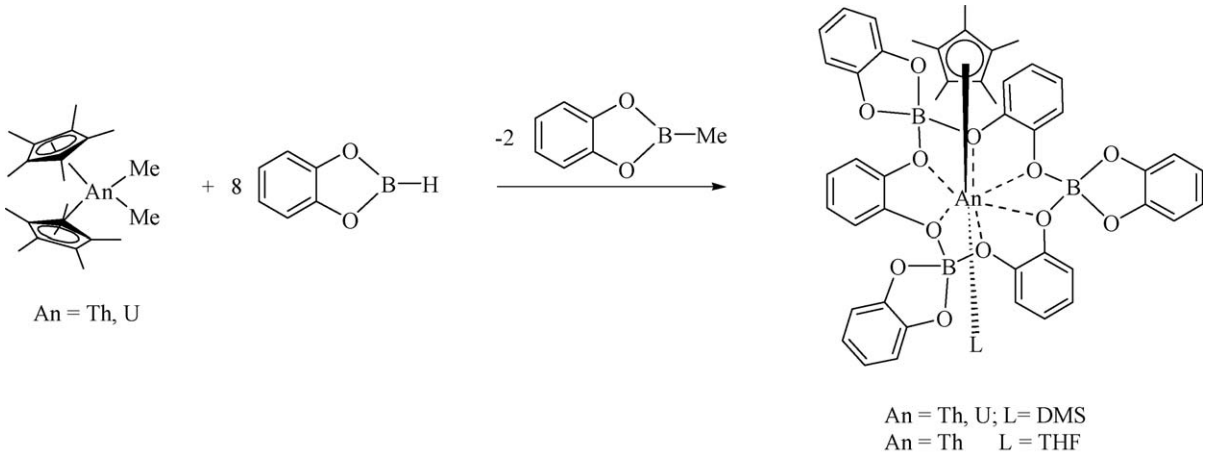

Scheme 69.

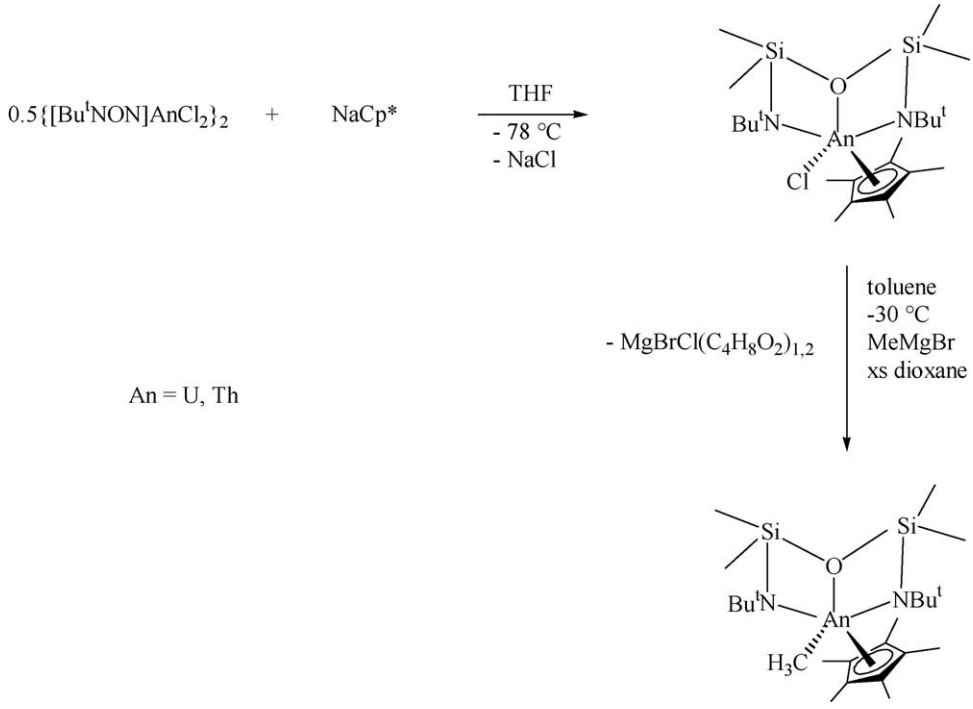

Scheme 70.

[284]. The reaction of $Cp^*_2UCl_2$ with $HNSPh_2{\cdot}H_2O$ in 1:1 stoichiometry produced $Cp^*_2UCl(OH)(HNSPh_2)$ as green crystals in good yield. This was the first structurally characterized *f*-element metallocene complexe containing a terminal hydroxy ligand (Fig. 80) [285].

Migratory insertion of benzonitrile into both An–C bonds of the bis(alkyl) and bis(aryl) complexes $Cp^*_2AnR_2$ (An = Th, U; R = Me, CH_2Ph) afforded the actinide ketimido complexes $Cp^*_2An[N{=}C(Ph)R]_2$. Thus for example, treatment of a colorless toluene solution of $Cp^*_2ThPh_2$ with excess benzonitrile instantly generated the highly iridescent orange-colored thorium(IV) bis(ketimido) complex $Cp^*_2Th[N{=}CPh_2]_2$, which was isolated as an orange crystalline solid in 82% yield (Scheme 71, Fig. 81) [286].

Density functional calculations have been used to investigate the structure and bonding in several unusual cyclopentadienyl complexes with nitrogen-containing ligands. The U(VI) imido complex $Cp_2U(NPh)_2$ and the U(IV) amido complex $Cp_2(NHPh)_2$ were examined and important orbitals involved in the U–N bonds analyzed [287]. Monoimido complexes of uranium(IV) were synthesized by metathesis or direct protonation reactions (Scheme 72). Obtained from Cp^*_2UMeCl and lithium anilide in the presence of tetramethylethylenediamine (TMEDA), the orange-brown complex $[Li(TMEDA)][Cp^*_2U(NC_6H_5)Cl]$ has been characterized by X-ray diffraction. It exhibits a typical "bent metallocene" structure with an average U–C(η^5-Cp^*) distance of 2.77(2) Å and a Cp^*(cent.)–U–Cp^*(cent.) angle of 132.4°. The U–Cl

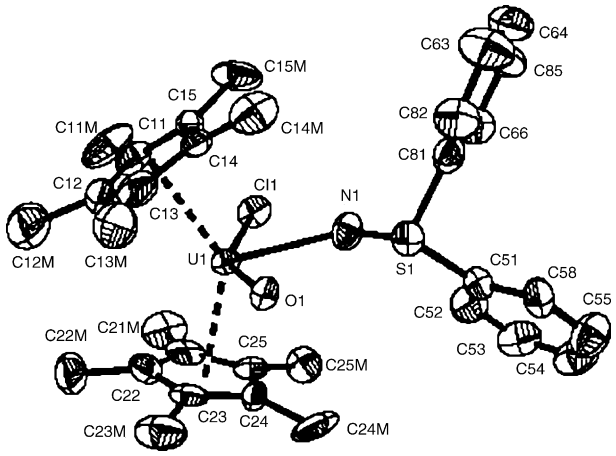

Fig. 80. Molecular structure of $Cp^*_2UCl(OH)(HNSPh_2)$ [285].

and U–N(NC_6H_5) bond lengths are 2.690(5) and 2.051(14) Å, respectively. The complex $Cp^*_2U(N\text{-}2,4,6\text{-}Bu^t_3C_6H_2)$, prepared by protonation of $Cp^*_2UMe_2$ with $H_2N\text{-}2,4,6\text{-}Bu^t_3C_6H_2$, was also structurally characterized. The most interesting feature of this molecule is the very short U–N bond length of 1.952(12) Å.

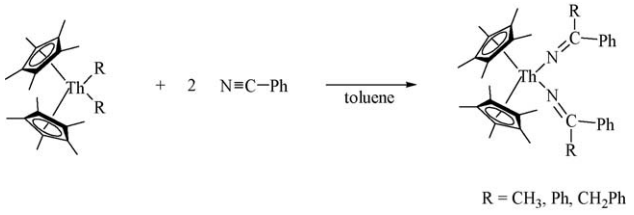

Scheme 71.

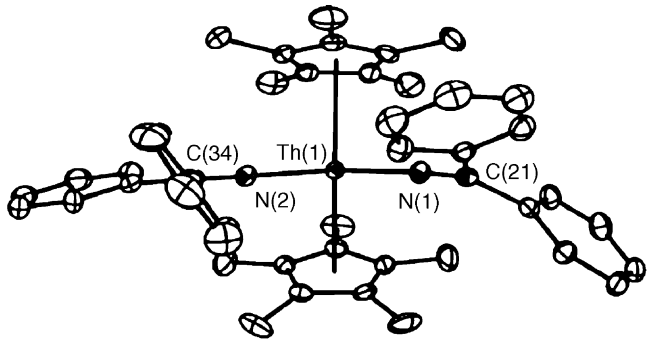

Fig. 81. Molecular structure of $Cp^*_2Th[N{=}CPh_2]_2$ [286].

Organometallic complexes of uranium(VI) with organoimido and oxo functional groups $Cp^*_2U(=NR)(=E)$ (E = NR or O) have also been prepared by two-electron oxidative atom transfer with using of organic azides, amine *N*-oxides or nitrous oxide. Another way of synthesizing these compounds is reductive cleavage of 1,2-disubstituted hydrazines (Scheme 73).

The uranium(IV) carbene complex $Cp^*_2U(O)[C(NMeCMe)_2]$ has been synthesized in the form of red-brown crystals from Cp^*_3U and the free carbene. It represents a rare example of a monometallic uranium mono-oxo compound (Fig. 82) [279]. The crystal structures of the known thorium and uranium complexes $Cp^*_2Th(CH_2Ph)_2$, $Cp^*_2ThMe_2$, $Cp^*_2U(CH_2Ph)_2$ and $Cp^*_2UMe_2$ have also been determined in the course of this investigation [286].

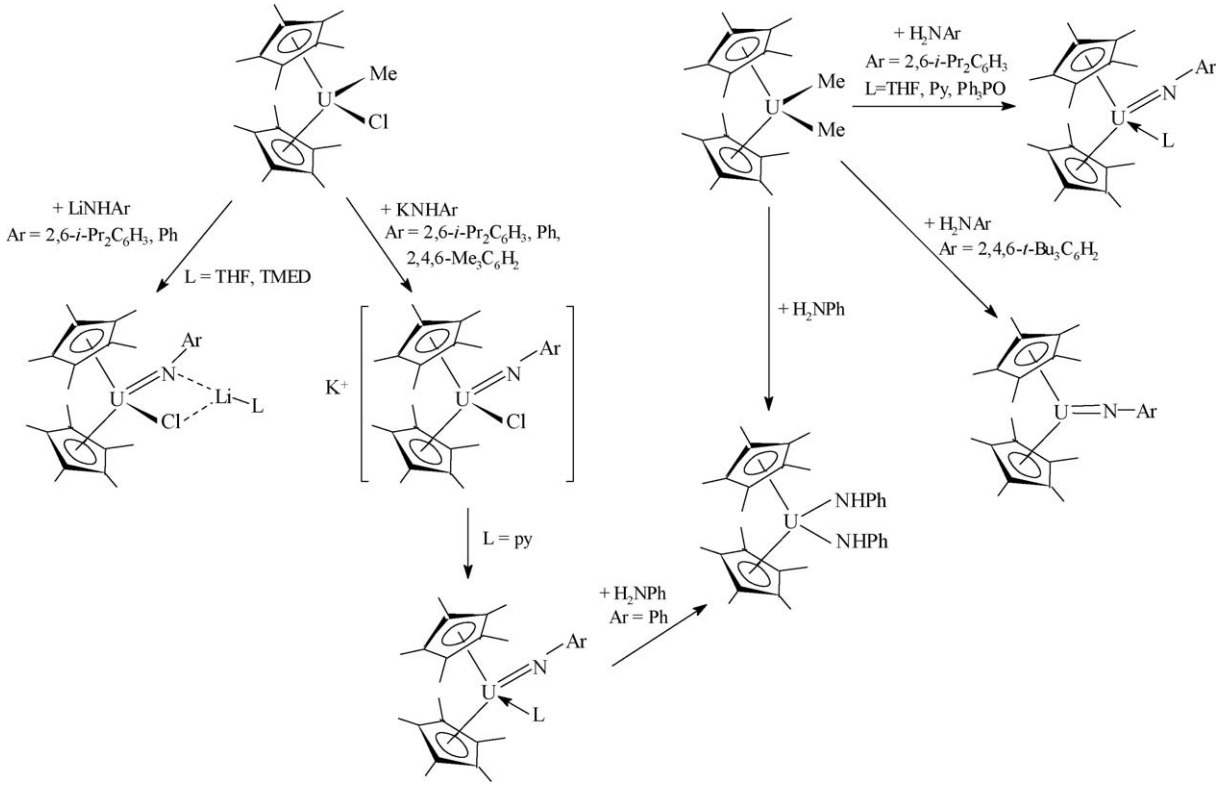

Scheme 72.

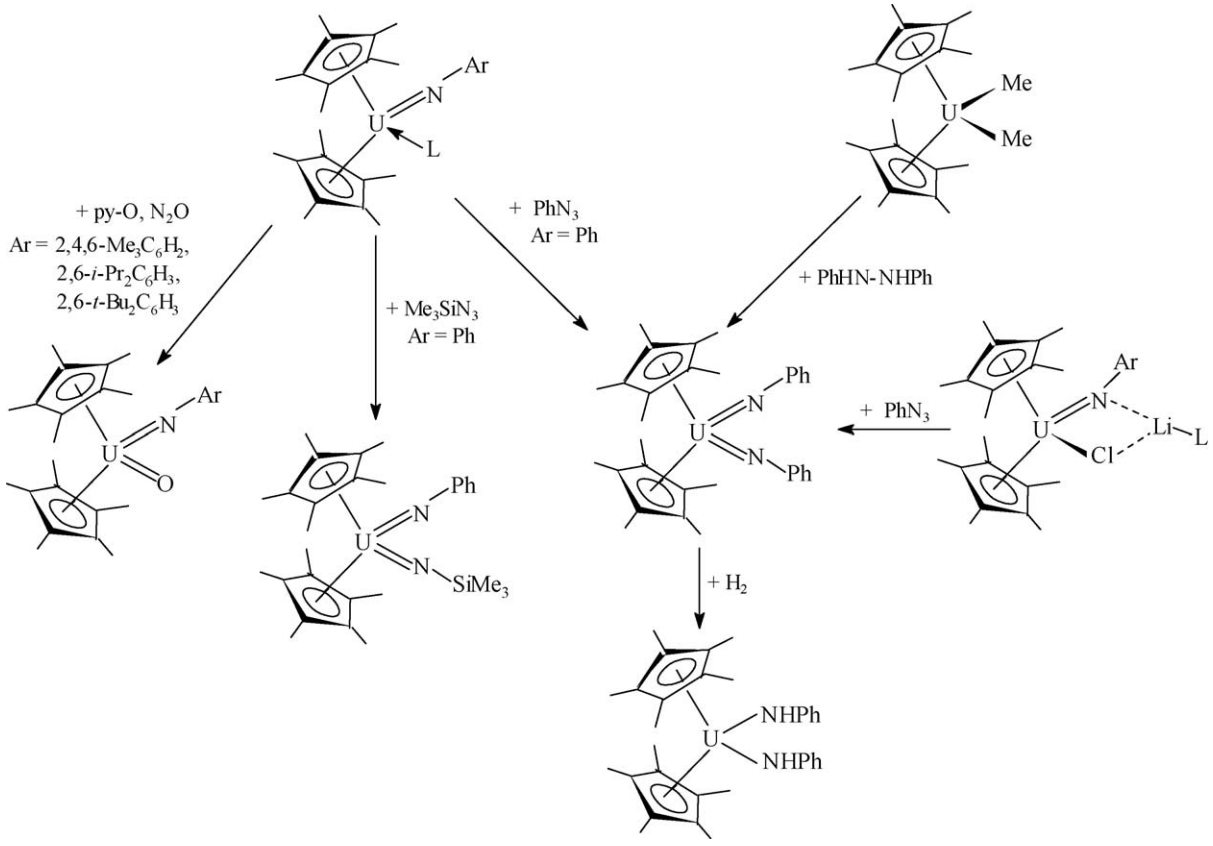

Scheme 73.

3.4.4. Pentalenediyl compounds

The electronic structure of $(\mu\text{-}N_2)[Cp^*U\{\eta^8\text{-}C_8H_4(SiPr^i_3)_2\text{-}1,4\}]_2$ has been investigated by density functional calculations [288].

3.5. Actinide arene complexes

The sterically crowded Cp^*_3U complex reacts with KC_8 or K/18-crown-6 in benzene to form the novel μ-benzene complex $(\mu\text{-}\eta^6\text{:}\eta^6\text{-}C_6H_6)[Cp^*_2U]_2$ as a brown solid in nearly quantitative yield. An alternative preparation involves the use of $[Cp^*_2U][(\mu\text{-}Ph)_2BPh_2]$ as starting material (Scheme 74). $(\mu\text{-}\eta^6\text{:}\eta^6\text{-}C_6H_6)[Cp^*_2U]_2$ reacts with $KN(SiMe_3)_2$ to afford the amide-substituted analogue $(\mu\text{-}\eta^6\text{:}\eta^6\text{-}C_6H_6)[Cp^*UN(SiMe_3)_2]_2$ Both compounds have nonplanar C_6H_6 rings sandwiched between the two uranium atoms. The solid-state structures of both arene complexes are illustrated in Figs. 83 and 84 [280].

By reducing the tetravalent $[K(DME)]_2[(Et_8\text{-calix-}[4]\text{-tetrapyrrole})Th(\mu\text{-}Cl)]_2$ with K(naphthalene), it was possible to obtain a unique example of a Th arene complex, $\{[(Et_8\text{-calix-}[4]\text{-tetrapyrrole})ThK(DME)](\mu,\mu'\text{-}\eta^4\text{:}\eta^6\text{-}C_{10}H_8)(\mu\text{-}K)\}_n$

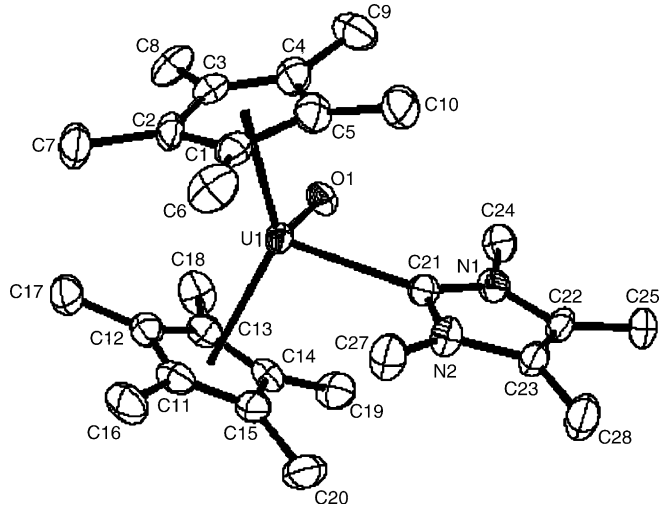

Fig. 82. Molecular structure of $Cp^*_2U(O)[C(NMeCMe)_2]$ [279].

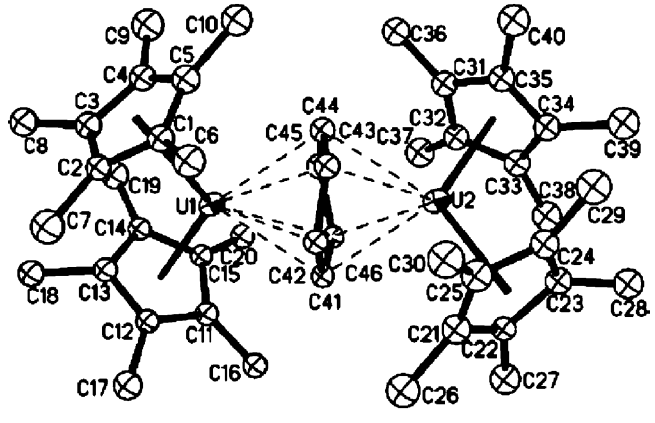

Fig. 83. Molecular structure of $(\mu\text{-}\eta^6\text{:}\eta^6\text{-}C_6H_6)[Cp^*_2U]_2$ [280].

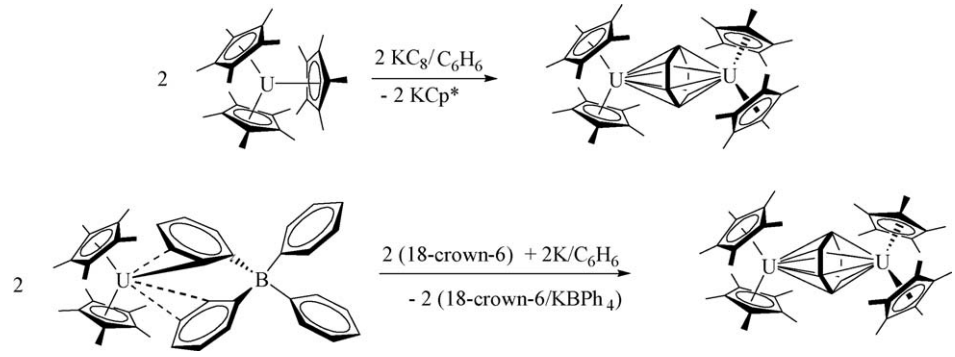

Scheme 74.

(Scheme 75). Exposure of a deep red toluene solution of the naphthalene complex to CO_2 at room temperature and 1 atm afforded colorless crystals of the new compound [(Et$_8$-calix-[4]-tetrapyrrole)ThK(DME)]$_2$[μ-*cis*-1,4-$(CO_2)_2C_{10}H_6$K(DME)$_{1.5}$]$_2$, resulting from the *cis*-insertion of two molecules of CO_2 at the 1- and 4-positions of the coordinated naphthalene ring (Scheme 75) [289].

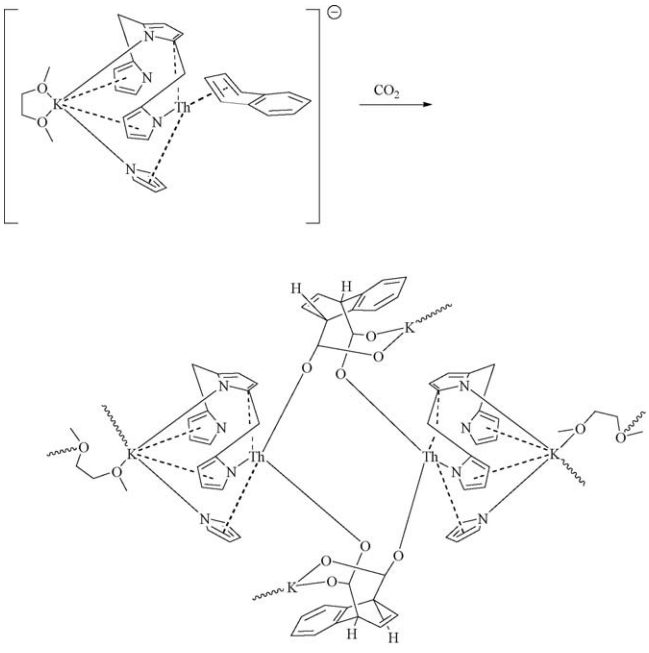

Scheme 75.

3.6. Actinide cyclooctatetraenyl compounds

A highly interesting essay on the discovery and chemistry of uranocene has been published by Seyferth under the title: "Uranocene. The first member of a new class of organometallic derivatives of the *f* elements" [290].

3.6.1. Cyclooctatetraenyl actinide(III) compounds

The mixed-sandwich uranium(III) complex (COT)Cp*U(HMPA) was isolated from the reaction of the cationic uranium complex [(COT)U(HMPA)$_3$][BPh$_4$] with KCp* (70% yield). Fig. 85 shows the molecular structure of (COT)Cp*U(HMPA). The analogous tetramethylphospholyl (=tmp) derivative (COT)U(tmp)(HMPA)$_2$ was obtained upon reduction of the cationic uranium(IV) complex [(COT)U(tmp)(HMPA)$_2$][BPh$_4$] with sodium amalgam [291].

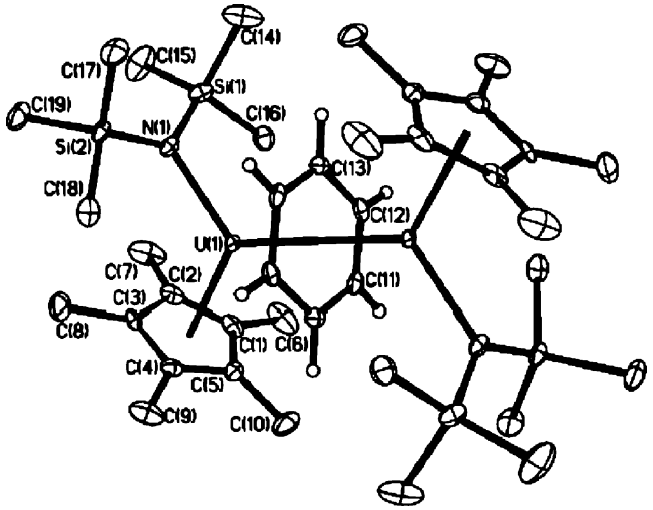

Fig. 84. Molecular structure of (μ-η^6:η^6-C_6H_6)[Cp*UN(SiMe$_3$)$_2$]$_2$ [280].

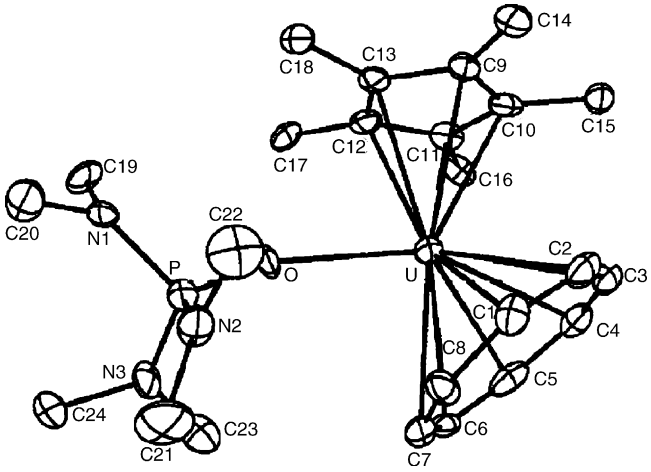

Fig. 85. Molecular structure of (COT)Cp*U(HMPA) [291].

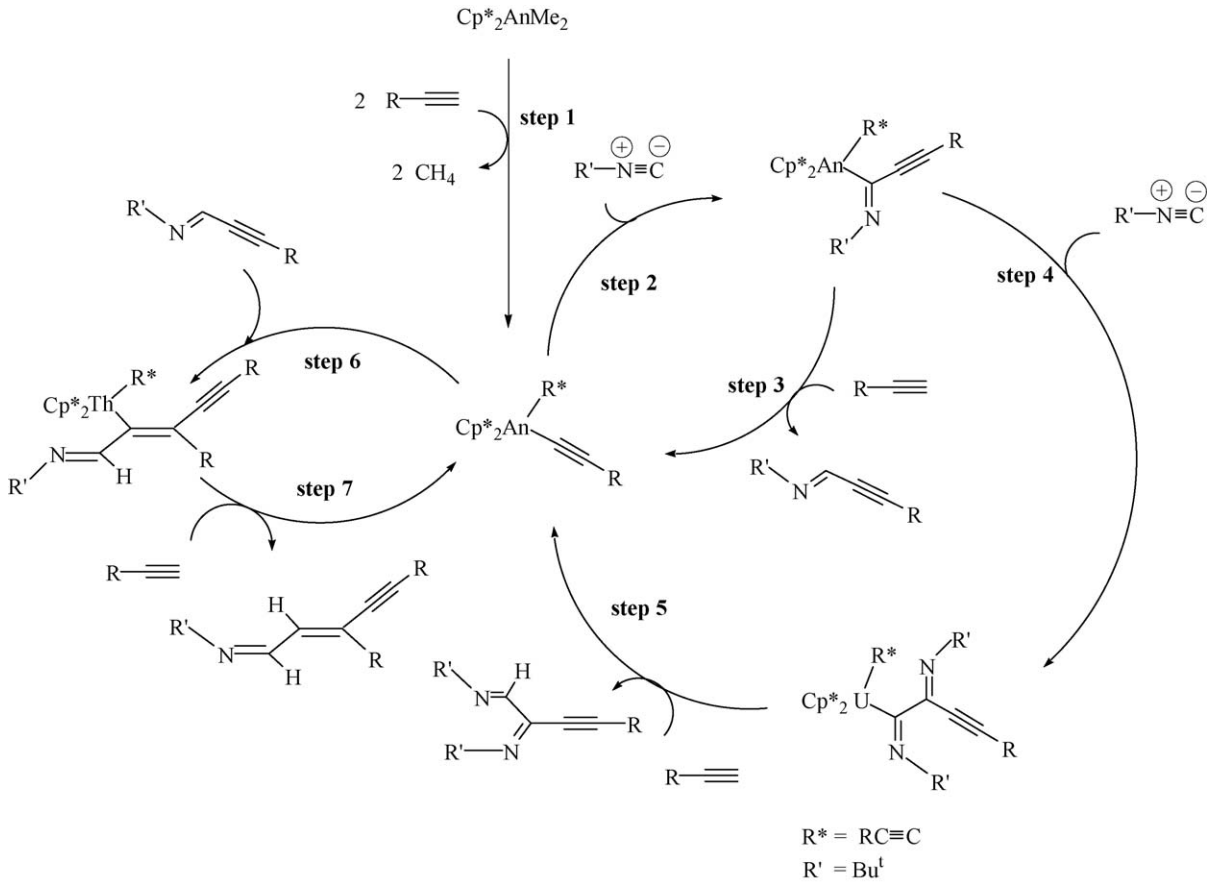

Scheme 76.

3.6.2. Mono(cyclooctatetraenyl) actinide(IV) compounds

Reaction of (COT)U(BH_4)$_2$(THF) with the dithiocarbonates dddtCO and dmioCO (dddt = 5,6-dihydro-1,4-dithiine-2,3-dithiolate; dmio = 1,3-dithiole-2-one-4,5-dithiolate) gave the neutral dithiolene compounds [(COT)U(dithiolene)]$_2$ in good yields (dithiolene = dddt, dmio, or 1,3-dithiole-4,5-dithiolate (mdt)). The reactions are accompanied by elimination of formaldehyde and borane. The X-ray crystal structures of [(COT)U(mdt)]$_2$ (Fig. 86) and monomeric (COT)U(mdt)(pyridine)$_2$ (Fig. 87) showed an interaction between the C=C double bond of the mdt ligand and the uranium atom, and the ^{1}H NMR spectra revealed a facile dithiolene ring inversion process in solution [292].

3.6.3. Bis(cyclooctatetraenyl) actinide(IV) compounds

High-resolution Raman spectra for uranocene and thorocene have been measured under liquid nitrogen [293].

3.7. Organoactinide catalysis

3.7.1. Organoactinide-catalyzed hydroamination reactions

Constrained-geometry complexes of the type [$Me_2Si(C_5Me_4)(NBu^t)$]An(NRR′)$_2$ (An = Th, U; R = R′ = Me; R = Me, R = Et; R = R′ = Et) have been reported to be effective precatalysts for intramolecular catalytic hydroamination/cyclization of aminoalkenes and aminoalkynes [277].

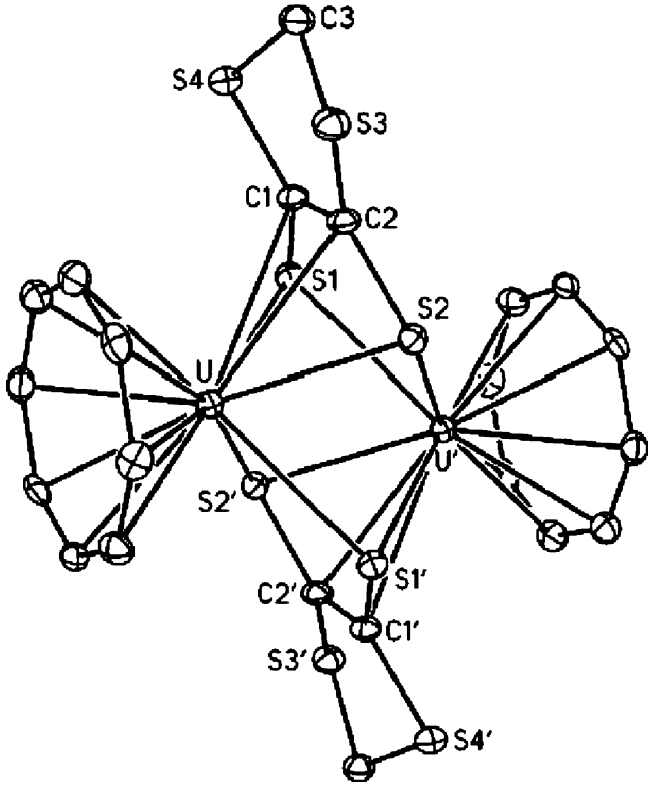

Fig. 86. Molecular structure of [(COT)U(mdt)]$_2$ [292].

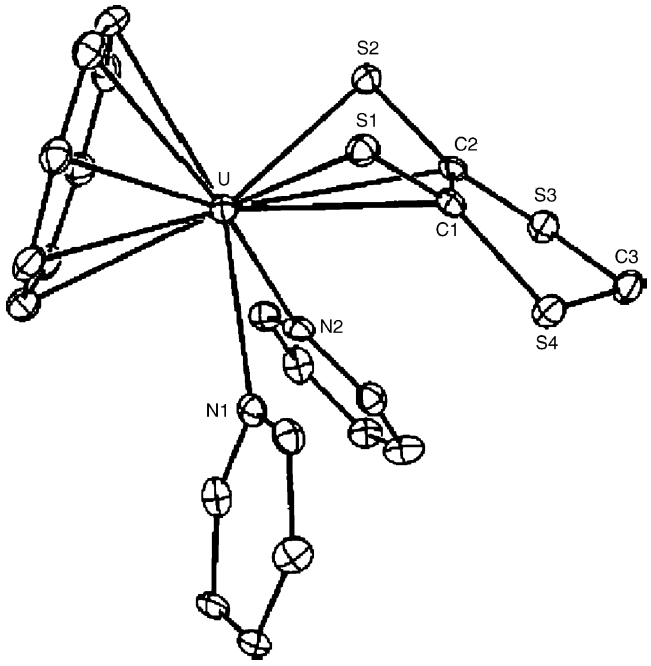

Fig. 87. Molecular structure of (COT)U(mdt)(pyridine)$_2$ [292].

3.7.2. Other organoactinide-catalyzed reactions

The actinide complexes $Cp^*_2AnMe_2$ (An = Th, U) have been found to effectively catalyze the coupling reaction of terminal alkynes and *t*-butylisonitrile, Bu^{t}NC. The catalytic conversion of the isonitrile and alkyne to 1-aza-1,3-enynes was achieved in toluene or benzene at 90–100 °C, while no reaction was observed in the absence of a catalyst. Scheme 76 illustrates a plausible mechanism for the catalytic coupling of Bu^{t}NC and terminal alkynes mediated by $Cp^*_2AnMe_2$ [294].

Selective alkylation of aromatic molecules (benzene, toluene) with α-chloronorbornene at room temperature to afford good yields the 1:1 addition products *exo*-1-chloro-2-arylnorbornane (aryl = Ph, C_6H_4Me-*p*) has been achieved with the metallocenium ion pair $[Cp^*_2ThMe][B(C_6F_5)_4]$ [295]. The solution structure and aggregation of the catalyst has been studied by NOE and PGSE NMR spectroscopy [296,297].

References

[1] P.B. Hitchcock, A.G. Hulkes, A.V. Khvostov, M.F. Lappert, A.V. Protchenko, Spec. Publ. Roy. Soc. 287 (2003) 86.
[2] Z. Hou, Y. Wakatsuki, Sci. Synth. 2 (2003) 849.
[3] V. Vetere, P. Maldivi, C. Adamo, J. Quant. Chem. 91 (2003) 321.
[4] V. Vetere, P. Maldivi, C. Adamo, J. Comput. Chem. 24 (2003) 850.
[5] J. Pilme, B. Silvi, M.E. Alikhani, J. Phys. Chem. A 107 (2003) 4506.
[6] D. Zhang, C. Liu, S. Bi, S. Yuan, Chem. Eur. J. 9 (2003) 484.
[7] F.-J. Ding, Huaxue Xuebao 61 (2003) 161.
[8] R.Z. Hinrichs, J.J. Schroden, H.F. Davis, J. Am. Chem. Soc. 125 (2003) 860.
[9] M.S. Hill, P.B. Hitchcock, Dalton Trans. (2003) 4570.
[10] D.-Y. Hwang, A.M. Mebel, Chem. Phys. Lett. 396 (2004) 75.
[11] B.O. Roos, P.-O. Widmark, L. Gagliardi, Faraday Discuss. 124 (2003) 57.
[12] R.J. Gillespie, S. Noury, J. Pilme, B. Silvi, Inorg. Chem. 43 (2004) 3248.
[13] E.D. Brady, D.L. Clark, J.C. Gordon, P.J. Hay, D.W. Keogh, R. Poli, B.L. Scott, J.G. Watkin, Inorg. Chem. 42 (2003) 6682.
[14] L. Perrin, L. Maron, O. Eisenstein, M.F. Lappert, New J. Chem. 27 (2003) 121.
[15] C. Guttenberger, B. Unrecht, H. Reddmann, H.-D. Amberger, Inorg. Chim. Acta 348 (2003) 165.
[16] S.F. Zhil'tsov, V.M. Makarov, N.E. Semkina, Russ. J. Gen. Chem. 73 (2003) 1395.
[17] L. Perrin, L. Maron, O. Eisenstein, ACS Symp. Ser. 885 (2004) 116.
[18] E.C. Sherer, C.J. Cramer, Organometallics 22 (2003) 1682.
[19] G.W. Rabe, B. Rhatigan, J.A. Golen, A.L. Rheingold, Acta Crystallogr. E 59 (2003) m99.
[20] G.W. Rabe, M. Zhang-Presse, F.A. Riederer, J.A. Golen, C.D. Incarvito, A.L. Rheingold, Inorg. Chem. 42 (2003) 7587.
[21] G.W. Rabe, M. Zhang-Presse, F.A. Riederer, G.P.A. Yap, Inorg. Chem. 42 (2003) 3527.
[22] A.G. Avent, C.F. Caro, P.B. Hitchcock, M.F. Lappert, Z. Li, X.-H. Wei, Dalton Trans. (2004) 1567.
[23] S. Arndt, P.M. Zeimentz, T.P. Spaniol, J. Okuda, M. Honda, K. Tatsumi, Dalton Trans. (2003) 3622.
[24] S. Arndt, T.P. Spaniol, J. Okuda, Angew. Chem. 115 (2003) 5229; S. Arndt, T.P. Spaniol, J. Okuda, Angew. Chem. Int. Ed. 42 (2003) 5075.
[25] D.J.H. Emslie, W.E. Piers, M. Parvez, Dalton Trans. (2003) 2615.
[26] A.G. Avent, G.F.N. Cloke, B.R. Elvidge, P.B. Hitchcock, Dalton Trans. (2004) 1083.
[27] Y. Lou, Y. Yao, Q. Shen, K. Yu, L. Weng, Eur. J. Inorg. Chem. (2003) 318.
[28] O. Eisenstein, P.B. Hitchcock, A.V. Khvostov, M.F. Lappert, L. Maron, L. Perrin, A.V. Protchenko, J. Am. Chem. Soc. 125 (2003) 10790.
[29] S. Harder, Angew. Chem. 116 (2004) 2768; S. Harder, Angew. Chem. Int. Ed. 43 (2004) 2714.
[30] Y.-J. Luo, Y.-M. Yao, Y. Zhang, Q. Shen, K.-B. Yu, Chinese J. Chem. 22 (2004) 187.
[31] F. Basuli, J. Tomaszewski, J.C. Huffman, D.J. Mindiola, Organometallics 22 (2003) 4705.
[32] L.K. Knight, E.W. Piers, P. Fleurat-Lessard, M. Parvez, R. McDonald, Organometallics 23 (2004) 2087.
[33] A.-M. Neculai, C.C. Cummins, D. Neculai, H.W. Roesky, G. Bunkòczi, B. Walfort, D. Stalke, Inorg. Chem. 42 (2003) 8803.
[34] D. Neculai, H.W. Roesky, A. Mirela, J. Magull, R. Herbst-Irmer, B. Walfort, D. Stalke, Organometallics 22 (2003) 2279.
[35] A.M. Neculai, D. Neculai, H.W. Roesky, J. Magull, Polyhedron 23 (2004) 183.
[36] A.G. Avent, P.B. Hitchcock, A.V. Khvostov, M.F. Lappert, A.V. Protchenko, Dalton Trans. (2004) 2272.
[37] S.C. Lawrence, B.D. Ward, S.R. Dubberley, C.M. Kozak, P. Mountford, Chem. Commun. (2003) 2880.
[38] C.G.J. Tazelaar, S. Bambirra, D. van Leusen, A. Meetsma, B. Hessen, J.H. Teuben, Organometallics 23 (2004) 936.
[39] K.C. Hultzsch, F. Hampel, T. Wagner, Organometallics 23 (2004) 2601.
[40] S. Bambirra, S.J. Boot, D. van Leusen, A. Meetsma, B. Hessen, Organometallics 23 (2004) 1891.
[41] C.-X. Cai, L. Toupet, C.W. Lehmann, J.-F. Carpentier, J. Organometall. Chem. 683 (2003) 131.
[42] C. Cui, A. Shafir, C.L. Reeder, J. Arnold, Organometallics 22 (2003) 3357.
[43] F. Estler, G. Eickerling, E. Herdtweck, R. Anwander, Organometallics 22 (2003) 1212.
[44] P.G. Hayes, G.C. Welch, D.J.H. Emslie, C.L. Noack, W.E. Piers, M. Parvez, Organometallics 22 (2003) 1577.
[45] S. Bambirra, D. van Leusen, A. Meetsma, B. Hessen, J.T. Teuben, Chem. Commun. (2003) 522.
[46] T.M. Cameron, J.C. Gordon, R. Michalczyk, B.L. Scott, Chem. Commun. (2003) 2282.
[47] L. Lavanant, T.-Y. Chou, Y. Chi, C.W. Lehmann, L. Toupet, J.-F. Carpentier, Organometallics 23 (2004) 5450.
[48] K. Izod, S.T. Liddle, W. Clegg, Chem. Commun. (2004) 1748.
[49] K. Izod, S.T. Liddle, W. McFarlane, W. Clegg, Organometallics 23 (2004) 2734.

[50] P.L. Arnold, S.A. Mungur, A.J. Blake, C. Wilson, Angew. Chem. 115 (2003) 6163;
P.L. Arnold, S.A. Mungur, A.J. Blake, C. Wilson, Angew. Chem. Int. Ed. 42 (2003) 5981.
[51] E.D. Glendening, J. Phys. Chem. A 108 (2004) 10165.
[52] N.A. Pimanova, S.F. Zhil'tsov, O.N. Druzhova, J. Gen. Chem. 73 (2003) 1188.
[53] T.J. Woodmann, M. Schormann, D.L. Hughes, M. Bochmann, Organometallics 22 (2003) 3028.
[54] T.J. Woodman, M. Schormann, M. Bochmann, Israel J. Chem. 42 (2003) 283.
[55] T.J. Woodman, M. Schormann, D.L. Hughes, M. Bochmann, Organometallics 23 (2004) 2972.
[56] C.J. Kuehl, C.K. Simpson, K.D. John, A.P. Sattelberger, C.N. Carlson, T.P. Hanusa, J. Organometall. Chem. 683 (2003) 149.
[57] T.J. Woodman, M. Schormann, M. Bochmann, Organometallics 22 (2003) 2938.
[58] Y. Nakayama, H. Yasuda, J. Organometall. Chem. 689 (2004) 4489.
[59] O. Tardif, M. Nishiura, Z. Hou, Tetrahedron 59 (2003) 10525.
[60] D. Wang, C. Zhao, D.L. Phillips, Organometallics 23 (2004) 1953.
[61] G.B. Deacon, C.M. Forsyth, N.M. Scott, Dalton Trans. (2003) 3216.
[62] M. Deng, Y. Yoa, Q. Shen, Y. Zhang, J. Lang, Y. Zhou, J. Organometall. Chem. 681 (2003) 174.
[63] W.J. Evans, J.M. Perotti, J.C. Brady, J.W. Ziller, J. Am. Chem. Soc. 125 (2003) 5204.
[64] G.V. Khoroshen'kov, A.A. Fagin, M.N. Bochkarev, S. Dechert, H. Schumann, Russ. Chem. Bull. 52 (2003) 1358.
[65] A. Maia, I. Sampaio Paulino, U. Schuchardt, W. de Oliveira, Inorg. Chem. Commun. 6 (2003) 304.
[66] G.R. Giesbrecht, D.L. Clark, J.C. Gordon, B.L. Scott, Appl. Organometall. Chem. 17 (2003) 473.
[67] G.R. Giesbrecht, G.E. Collis, C.J. Gordon, D.L. Clark, B.L. Scott, N.J. Hardman, J. Organometall. Chem. 689 (2004) 2177.
[68] I.L. Fedushkin, V.I. Nevodchikov, M.N. Bochkarev, S. Dechert, H. Schumann, Russ. Chem. Bull. 52 (2003) 154.
[69] Y. Yao, Y. Zhang, Z. Zhang, Q. Shen, K. Yu, Organometallics 22 (2003) 2876.
[70] Y. Zhang, Y.-M. Yao, Y.-J. Luo, Q. Shen, Y. Cui, K.-B. Yu, Polyhedron 22 (2003) 1241.
[71] L.-J. Zhang, X.-J. Lu, H.-Z. Ma, W. Zhang, Hecheng Huaxue 11 (2003) 363.
[72] M.T. Gamer, P.W. Roesky, Inorg. Chem. 43 (2004) 4903.
[73] M. Zhu, Y. Li, J. Luo, X. Zhou, Chinese Sci. Bull. 48 (2003) 2041.
[74] S. Arndt, T.P. Spaniol, J. Okuda, Organometallics 22 (2003) 775.
[75] T.P. Spaniol, J. Okuda, M. Kitamura, T. Takahashi, J. Organometall. Chem. 684 (2003) 194.
[76] P. Voth, S. Arndt, T.P. Spaniol, J. Okuda, Organometallics 22 (2003) 65.
[77] P. Voth, T.P. Spaniol, J. Okuda, Organometallics 22 (2003) 3921.
[78] K.C. Hultzsch, P. Voth, T.P. Spaniol, J. Okuda, Z. Anorg. Allg. Chem. 629 (2003) 1272.
[79] O. Tardif, J. Kurazumi, M. Nishiura, A. Horiuchi, Z. Hou, Kidorui 42 (2003) 50.
[80] O. Tardif, M. Nishiura, Z. Hou, Organometallics 22 (2003) 1171.
[81] D. Cui, O. Tardif, Z. Hou, J. Am. Chem. Soc. 126 (2004) 1312.
[82] O. Tardif, D. Hashizume, Z. Hou, J. Am. Chem. Soc. 126 (2004) 8080.
[83] F. Alary, J.-L. Heully, R. Poteau, L. Maron, G. Trinquier, J.-P. Daudey, J. Am. Chem. Soc. 125 (2003) 11051.
[84] F. Bonnet, M. Visseaux, D. Barbier-Baudry, A. Hafid, E. Vigier, M.M. Kubicki, Inorg. Chem. 43 (2004) 3682.
[85] D.J. Beetstra, A. Meetsma, B. Hessen, J.H. Teuben, Organometallics 22 (2003) 4372.
[86] I.L. Fedushkin, M.N. Bochkarev, S. Muehle, H. Schumann, Russ. Chem. Bull. 52 (2003) 2005.
[87] Y. Luo, P. Selvam, Y. Ito, A. Endou, M. Kubo, A. Miyamoto, J. Organometall. Chem. 679 (2003) 84.
[88] Y. Luo, P. Selvam, M. Koyama, M. Kubo, A. Miyamoto, Inorg. Chem. Commun. 7 (2004) 566.
[89] Y. Lou, P. Selvam, Y. Ito, M. Kubo, A. Miyamoto, Inorg. Chem. Commun. 6 (2003) 1243.
[90] P. Nicolas, P. Royo, M.V. Galakhov, O. Blacque, H. Jacobsen, H. Berke, Dalton Trans. (2004) 2943.
[91] L. Maron, L. Perrin, O. Eisenstein, Dalton Trans. (2003) 4313.
[92] X.-G. Zhou, C.-M. Zhang, J. Luo, Y.-H. Chen, Z.-H. Shao, Q. Li, Fudan Xuebao, Ziran Kexueban 42 (2003) 1025.
[93] H. Schumann, A. Heim, J. Demtschuk, S.H. Mühle, Organometallics 22 (2003) 118.
[94] O. Schmitt, G. Wolmershäuser, H. Sitzmann, Eur. J. Inorg. Chem. (2003) 3105.
[95] H. Schumann, K. Herrmann, F. Erbstein, Z. Naturforsch. 58b (2003) 832.
[96] H. Schumann, K. Herrmann, S.H. Mühle, S. Dechert, Z. Anorg. Allg. Chem. 629 (2003) 1184.
[97] M. Zhu, L.-B. Zhang, Y.-H. Chen, X.-G. Zhou, R.-F. Cai, L.-H. Weng, Chinese J. Chem. 22 (2004) 935.
[98] K. Schierwater, H. Hanika-Heidl, M. Bollmann, D.R. Fischer, R.K. Harris, D.C. Apperley, Coord. Chem. Rev. 242 (2003) 15.
[99] F.-G. Yuan, L. Chen, L.-H. Wen, J. Yang, Youji Huaxue 23 (2003) 646.
[100] M. Deng, Y. Zhou, Y. Yao, Q. Shen, L. Weng, Zhongguo Xitu Xuebao 21 (2003) 626.
[101] T. Hahn, E. Hey-Hawkins, M. Hilder, P.C. Junk, M.K. Smith, Inorg. Chim. Acta 357 (2004) 2125.
[102] G.B. Deacon, C.C. Quitmann, K. Müller-Buschbaum, G. Meyer, Z. Anorg. Allg. Chem. 629 (2003) 589.
[103] J. Zhang, R. Cai, L. Weng, X. Zhou, J. Organometall. Chem. 672 (2003) 94.
[104] J. Zhang, R. Cai, L. Weng, X. Zhou, Organometallics 23 (2004) 3303.
[105] J. Zhang, R. Cai, L. Weng, X. Zhou, Organometallics 22 (2003) 5385.
[106] C. Zhang, R. Liu, X. Zhou, Z. Chen, L. Weng, Y. Lin, Organometallics 23 (2004) 3246.
[107] A. Strasser, A. Vogler, Chem. Phys. Lett. 379 (2003) 287.
[108] H.-D. Amberger, H. Reddmann, H.H. Karsch, V.W. Graf, C. Quian, B. Wang, J. Organometall. Chem. 677 (2003) 35.
[109] H. Reddmann, S. Jank, H. Schultze, H.-D. Amberger, N.M. Edelstein, Inorg. Chim. Acta 344 (2003) 243.
[110] H.-D. Amberger, H. Reddmann, S. Jank, M.I. Lopes, N. Marques, Eur. J. Inorg. Chem. (2004) 98.
[111] H. Schulz, C. Hagen, H. Reddmann, H.-D. Amberger, Z. Allg. Anorg. Chem. 630 (2004) 268.
[112] S. Jank, H. Reddmann, H.-D. Amberger, C. Apostolidis, J. Organometall. Chem. 689 (2004) 3143.
[113] H.-D. Amberger, H. Reddmann, H. Schultze, S. Jank, B. Kanellakopulos, C. Apostolidis, Spectrochim. Acta (Part A: Mol. Biomol. Spectr.) 59 (2003) 2527.
[114] C. Apostolidis, A. Morgenstern, O. Walter, H. Reddmann, H.-D. Amberger, Z. Allg. Anorg. Chem. 630 (2004) 928.
[115] T.-Q. Liu, F.-C. Ding, Y.-H. Lin, J.-X. Yu, Q.-S. Shi, Q. Shen, Youji Huaxue 23 (2003) 1029.
[116] P.C. Junk, Appl. Organometall. Chem. 17 (2003) 875.
[117] T. Mehdoui, J.-C. Berthet, P. Thuéry, M.J. Ephritikhine, Dalton Trans. (2004) 579.
[118] M. Nishiura, Z. Hou, Y. Wakatsuki, Organometallics 23 (2004) 1359.
[119] G.B. Deacon, C.M. Forsyth, Organometallics 22 (2003) 1349.
[120] L. Perrin, L. Maron, O. Eisenstein, D.J. Schwartz, C.J. Burns, R.A. Andersen, Organometallics 22 (2003) 5447.
[121] W.J. Evans, J.M. Perotti, J.W. Ziller, D.F. Moser, R. West, Organometallics 22 (2003) 1160.
[122] Z. Hou, Y. Zhang, M. Nishiura, Y. Wakatsuki, Organometallics 22 (2003) 129.
[123] W.J. Evans, D.G. Giarikos, P.S. Workman, J.W. Ziller, Inorg. Chem. 43 (2004) 5754.
[124] T.M. Cameron, J.C. Gordon, B.L. Scott, W. Tumas, Chem. Commun. (2004) 1398.
[125] T.M. Cameron, J.C. Gordon, B.L. Scott, Organometallics 23 (2004) 2995.

[126] L.D. Henderson, G.D. MacInnis, W.E. Piers, M. Parvez, Can. J. Chem. 82 (2004) 162.
[127] P.C. Junk, M.K. Smith, Appl. Organometall. Chem. 18 (2004) 252.
[128] S. Kaita, Z. Hou, M. Nishiura, Y. Doi, J. Kurazumi, A.C. Horiuchi, Y. Wakatsuki, Macromol. Rapid Commun. 24 (2003) 179.
[129] (a) W.J. Evans, B.L. Davis, G.W. Nyce, J.M. Perotti, J.W. Ziller, J. Organometall. Chem. 677 (2003) 89;
(b) J.W. Evans, D.S. Lee, C. Lie, J.W. Ziller, Angew. Chem. 116 (2004) 5633;
J.W. Evans, D.S. Lee, C. Lie, J.W. Ziller, Angew. Chem. Int. Ed. 43 (2004) 5517.
[130] A.A. Trifonov, Y.A. Kurskii, M.N. Bochkarev, S. Muehle, S. Dechert, H. Schumann, Russ. Chem. Bull. 52 (2003) 601.
[131] R.E. Da Re, C.J. Kuehl, M.G. Brown, R.C. Rocha, E.D. Bauer, K.D. John, D.E. Morris, A.P. Shreve, J.L. Sarrao, Inorg. Chem. 42 (2003) 5551.
[132] C.J. Kuehl, R.E. Da Re, B.L. Scott, D.E. Morris, K.D. John, Chem. Commun. (2003) 2336.
[133] M.L. Cole, P.C. Junk, New J. Chem. 27 (2003) 1032.
[134] M.T. Gamer, P.W. Roesky, Organometallics 23 (2004) 5540.
[135] C.P. Casey, J.A. Tunge, T.-Y. Lee, M.A. Fagan, J. Am. Chem. Soc. 125 (2003) 2641.
[136] L. Perrin, L. Maron, O. Eisenstein, New J. Chem. 28 (2004) 1255.
[137] S. Kaita, N. Koga, Z. Hou, Y. Doi, Y. Wakatsuki, Organometallics 22 (2003) 3077.
[138] Z. Hou, C. Yoda, T. Koizumi, M. Nishiura, Y. Wakatsuki, S. Fukuzawa, J. Takats, Organometallics 22 (2003) 3586.
[139] I.L. Fedushkin, Y.A. Kurskii, T.V. Balashova, M.N. Bochkarev, S. Mühle, S. Dechert, H. Schumann, Russ. Chem. Bull. 52 (2003) 1363.
[140] W.J. Evans, M.A. Johnston, M.A. Greci, T.S. Gummersheimer, J.W. Ziller, Polyhedron 22 (2003) 119.
[141] A.A. Trifonov, E.A. Fedorova, G.K. Fukin, N.O. Druzhkov, M.N. Bochkarev, Angew. Chem. 116 (2004) 5155;
A.A. Trifonov, E.A. Fedorova, G.K. Fukin, N.O. Druzhkov, M.N. Bochkarev, Angew. Chem. Int. Ed. 43 (2004) 5045.
[142] K. Zhang, W. Zhang, S. Wang, E. Sheng, G. Yang, M. Xie, S. Zhou, Y. Feng, L. Mao, Z. Huang, Dalton Trans. (2004) 1029.
[143] E. Sheng, S. Wang, G. Yang, S. Zhou, L. Cheng, K. Zhang, Z. Huang, Organometallics 22 (2003) 684.
[144] E. Sheng, S. Zhou, S. Wang, G. Yang, Y. Wu, Y. Feng, L. Mao, Z. Huang, Eur. J. Inorg. Chem. (2004) 2923.
[145] J. Cheng, D. Cui, W. Chen, N. Hu, T. Tang, B. Huang, J. Organometall. Chem. 689 (2004) 2646.
[146] S. Wang, S. Zhou, E. Sheng, M. Xie, K. Zhang, L. Cheng, Y. Feng, L. Mao, Z. Huang, Organometallics 22 (2003) 3546.
[147] A.T. Trifonov, T.P. Spaniol, J. Okuda, Eur. J. Inorg. Chem. (2003) 926.
[148] E. Kirillov, L. Toupet, C.W. Lehmann, A. Razavi, J.-F. Carpentier, Organometallics 22 (2003) 4467.
[149] E. Kirillov, C.W. Lehmann, A. Razavi, J.-F. Carpentier, Eur. J. Inorg. Chem. (2004) 943.
[150] J. Gavenonis, D.T. Tilley, J. Organometall. Chem. 689 (2004) 870.
[151] D.-M. Cui, T. Tang, J.-H. Cheng, W.-Q. Chen, B.-T. Huang, Chinese J. Chem. 21 (2003) 153.
[152] M.-H. Qi, Q. Shen, X.-P. Chen, L.-H. Weng, Yingyong Huaxue 20 (2003) 629.
[153] J.-H. Cheng, D.-M. Cui, W.-Q. Chen, N.-H. Hu, T. Tang, B.-T. Huang, Gaodeng Xuexiao Huaxue Xuebao 24 (2003) 973.
[154] J. Cheng, D. Cui, W. Chen, T. Tang, B. Huang, Polyhedron 23 (2004) 1075.
[155] H.-Y. Sun, J. Du, X.-M. Xie, T. Gao, Z.-Y. Yue, P.-F. Yan, Heilongjiang Daxue Ziran Kexue Xuebao 20 (2003) 108.
[156] C. Qian, G. Zou, W. Jiang, Y. Chen, J. Sun, N. Li, Organometallics 23 (2004) 4980.
[157] E. Kirillov, L. Toupet, C.W. Lehmann, A. Razavi, S. Kahlal, J.-Y. Saillard, J.-F. Carpentier, Organometallics 22 (2003) 4038.
[158] E. Kirillov, C.W. Lehmann, A. Razavi, J.-F. Carpentier, Organometallics 23 (2004) 2768.
[159] M.G. Klimpel, P. Sirsch, W. Scherer, R. Anwander, Angew. Chem. 115 (2003) 594;
M.G. Klimpel, P. Sirsch, W. Scherer, R. Anwander, Angew. Chem. Int. Ed. 42 (2003) 574.
[160] C.D. Bérubé, S. Gambarotta, G.P.A. Yap, P.G. Cozzi, Organometallics 22 (2003) 434.
[161] J. Wang, A.K.J. Dick, M.G. Gardiner, B.F. Yates, E.J. Peacock, B.W. Skelton, A.H. White, Eur. J. Inorg. Chem. (2004) 1992.
[162] G.B. Deacon, C.M. Forsyth, A. Gitlits, B.W. Skelton, A.H. White, Dalton Trans. (2004) 1239.
[163] C.C. Quitmann, K. Mueller-Buschbaum, Z. Naturforsch. B 59 (2004) 562.
[164] K. Mueller-Buschbaum, Z. Allg. Anorg. Chem. 630 (2004) 895.
[165] C.D. Bérubé, M. Yazdanbakhsh, S. Gambarotta, G.P.A. Yap, Organometallics 22 (2003) 3742.
[166] D. Turcitu, F. Nief, L. Ricard, Chem. Eur. J. 9 (2003) 4916.
[167] G.K.B. Clentsmith, F.G.N. Cloke, J.C. Green, J. Hanks, P.B. Hitchcock, J.F. Nixon, Angew. Chem. 115 (2003) 1068;
G.K.B. Clentsmith, F.G.N. Cloke, J.C. Green, J. Hanks, P.B. Hitchcock, J.F. Nixon, Angew. Chem. Int. Ed. 42 (2003) 1038.
[168] J. Wang, S. Li, C. Zheng, J.A. Maguire, B. Sarkar, W. Kaim, N.S. Hosmane, Organometallics 22 (2003) 4334.
[169] J. Wang, S. Li, C. Zheng, J.A. Maguire, W. Kaim, N.S. Hosmane, Inorg. Chem. Commun. 6 (2003) 1220.
[170] J. Wang, S. Li, C. Zheng, N.S. Hosmane, J.A. Maguire, H.W. Roesky, C.C. Cummins, W. Kaim, Organometallics 22 (2003) 4390.
[171] J. Wang, S. Li, C. Zheng, A. Li, N.S. Hosmane, J.A. Maguire, H.W. Roesky, C.C. Cummins, W. Kaim, Organometallics 23 (2004) 4621.
[172] J. Wang, S. Li, C. Zheng, J.A. Maguire, N.S. Hosmane, Inorg. Chem. Commun. 6 (2003) 549.
[173] A. Li, J. Wang, C. Zheng, J.A. Maguire, N.S. Hosmane, Organometallics 23 (2004) 3091.
[174] S. Wang, Y. Wang, M.-S. Cheung, H.-S. Chan, Z. Xie, Tetrahedron 59 (2003) 10373.
[175] S. Wang, H.-W. Li, Z. Xie, Organometallics 23 (2004) 3780.
[176] S. Wang, H.-W. Li, Z. Xie, Organometallics 23 (2004) 2469.
[177] M.-S. Cheung, H.-S. Chan, Z. Xie, Organometallics 23 (2004) 517.
[178] H. Wang, H. Wang, H.-W. Li, Z. Xie, Organometallics 23 (2004) 875.
[179] F. Rabilloud, D. Rayane, A.R. Allouche, R. Antoine, M. Aubert-Frécon, M. Broyer, I. Compagnon, P. Dugourd, J. Phys. Chem. A 107 (2003) 11347.
[180] S. Kambalapalli, J.V. Ortiz, J. Phys. Chem. A 108 (2004) 2988.
[181] P.L. Arnold, M.A. Petrukhina, V.E. Bochenkov, T.I. Shabatina, V.V. Zagorskii, G.B. Sergeev, F.G.N. Cloke, J. Organometall. Chem. 688 (2003) 49.
[182] I.L. Fedushkin, G.V. Khoroshenĭkov, M.N. Bochkarev, S. Mühle, H. Schumann, Russ. Chem. Bull. 52 (2003) 1358.
[183] P.G. Hayes, W.E. Piers, M. Parvez, J. Am. Chem. Soc. 125 (2003) 5622.
[184] Y. Yao, G. Qi, Q. Shen, J. Hu, Y. Lin, Chin. Sci. Bull. 48 (2003) 2164.
[185] P.W. Roesky, M.T. Gamer, N. Marinos, Chem. Eur. J. 10 (2004) 3537.
[186] G.W. Rabe, M. Zhang-Presse, J.A. Golen, A.L. Rheingold, Acta Crystallogr. E 59 (2003) m1102.
[187] G.W. Rabe, M. Zhang-Presse, J.A. Golen, A.L. Rheingold, Acta Crystallogr. E 59 (2003) m255.
[188] G.W. Rabe, M. Zhang-Presse, G.P.A. Yap, Inorg. Chim. Acta 348 (2003) 245.
[189] A. Streitwieser, S.A. Kinsley, C.H. Jenson, J.T. Rigsbee, Organometallics 23 (2004) 5169.
[190] T. Inoue, T. Tomiyama, T. Sugai, T. Okazaki, T. Suematsu, N. Fujii, H. Utsumi, K. Nojima, H. Shinohara, J. Phys. Chem. B 108 (2004) 7573.
[191] M. Krause, M. Hulman, H. Kuzmany, O. Dubay, G. Kresse, K. Vietze, G. Seifert, C. Wang, Phys. Rev. Lett. 93 (2004) 1374031.
[192] H.-D. Arndt, R. Welz, S. Mueller, B. Ziemer, U. Koert, Chem. Eur. J. 10 (2004) 3945.
[193] H. Shimotani, T. Ito, Y. Iwasa, A. Taninaka, H. Shinohara, E. Nishibori, M. Takata, M. Sakata, J. Am. Chem. Soc. 126 (2004) 364.
[194] D.J. Berg, R.A. Andersen, Organometallics 22 (2003) 627.
[195] G.R. Giesbrecht, J.C. Gordon, D.L. Clark, P.J. Hay, B.L. Scott, D.C. Tait, J. Am. Chem. Soc. 126 (2004) 6387.

[196] H. Yasuda, Spec. Publ.—Roy. Soc. Chem. 287 (2003) 152.
[197] U. Reißmann, F.T. Edelmann, Z. Anorg. Allg. Chem. 629 (2003) 2433.
[198] M.-Y. Deng, Y.-M. Yoa, Y.-F. Zhou, L.-F. Zhang, Q. Shen, Chinese J. Chem. 21 (2003) 574.
[199] M. Nishiura, Z. Hou, Y. Wakatsuki, T. Yamaki, T. Miyamoto, J. Am. Chem. Soc. 125 (2003) 1184.
[200] T.R. Jensen, T.J. Marks, Macromolcules 36 (2003) 1775.
[201] Y. Luo, P. Selvam, A. Endou, M. Kubo, A. Miyamoto, J. Am. Chem. Soc. 125 (2003) 16210.
[202] T.R. Jensen, J.J. O'Donnell III, T.J. Marks, Organometallics 23 (2004) 740.
[203] Y. Luo, P. Selvam, Y. Ito, S. Takami, M. Kubo, A. Imamura, A. Miyamoto, Organometallics 22 (2003) 2181.
[204] E. Kirillov, C.W. Lehmann, A. Razavi, J.-F. Carpentier, J. Am. Chem. Soc. 126 (2004) 12240.
[205] Y. Luo, J. Baldamus, Z. Hou, J. Am. Chem. Soc. 126 (2004) 13910.
[206] A.M. Kawaoka, T.J. Marks, J. Am. Chem. Soc. 126 (2004) 12764.
[207] R.G. Lopez, C. Boisson, F. D'Agosto, R. Spitz, F. Boisson, D. Bertin, P. Tordo, Macromolecules 37 (2004) 3540.
[208] L.A. Nekhaeva, G.N. Bondarenko, V.M. Frolov, Kinet. Catal. 44 (2003) 631.
[209] L.A. Nekhaeva, V.M. Frolov, N.A. Konovalenko, L.I. Vyshinskaya, I.N. Tikhomirova, V.L. Khodzhaeva, B.F. Shklyaruk, E.M. Antipov, Vysokomolekulyarnye Soedineniya, Seriya A i Seriya B 45 (2003) 540.
[210] G.-H. Kwag, J.-G. Lee, C.-B. Bae, S.-N. Lee, Polymer 44 (2003) 6555.
[211] H. Berndt, H. Landmesser, J. Mol. Catal. A: Chem. 197 (2003) 245.
[212] J. Gromada, L. le Pichon, A. Mortreux, F. Leising, J.-F. Carpentier, J. Organometall. Chem. 683 (2003) 44.
[213] C. Boisson, V. Monteil, D. Ribour, R. Spitz, F. Barbotin, Macromol. Chem. Phys. 204 (2003) 1747.
[214] V. Monteil, R. Spitz, F. Barbotin, C. Boisson, Macromol. Chem. Phys. 205 (2004) 737.
[215] S. Kaita, Y. Takeguchi, Z. Hou, M. Nishiura, Y. Doi, Y. Wakatsuki, Macromolcules 36 (2003) 7923.
[216] A. Fischbach, M.G. Klimpel, M. Widenmeyer, E. Herdtweck, W. Scherer, R. Anwander, Angew. Chem. 116 (2004) 2284;
A. Fischbach, M.G. Klimpel, M. Widenmeyer, E. Herdtweck, W. Scherer, R. Anwander, Angew. Chem. Int. Ed. 43 (2004) 2234.
[217] S. Kaita, Y. Doi, K. Kaneko, A.C. Horiuchi, Y. Wakatsuki, Macromolecules 37 (2004) 5860.
[218] F. Bonnet, M. Visseaux, D. Barbier-Baudry, J. Organometall. Chem. 689 (2004) 264.
[219] F. Bonnet, M. Visseaux, D. Barbier-Baudry, E. Vigier, M.M. Kubicki, Chem. Eur. J. 10 (2004) 2428.
[220] H. Sugiyama, S. Gambarotta, G.P.A. Yap, D.R. Wilson, S.K.-H. Thiele, Organometallics 23 (2004) 5054.
[221] D. Cui, T. Tang, W. Bi, J. Cheng, W. Chen, B. Huang, J. Polym. Sci., Part A: Polym. Chem. 41 (2003) 2667.
[222] C. Tsutsumi, K. Nakagawa, H. Shirahama, H. Yasuda, Polym. Int. 52 (2003) 439.
[223] Y. Satoh, N. Ikitake, Y. Nakayama, S. Okuno, H. Yasuda, J. Organometall. Chem. 667 (2003) 42.
[224] J.-L. Chen, Y.-M. Yao, Y.-J. Luo, L.-Y. Zhou, Y. Zhang, Q. Shen, J. Organometall. Chem. 689 (2004) 1019.
[225] I. Palard, A. Soum, S.M. Guillaume, Chem. Eur. J. 10 (2004) 4054.
[226] H. Yasuda, G. Desurmont, Polym. Intern. 53 (2004) 1017.
[227] M.W. Neiser, J. Okuda, M. Schmidt, Macromolcules 36 (2003) 5437.
[228] M.W. Neiser, S. Muth, U. Kolb, J.R. Harris, J. Okuda, M. Schmidt, Angew. Chem. 116 (2004) 3255;
M.W. Neiser, S. Muth, U. Kolb, J.R. Harris, J. Okuda, M. Schmidt, Angew. Chem. Int. Ed. 43 (2004) 3192.
[229] H. Yasuda, Y. Nakayama, Y. Satoh, Z. Shen, X. Ni, M. Inoue, S. Namba, Polym. Int. 53 (2004) 1682.
[230] G. Qi, Y. Nitto, A. Saiki, T. Tomohiro, Y. Nakayama, H. Yasuda, Tetrahedron 59 (2003) 10409.
[231] L. Mei, H.-Z. Ma, Q.-D. Su, Q.-R. Li, Asian J. Chem. 15 (2003) 259.
[232] L. Mei, H.-Z. Ma, Q.-D. Su, Asian J. Chem. 15 (2003) 497.
[233] X. Xie, J. Huang, Appl. Organometall. Chem. 18 (2004) 282.
[234] Y.-L. Qian, M.D. Bala, X.-M. Xie, J.-L. Huang, Chinese J. Chem. 22 (2004) 568.
[235] M. Nishiura, M. Tanikawa, M. Hoshino, T. Miyamoto, Z. Hou, Kidorui 42 (2003) 54.
[236] Y. Horino, T. Livinghouse, Organometallics 23 (2004) 12.
[237] A.A. Trifonov, T.P. Spaniol, J. Okuda, Dalton Trans. (2004) 2245.
[238] K. Takaki, K. Komeyama, G. Koshoji, K. Takehira, Kidorui 42 (2003) 52.
[239] A.M. Seyam, B.D. Stubbert, T.R. Jensen, J.J. O'Donnell III, C. Stern, T.J. Marks, Inorg. Chim. Acta 357 (2004) 4029.
[240] J.-S. Ryu, G.Y. Li, T.J. Marks, J. Am. Chem. Soc. 125 (2003) 12584.
[241] A. Motta, G. Lanza, I.L. Fragala, T.J. Marks, Organometallics 23 (2004) 4097.
[242] S. Hong, A.M. Kawaoka, T.J. Marks, J. Am. Chem. Soc. 125 (2003) 15878.
[243] J.-S. Ryu, T.J. Marks, F.E. McDonald, J. Org. Chem. 69 (2004) 1038.
[244] G.A. Molander, S.K. Pack, J. Org. Chem. 68 (2003) 9214.
[245] G.A. Molander, S.K. Pack, Tetrahedron 59 (2003) 10581.
[246] S. Hong, S. Tian, M.V. Metz, T.J. Marks, J. Am. Chem. Soc. 125 (2003) 14768.
[247] D.V. Gribkov, K.C. Hultzsch, Chem. Commun. (2004) 730.
[248] F. Lauterwasser, P.G. Hayes, S. Braese, W.E. Piers, L.L. Schafer, Organometallics 23 (2004) 2234.
[249] A.M. Kawaoka, M.R. Douglass, T.J. Marks, Organometallics 22 (2003) 4630.
[250] K. Takaki, G. Koshoji, K. Komeyama, M. Takeda, T. Shishido, A. Kitani, K. Takehira, J. Org. Chem. 68 (2003) 6554.
[251] A.D. Sadow, T.D. Tilley, Angew. Chem. 115 (2003) 827;
A.D. Sadow, T.D. Tilley, Angew. Chem. Int. Ed. 42 (2003) 803.
[252] A.D. Sadow, T.D. Tilley, J. Am. Chem. Soc. 125 (2003) 7971.
[253] C.C. Bausch, J.S. Johnson, J. Org. Chem. 69 (2004) 4283.
[254] C. Zhao, D. Wang, D.L. Phillips, J. Am. Chem. Soc. 125 (2003) 15200.
[255] D. Wang, C. Zhao, D.L. Phillips, J. Org. Chem. 69 (2004) 5512.
[256] S.T. Cacatian, P.L. Fuchs, Tetrahedron 59 (2003) 7177.
[257] A.G.H. Wee, D.D. McLeod, J. Org. Chem. 68 (2003) 6268.
[258] F.-X. Felpin, K. Boubekeur, J. Lebreton, Eur. J. Org. Chem. (2003) 4518.
[259] A. Wada, Y. Takakura, K. Yamazaki, T. Takahashi, M. Ito, Lett. Org. Chem. 1 (2004) 59.
[260] J. Li, Y. Liu, Y. Zhang, J. Chem. Res., Synopses (2003) 438.
[261] X. Wang, J. Li, Y. Zhang, Synth. Commun. 33 (2003) 3575.
[262] D.-S. Hsu, C.-C. Liao, Org. Lett. 5 (2003) 4741.
[263] L.F. Rybakova, S.V. Tsygankova, D.M. Roitershtein, E.S. Petrov, Russ. J. Gen. Chem. 74 (2004) 141.
[264] X. He, M. Trudeau, D. Antonelli, J. Mater. Chem. 13 (2003) 75.
[265] X. He, M. Trudeau, D. Antonelli, J. Mater. Chem. 13 (2003) 75.
[266] G. Scarel, E. Bonera, C. Wiemer, G. Tallarida, S. Spiga, M. Fanciulli, I.L. Fedushkin, H. Schumann, Y. Lebedinski, A. Zenkevich, Appl. Phys. Lett. 85 (2004) 630.
[267] T. Akane, S. Jinno, Y. Yang, T. Kuno, T. Hirata, Y. Isogai, N. Watanabe, Y. Fujiwara, A. Nakamura, Y. Takeda, Appl. Surf. Sci. 216 (2003) 537.
[268] A. Dormond, D. Barbier-Baudry, Sci. Synth. 2 (2003) 943.
[269] L. Andrews, B. Liang, J. Li, B.E. Bursten, J. Am. Chem. Soc. 125 (2003) 3126.
[270] K.C. Jantunen, R.J. Batchelor, D.B. Leznoff, Organometallics 23 (2004) 2186.
[271] H. Nakai, X. Hu, L.N. Zakharov, A.L. Rheingold, K. Meyer, Inorg. Chem. 43 (2004) 855.
[272] M.J. Sarsfield, M. Helliwell, J. Am. Chem. Soc. 126 (2004) 1036.
[273] C.N. Carlson, T.P. Hanusa, W.W. Brennessel, J. Am. Chem. Soc. 126 (2004) 10550.
[274] R.J. Wright, P.P. Power, B.L. Scott, J.L. Kiplinger, Organometallics 23 (2004) 4801.
[275] T. Mehdoui, J.-C. Berthet, P. Thuery, M. Ephritikhine, Dalton Trans. (2004) 579.
[276] T. Nagao, J. Igarashi, Physica B 329–333 (2003) 628.
[277] B.D. Stubbert, C.L. Stern, T.J. Marks, Organometallics 22 (2003) 4836.

[278] J.T. Golden, D.N. Kazul'kin, B.L. Scott, A.Z. Voskoboynikov, C.J. Burns, Organometallics 22 (2003) 3971.
[279] W.J. Evans, S.A. Kozimor, J.W. Ziller, Polyhedron 23 (2004) 2689.
[280] W.J. Evans, S.A. Kozimor, J.W. Ziller, N. Kaltsoyannis, J. Am. Chem. Soc. 126 (2004) 14533.
[281] W.J. Evans, S.A. Kozimor, J.W. Ziller, J. Am. Chem. Soc. 125 (2003) 14264.
[282] W.J. Evans, S.A. Kozimor, G.W. Nyce, J.W. Ziller, J. Am. Chem. Soc. 125 (2003) 13831.
[283] E. Barnea, T. Andrea, M. Kapon, M.S. Eisen, J. Am. Chem. Soc. 126 (2004) 5066.
[284] D.E. Morris, R.E.D. Re, K.C. Jantunen, I. Castro-Rodriguez, J.L. Kiplinger, Organometallics 23 (2004) 5142.
[285] K.A.N.S. Ariyaratne, R.E. Cramer, G.B. Jameson, J.W. Gilje, J. Organometall. Chem. 689 (2004) 2029.
[286] K.C. Jantunen, C.J. Burns, I. Castro-Rodriguez, R.E. Da Re, J.T. Golden, D.E. Morris, B.L. Scott, F.L. Taw, J.L. Kiplinger, Organometallics 23 (2004) 4682.
[287] P.J. Hay, Faraday Discuss. 124 (2003) 69.
[288] F.G.N. Cloke, J.C. Green, N. Kaltsoyannis, Organometallics 23 (2004) 832.
[289] I. Korobkov, S. Gambarotta, Organometallics 23 (2004) 5379.
[290] D. Seyferth, Organometallics 23 (2004) 3562.
[291] S.M. Cendrowski-Guillaume, G. Le Gland, M. Nierlich, M. Ephritikhine, Eur. J. Inorg. Chem. (2003) 1388.
[292] T. Arliguie, P. Thuéry, M. Fourmigué, M. Ephritikhine, Organometallics 22 (2003) 3000.
[293] J.S. Hager, J. Zahardis, R.M. Pagni, R.N. Compton, J. Li, J. Chem. Phys. 120 (2004) 2708.
[294] E. Barnea, T. Andrea, M. Kapon, J.-C. Berthet, M. Ephritikhine, M.S. Eisen, J. Am. Chem. Soc. 126 (2004) 10860.
[295] A.K. Dash, T.R. Jensen, C.L. Stern, T.J. Marks, J. Am. Chem. Soc. 126 (2004) 12528.
[296] N.G. Stahl, C. Zuccaccia, T.R. Jensen, T.J. Marks, J. Am. Chem. Soc. 125 (2003) 5256.
[297] C. Zuccaccia, N.G. Stahl, A. Macchioni, M.-C. Chen, J.A. Roberts, T.J. Marks, J. Am. Chem. Soc. 126 (2004) 1448.